BRL-TR-2974

DTIC FILE COPY

4

TECHNICAL REPORT BRL-TR-2974

BRL

1938 – Serving the Army for Fifty Years – 1988

AD-A205 464

AN UPDATED LUMPED PARAMETER CODE FOR REGENERATIVE LIQUID PROPELLANT IN-LINE GUNS

TERENCE P. COFFEE

DECEMBER 1988

APPROVED FOR PUBLIC RELEASE; DISTRIBUTION UNLIMITED.

U.S. ARMY LABORATORY COMMAND

BALLISTIC RESEARCH LABORATORY

ABERDEEN PROVING GROUND, MARYLAND

DESTRUCTION NOTICE

Destroy this report when it is no longer needed. DO NOT return it to the originator.

Additional copies of this report may be obtained from the National Technical Information Service, U.S. Department of Commerce, Springfield, VA 22161.

The findings of this report are not to be construed as an official Department of the Army position, unless so designated by other authorized documents.

The use of trade names or manufacturers' names in this report does not constitute indorsement of any commercial product.

UNCLASSIFIED

SECURITY CLASSIFICATION OF THIS PAGE

REPORT DOCUMENTATION PAGE

Form Approved OMB No. 0704-0188

1a. REPORT SECURITY CLASSIFICATION Unclassified	1b. RESTRICTIVE MARKINGS
2a. SECURITY CLASSIFICATION AUTHORITY	3. DISTRIBUTION / AVAILABILITY OF REPORT APPROVED FOR PUBLIC RELEASE; DISTRIBUTION UNLIMITED.
2b. DECLASSIFICATION / DOWNGRADING SCHEDULE	
4. PERFORMING ORGANIZATION REPORT NUMBER(S) BRL-TR-2974	5. MONITORING ORGANIZATION REPORT NUMBER(S)
6a. NAME OF PERFORMING ORGANIZATION US Army Ballistic Rsch Lab 6b. OFFICE SYMBOL (*If applicable*) SLCBR-IB	7a. NAME OF MONITORING ORGANIZATION
6c. ADDRESS (*City, State, and ZIP Code*) Aberdeen Proving Ground, MD 21005-5066	7b. ADDRESS (*City, State, and ZIP Code*)
8a. NAME OF FUNDING / SPONSORING ORGANIZATION 8b. OFFICE SYMBOL (*If applicable*)	9. PROCUREMENT INSTRUMENT IDENTIFICATION NUMBER
8c. ADDRESS (*City, State, and ZIP Code*)	10. SOURCE OF FUNDING NUMBERS PROGRAM ELEMENT NO. / PROJECT NO. / TASK NO. / WORK UNIT ACCESSION NO.

11. TITLE (*Include Security Classification*)
AN UPDATED LUMPED PARAMETER CODE FOR REGENERATIVE LIQUID PROPELLANT IN-LINE GUNS

12. PERSONAL AUTHOR(S)
Coffee, Terence P.

13a. TYPE OF REPORT	13b. TIME COVERED	14. DATE OF REPORT (*Year, Month, Day*)	15. PAGE COUNT
TR	FROM ______ TO ______		

16. SUPPLEMENTARY NOTATION

17. COSATI CODES		
FIELD	GROUP	SUB-GROUP

18. SUBJECT TERMS (*Continue on reverse if necessary and identify by block number*)
liquid monopropellant, propellant injection, regenerative gun, droplet burning, lumped parameter model, numerical solution

19. ABSTRACT (*Continue on reverse if necessary and identify by block number*)

In a previous report, a lumped parameter code for regenerative liquid propellant guns was described.[1] Since then improvements have been made in the governing equations. A number of options have been added to the code, and some options have been removed. This report is an update to the description of the regenerative liquid propellant in-line gun code.

The governing ordinary differential equations for the lumped parameter model of a regenerative liquid gun are given. The different options and assumptions are described. The equations are solved numerically using EPISODE, an efficient and robust computer code for the integration of ordinary differential equations. An example is given where the code is compared to an experimental gun firing, and the process of choosing reasonable input parameters is discussed.

20. DISTRIBUTION / AVAILABILITY OF ABSTRACT	21. ABSTRACT SECURITY CLASSIFICATION	
☒ UNCLASSIFIED/UNLIMITED ☐ SAME AS RPT. ☐ DTIC USERS	Unclassified	
22a. NAME OF RESPONSIBLE INDIVIDUAL	22b. TELEPHONE (*Include Area Code*)	22c. OFFICE SYMBOL
Terence P. Coffee	(301) 278-6169	SLCBR-IB-B

DD Form 1473, JUN 86 *Previous editions are obsolete.* SECURITY CLASSIFICATION OF THIS PAGE

TABLE OF CONTENTS

		Page
	LIST OF FIGURES	vii
I.	INTRODUCTION	1
II.	THE REGENERATIVE LIQUID PROPELLANT GUN	1
III.	BASIC ASSUMPTIONS	2
IV.	GOVERNING EQUATIONS	5
	A. LIQUID RESERVIOR	5
	B. COMBUSTION CHAMBER	8
	C. GUN TUBE	10
V.	VENT OPTIONS	14
	A. VENT1	14
	B. VENT2	15
	C. VENT3	17
VI.	PISTON RESISTANCE OPTIONS	18
	A. PIS1	19
VII.	PROJECTILE RESISTANCE OPTIONS	19
	A. PROJ1	19
VIII.	DISCHARGE COEFFICIENT - INTO CHAMBER	20
	A. DIS1	20
IX.	DISCHARGE COEFFICIENT - INTO GUN TUBE	20
	A. DIS1	20
X.	MASS FLUX OPTIONS - INTO CHAMBER	20
	A. FLUX1	20
	B. FLUX2	21
	C. FLUX3	21

XI.	MASS FLUX OPTIONS - INTO GUN TUBE		22
	A.	FLUX1	22
	B.	FLUX2	22
XII.	GUN TUBE PRESSURE DISTRIBUTION OPTIONS		22
	A.	TUBE1	22
	B.	TUBE2	23
	C.	TUBE3	23
	D.	TUBE4	24
XIII.	PRIMER OPTIONS		24
	A.	PRIM1	24
	B.	PRIM2	25
	C.	PRIM3	25
XIV.	GUN TUBE HEAT LOSS OPTIONS		25
	A.	HEAT1	26
	B.	HEAT2	26
XV.	CHAMBER HEAT LOSS OPTIONS		28
	A.	HEAT1	28
	B.	HEAT2	28
XVI.	AIR SHOCK		29
	A.	SHOCK1	29
	B.	SHOCK2	29
XVII.	BUFFER OPTIONS		30
	A.	BUFF1	30
	B.	BUFF2	30
XVIII.	REPEAT OPTIONS		31
	A.	REP1	31
	B.	REP2	31
	C.	REP3	32
XIX.	CHAMBER PRESSURE OPTIONS		32
	A.	CHAM1	32
	B.	CHAM2	33

XX.	DROPLET BURNING OPTIONS	33
	A. DROP1	38
	B. DROP2	39
	C. DROP3	39
XXI.	MASS AND ENERGY BALANCE	39
XXII.	NUMERICAL METHOD	42
XXIII.	BRL 30MM GUN FIXTURE	45
XXIV.	CONCLUSIONS	68
	ACKNOWLEDGEMENT	68
	GLOSSARY	69
	REFERENCES	77
	APPENDIX A	81
	APPENDIX B	89
	APPENDIX C	99
	APPENDIX D	103
	APPENDIX E	107
	APPENDIX F	111
	DISTRIBUTION LIST	115

LIST OF FIGURES

Figure		Page
1	A Regenerative Liquid Propellant Gun with Injection Orifices.	3
2	A Regenerative Liquid Propellant Gun with an Annular Piston.	3
3	Scale Model Drawing of the Liquid Reservoir, Initial Position (after Pre-pressurization).	46
4	Experimental Liquid Pressure (line) and Chamber Pressure (dot).	47
5	Experimental Piston Travel.	47
6	Experimental Projectile Velocity.	48
7	Derived Discharge Coefficient versus Time.	49
8	Derived Discharge Coefficient versus Piston Travel.	49
9	Chamber Pressure. Experiment (line). Model - Instantaneous burning - $C_D = 0.95$ (dot).	55
10	Chamber Pressure - Centered. Experiment (line). Model - Instantaneous Burning - $C_D = 0.95$ (dot).	55
11	Liquid Pressure - Centered. Experiment (line). Model - Instantaneous Burning - $C_D = 0.95$ (dot).	56
12	Piston Travel - Centered. Experiment (line). Model - Instantaneous Burning - $C_D = 0.95$ (dot).	56
13	Projectile Velocity - Centered. Experiment (line). Model - Instantaneous Burning - $C_D = 0.95$ (dot).	57
14	Chamber Pressure. Experiment (line). Model - Droplet Formation - $C_D = 0.95$ (dot).	58
15	Liquid Pressure. Experiment (line). Model - Droplet Formation - $C_D = 0.95$ (dot).	58

16 Piston Travel. Experiment (line).
Model - Droplet Formation - C_D = 0.95 (dot). 59

17 Projectile Velocity. Experiment (line).
Model - Droplet Formation - C_D = 0.95 (dot). 59

18 Chamber Pressure - Centered. Experiment (line).
Model - Instantaneous Burning - C_D = 0.95 -
Long Belleville (dot). 61

19 Liquid Pressure - Centered. Experiment (line).
Model - Instantaneous Burning - C_D = 0.95 -
Long Belleville (dot). 61

20 Piston Travel - Centered. Experiment (line).
Model - Instantaneous Burning - C_D = 0.95 -
Long Belleville (dot). 62

21 Projectile Velocity - Centered. Experiment (line).
Model - Instantaneous Burning - C_D = 0.95 -
Long Belleville (dot). 62

22 Chamber Pressure. Experiment (line).
Model - Droplet Formation - C_D = 0.95 -
Long Belleville (dot). 63

23 Liquid Pressure. Experiment (line).
Model - Droplet Formation - C_D = 0.95 -
Long Belleville (dot). 63

24 Piston Travel. Experiment (line).
Model - Droplet Formation - C_D = 0.95 -
Long Belleville (dot). 64

25 Projectile Velocity. Experiment (line).
Model - Droplet Formation - C_D = 0.95 -
Long Belleville (dot). 64

26 Chamber Pressure. Experiment (line).
Model - Droplet Formation - C_D Adjusted -
Long Belleville (dot). 65

27	Liquid Pressure. Experiment (line). Model - Droplet Formation - C_D Adjusted - Long Belleville (dot).	65
28	Piston Travel. Experiment (line). Model - Droplet Formation - C_D Adjusted - Long Belleville (dot).	66
29	Projectile Velocity. Experiment (line). Model - Droplet Formation - C_D Adjusted - Long Belleville (dot).	66
30	Discharge Coefficient. Derived from Experiment (line). Model - Droplet Formation - C_D Adjusted - Long Belleville (dot).	67

I. INTRODUCTION

In this paper an update is given to the description of a regenerative liquid propellant gun code.[1] Most of the basic governing equations for the lumped parameter model are the same as before, but are repeated here for convenience. The derivations are in the previous report. The changes in the equations are described, and the reasons for the changes are given. The code has been used to test the effect of various assumptions. A number of options have been added to the code, and some options that are no longer considered useful have been removed. A complete description of the present group of options is given. In the future, new options will undoubtably be added. The code is compared to experimental data for a 30mm gun fixture at the BRL.

II. THE REGENERATIVE LIQUID PROPELLANT GUN

Fig. 1 shows a diagram of one possible design of a regenerative liquid propellant gun with an in-line piston. The monopropellant is pumped into the liquid reservoir at the beginning of the firing cycle. A primer is ignited and injects hot gas into the combustion chamber. As the chamber is pressurized, the piston is pushed back. Because of the piston area differential between the two regions, the piston will move back even when the liquid pressure is higher than the combustion chamber pressure. The pressure differential forces liquid propellant through the holes in the piston face. The propellant ignites and burns in the combustion chamber. The higher chamber pressure accelerates the piston, leading to more rapid injection. Eventually, the pressure pushes the projectile down the gun tube.

The behavior in the combustion chamber is very complicated. A primer forces hot gas into the chamber, leading to a gradual pressure rise. Liquid jets are forced out of the vent holes. These jets may break up into droplets because of hydrodynamic forces or due to impact on the wall of the chamber. The droplets formed may break up further or

coalese. The propellant will eventually ignite, and may burn as individual droplets or as envelope flames. A recirculation flow will be set up in the chamber, further complicating the behavior of the liquid jets. As the projectile starts to move down the gun tube, gas (and perhaps some unburned propellant) will flow into the tube. Unlike most solid propellant guns, there is generally a large abrupt area change between the combustion chamber and the gun tube. This will further complicate the flow patterns. These processes are not well understood even at low pressures.

The design of the piston considered here was used in early test fixtures,[2,3] but is not convenient for actual guns. The vent holes must be plugged before each shot, making rapid fire impractical. Fig. 2 shows a more practical gun design (concept VI). The piston is wrapped around a fixed central bolt. The liquid propellant is injected through the annulus between the piston and the bolt. The present code also handles this type of gun.

Another design being considered at the present time allows the central bolt to move as well as the piston (concept VIC). The code cannot presently handle this case.

An alternate to the in-line piston configurations is the reverse annular piston (RAP) gun. For this case the piston is wrapped around the gun tube and moves in the same direction as the projectile. Liquid is injected directly into the gun tube. A separate code has been developed for this type of fixture, and this will be described in a separate report.

III. BASIC ASSUMPTIONS

The propellant in the liquid reservoir is assumed to be a homogeneous, isothermal fluid. Because of the high pressures in a gun, the liquid is considered to be compressible.

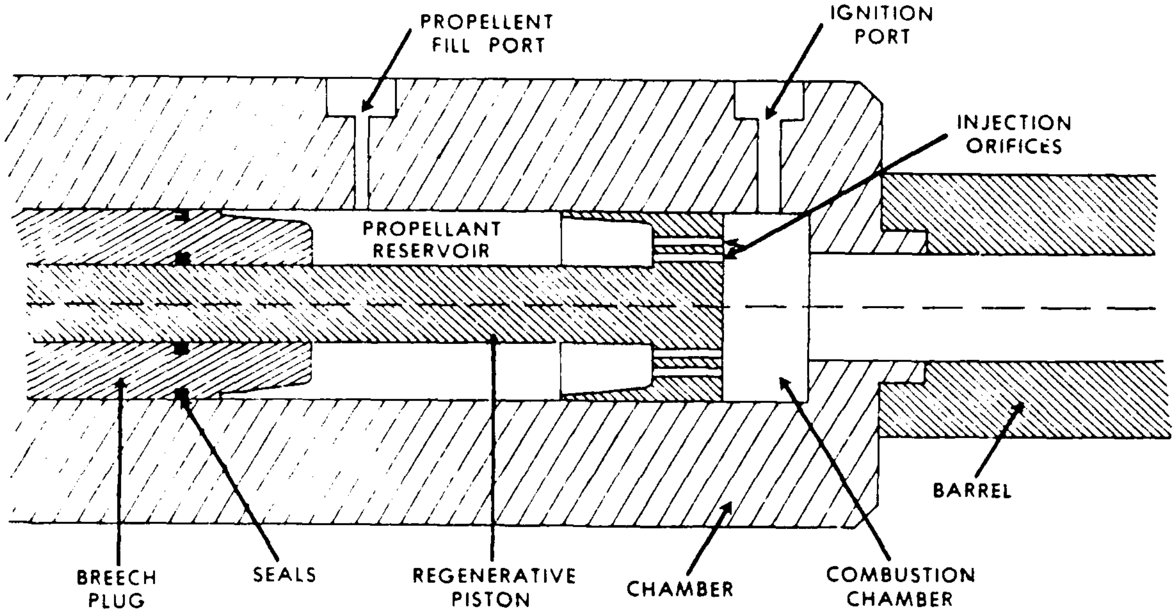

Figure 1. A Regenerative Liquid Propellant Gun with Injection Orifices.

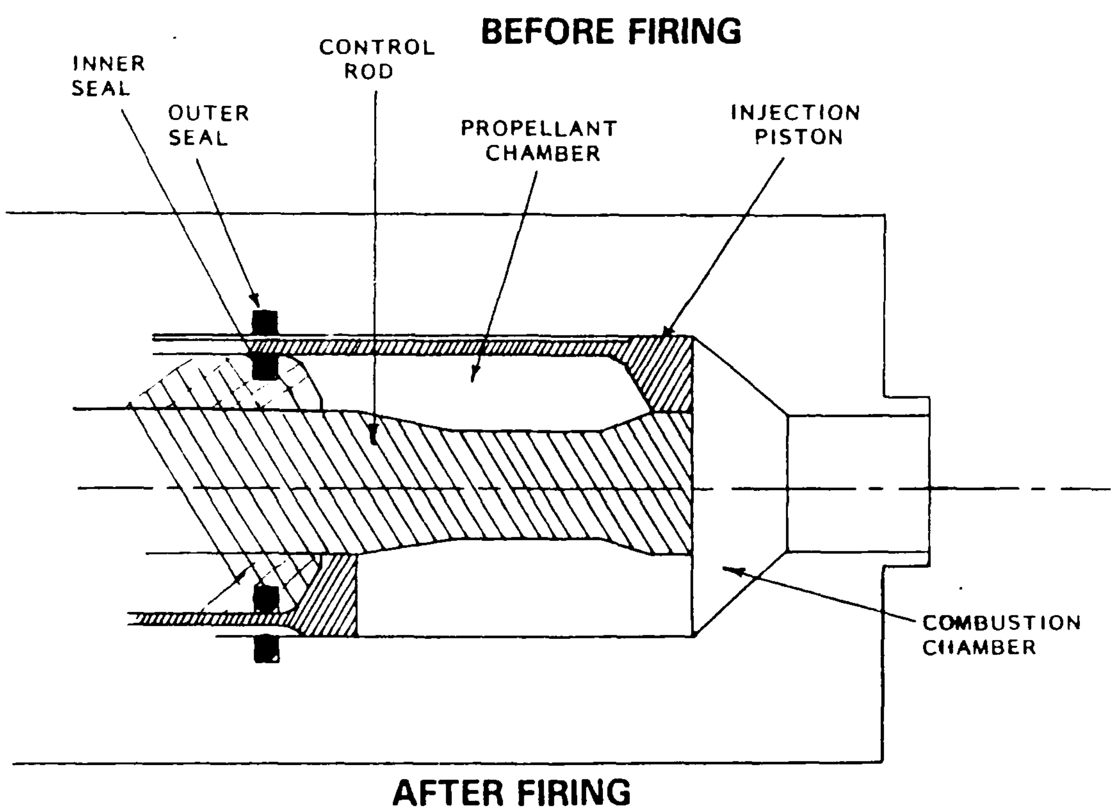

Figure 2. A Regenerative Liquid Propellant Gun with an Annular Piston.

The orifice flow through the vents in the piston is difficult to model. The assumption is made that the piston is infinitely thin, so the orifice behaviour can be ignored. The mass flux into the chamber is normally computed assuming steady state Bernoulli flow. Comparisons with transient lumped parameter, one-dimensinal, and two-dimensional models of the liquid reservoir indicate that this is a reasonable assumption.[4]

At present, there is no reasonable procedure for predicting the flow patterns in the combustion chamber. The chamber fluid is assumed to be homogeneous and stagnant. Lacking any detailed information on flow in the chamber, the fluid velocity in the chamber is simply set uniformly equal to zero.

The propellant combustion is coupled closely with the fluid flow in the chamber, and is also very hard to model. As a first approximation, the liquid is assumed to combust instantaneously as soon as it enters the combustion chamber, releasing all its energy.

There is evidence that liquid accumulates in the combustion chamber at the beginning of the firing cycle, affecting the behavior of the gun. Later finite burning rate models for the liquid propellant will be introduced, in an attempt to model, at least crudely, the effects of possible propellant accumulation.

The primer is assumed to be the same liquid as the propellant. Normally the combustion and injection of the primer is not considered in detail. Instead, the initial pressure in the combustion chamber is an input parameter. Then the amount of propellant needed to produce this pressure is calculated. and this is taken as the mass of the primer. The piston and projectile are not allowed to move during the burning of the primer. Later more complicated primer options will be discussed.

There is usually a large area change between the combustion chamber and the gun tube. The mass flux into the gun tube is computed assuming steady state isentropic flow. Since the conditions in the chamber are not well known, the accuracy of this assumption is uncertain.

The gun tube is also treated as a lumped parameter region, using modifications of the Lagrange pressure distribution that has successfully modeled the behavior of solid propellant guns[5]. By comparisons with a one-dimensional model, improved versions of the Lagrange pressure distribution for liquid propellant guns have been developed.[6]

Below, we derive the governing equations for the simple lumped parameter model described above, assuming the gun of Fig. 1. Then a list of options will be given, with the appropriate modifications to the base governing equations.

IV. GOVERNING EQUATIONS

With the above assumptions, the regenerative gun behavior can be modeled by 13 ordinary differential equations. These equations are marked by numbers at the left in square brackets ([1] to [13]). Some algebraic equations are required to compute the coefficients of the ordinary differential equations. The equations describe the three lumped parameter regions (liquid reservoir, combustion chamber, and gun tube), the mass flux between the regions, and the piston and projectile motion. For historical reasons, the regions are numbered 1, 3, and 4. The RAP gun has an additional region, the intermediate chamber, numbered 2. The derivations that have not changed are in the previous report.[1] The notation is given in the glossary.

A. LIQUID RESERVOIR

The equations governing the piston motion are straightforward. Let

V_1 be the volume of the propellant chamber, and A_1 be the area of the propellant side of the piston (this area includes the vent holes). Let s_{ps} be the piston travel (to the left) and v_{ps} be the piston velocity. Then

[1] $$\frac{dV_1}{dt} = -v_{ps} A_1 \ . \qquad (1)$$

The acceleration of the piston equals the force on the piston divided by the mass of the piston. That is,

[2] $$\frac{dv_{ps}}{dt} = \frac{g_o}{M_{ps}} [p_3 (A_3 - A_v) - (p_1 + p_{ps}) (A_1 - A_v)] \ , \qquad (2)$$

where A_3 is the area of the combustion side of the piston, p_1 is the pressure in the liquid chamber, p_3 is the pressure in the combustion chamber, and M_{ps} is the mass of the piston. The quantity $g_o = 10^7$ g/s-cm-Mpa is a conversion constant to put the acceleration in the desired units of cm^2/s. By assumption, the pressures are constant throughout the two chambers. The quantity p_{ps} is an empirical correction to simulate the effects of frictional resistance (see options). The piston is assumed initially to be prevented from moving toward the gun tube. So if the initial acceleration is negative, it is changed to zero. Also, the quantity p_{ps} is solely a resistance pressure. If the p_{ps} term is larger than the other pressure terms, the acceleration is set equal to zero. Also, if at a later time the piston reverses direction, the sign of p_{ps} is changed. The equation governing the piston travel is

[3] $$\frac{ds_{ps}}{dt} = v_{ps} \ . \qquad (3)$$

From conservations of mass,

[4] $$\frac{d\rho_1}{dt} = - \frac{\rho_1}{V_1}\frac{dV_1}{dt} - \frac{m_{13}}{V_1} , \qquad (4)$$

where ρ_1 is the density of the liquid and m_{13} is the mass flux out of the reservoir. The energy equation can be rewritten as

[5] $$\frac{dp_1}{dt} = \frac{c_1^2}{g_o}\frac{d\rho_1}{dt} , \qquad (5)$$

where c_1 is the speed of sound in the liquid.

Heat transfer and temperature changes in the liquid propellant are expected to be small, and are ignored. Then the speed of sound is given by

$$c_1 = \sqrt{g_o K / \rho_1} , \qquad (6)$$

where K is the adiabatic bulk modulus. For the common liquid propellants, this can be fit very accurately by[7]

$$K = K_1 + K_2 \, p_1 . \qquad (7)$$

The corresponding equation of state is

$$p_1 = \frac{K_1}{K_2} \left[(\rho_1/\rho_o)^{K_2} - 1 \right] . \qquad (8)$$

The ordinary differential equations [5] for the pressure is not actually required. Once the density is known, the pressure can be computed from the equation of state (8).

Recently a new equation of state has been derived that also includes the temperature dependence.[8] This could be used instead to include temperature changes in the liquid. The new equation predicts that temperature effects are minimal and predicts almost the same pressure

dependence as eq. (8).

The mass flux out of the reservoir is assumed to be steady state Bernoulli flow

$$m_{13} = C_D A_v \sqrt{2g_o \rho_1 (p_1 - p_3)} \; . \qquad (9)$$

The discharge coefficient C_D is an empirical correction to the equations to take into account frictional losses. Since the mass flux for a gun firing is not steady state, C_D may also be used to approximate the time delay in reaching steady state.

B. COMBUSTION CHAMBER

Now consider the combustion chamber. By analogy with eq. [1],

[6] $$\frac{dV_3}{dt} = v_{ps} A_3 \; , \qquad (10)$$

where V_3 is the volume of the combustion chamber and A_3 is the area of the combustion side of the piston (including holes). Similarly, from conservation of mass

[7] $$\frac{d\rho_3}{dt} = - \frac{\rho_3}{V_3} \frac{dV_3}{dt} + \frac{m_{13} - m_{34}}{V_3} \; , \qquad (11)$$

where ρ_3 is the density of the gas in the combustion chamber and m_{34} is the mass flux into the gun tube. The energy equation is

[8] $$\frac{dp_3}{dt} = \frac{c_3^2}{g_o} \frac{d\rho_3}{dt} + \frac{m_{13} (h_{L1} - h_{G3}) (\gamma - 1)}{V_3 - b M_3} \; , \qquad (12)$$

where c_3 is the speed of sound in the chamber, h_{L1} is the enthalpy of the liquid, and h_{G3} is the enthalpy of the combustion chamber gas. This is based on the Noble-Abel equation of state[5]

$$p_3 = \rho_3 R_s T_3 / (1 - b \rho_3) , \tag{13}$$

where T_3 is the temperature in region 3, R_s is the specific gas constant (universal gas constant divided by molecular weight of the gas), and b is the covolume. This can also be written as

$$p_3 = \rho_3 (\gamma - 1) c_v T_3 / (1 - b \rho_3) , \tag{14}$$

where c_v is the specific heat at constant volume and γ is the specific heat ratio c_p/c_v. The corresponding equation for the speed of sound is

$$c_3 = \sqrt{\frac{g_o \gamma p_3}{\rho_3 (1 - b \rho_3)}} . \tag{15}$$

Normally, gas will flow from the combustion chamber into the gun tube, so the mass flux m_{34} does not contribute to the energy equation. But if the gas flows from the tube into the chamber, there will be an additional source term. This occurs so infrequently and the reverse mass flux is so small, it is sufficient to just set the mass flux equal to zero in this case.

The energy content of a propellant is normally given in terms of impetus λ. Consider a quantity of propellant in a constant volume closed chamber. The propellant combusts, and the result is a gas with some molecular weight M_g and temperature T_o (called the isochoric temperature). The impetus is defined as

$$\lambda = R_u T_o / M_g , \tag{16}$$

where R_u is the universal gas constant. Impetus can be obtained from a closed bomb experiment, if the proper corrections are made for the primer and the heat loss to the chamber walls. For liquid propellants, the impetus is usually calculated by a thermodynamics code.[9] The values of the molecular weight, the specific heats, and the covolume of the

product gases are evaluated at the isochoric temperature and then assumed to be constant with respect to temperature and pressure. The impetus does depend on the initial loading density (grams of propellant per unit volume). Values are chosen at a standard loading density of 0.2. The effects of changing the loading density are negligable.

For our case, it is more convenient to work with the chemical energy

$$e_1 = \lambda / (\gamma - 1) \ . \tag{17}$$

The enthalpy of the liquid is given by

$$h_{L1} = e_1 + p_1 / \rho_1 \ . \tag{18}$$

The enthalpy of the gas is given by

$$h_{G3} = c_v T_3 + p_3 / \rho_3 = c_p T_3 + b \, p_3 \ . \tag{19}$$

C. GUN TUBE

Finally, the gun tube (region 4) is considered. The volume has the standard equation

[9] $$\frac{dV_4}{dt} = v_{pj} A_4 \ , \tag{20}$$

where v_{pj} is the velocity of the projectile and A_4 is the area of the gun tube. The rapid projectile motion creates a large pressure gradient. The standard approach is to assume a Lagrange pressure distribution,[5] that is, assume that the density is constant with respect to space. It follows from the one-dimensional continuity equation that the gas velocity is a linear function of distance. The gas velocity at the base of the projectile is equal to the velocity of the projectile.

In solid propellant guns, the gas velocity at the other end of the gun (breech) is assumed to be zero. Since there is a mass flow into the gun tube, this is not correct for our model. However, the derivation with a velocity at the entrance is much more complicated, and the standard Lagrange distribution is used as a first approximation. Recently more realistic pressure distributions have been studied.[6]

Integrating the momentum equation,

$$p(x) = p_L - (p_R - p_{pj})\frac{M_4}{2M_{pj}}\ \frac{x^2}{{x_R}^2}\ , \tag{21}$$

where x_R is the distance from the tube entrance to the base of the projectile, p_L is the pressure at the gun tube throat, p_R is the pressure at the base of the projectile, M_4 is the mass of the gas in the tube, M_{pj} is the mass of the projectile, and p_{pj} is the resistance pressure. The latter is an input parameter, which takes into account the shot start engraving force and the frictional forces between the projectile and the bore. Evaluating at $x=x_R$ yields

$$p_R = p_L - \frac{M_4}{2M_{pj}}\ (p_R - p_{pj})\ . \tag{22}$$

Integrating from the throat to the projectile base yields

$$p_4 = p_L - \frac{M_4}{6M_{pj}}\ (p_R - p_{pj})\ , \tag{23}$$

where p_4 is the space mean pressure. Then the above two equations can be solved for p_L and p_R.

Eq. (22) and (23) are based on the assumption that the projectile has started to move, creating a pressure differential. If the projectile has not moved, then region 4 is treated as just an extension

of region 3, that is,

$$p_4 = p_R = p_L = p_3 \ . \tag{24}$$

Given the pressure on the projectile, the acceleration equation is

[10] $$\frac{dv_{pj}}{dt} = (p_R - p_{pj})\ A_4\ g_o\ /\ M_{pj} \ . \tag{25}$$

As with the piston, the pressure p_{pj} is only a resistive pressure. If $p_{pj} > p_R$, the projectile does not move. The projectile travel s_{pj} is given by

[11] $$\frac{ds_{pj}}{dt} = v_{pj} \ . \tag{26}$$

The last two differential equations are exactly analogous to region 3. That is,

[12] $$\frac{d\rho_4}{dt} = -\frac{\rho_4}{V_4}\frac{dV_4}{dt} + \frac{m_{34}}{V_4} \ , \tag{27}$$

where ρ_4 is the space mean average density of the gas in region 4, and

[13] $$\frac{dp_4}{dt} = \frac{{c_4}^2}{g_o}\frac{d\rho_4}{dt} + \frac{m_{34}\ (h_{G3} - h_{G4})\ (\gamma - 1)}{V_4 - b\ M_4} \ . \tag{28}$$

The average speed of sound in the tube is

$$c_4 = \sqrt{\frac{g_o\ \gamma\ p_4}{\rho_4\ (1 - b\ \rho_4)}} \ . \tag{29}$$

In early versions of the code, the mass flux into the gun tube was approximated by steady state Bernoulli flow. However, Bernoulli flow assumes an incompressible, isothermal fluid. This is a good

approximation for liquids, but not for gases. A more reasonable assumption is isentropic flow (that is, adiabatic and reversible).[10,11] The gas in the combustion chamber is considered to be stagnant. The gas expands isentropically into the gun tube throat. The expanded gas then mixes with the gun tube gas already present. The process equations for a Noble-Abel equation of state are

$$T\ (1/\rho - b)^{(\gamma-1)} = \text{constant}\ , \tag{30}$$

and

$$p\ (1/\rho - b)^{\gamma} = \text{constant}\ . \tag{31}$$

Assume that $p_t = p_L$. The pressure will equilibrate much more rapidly than the temperature or density. The process equations (30) and (31) can be used to find the throat temperature T_t and density ρ_t. Then the one-dimensional momentum equation can be integrated from the stagnant conditions in the chamber to the throat, resulting in

$$v_t = \sqrt{2g_o\ \{b(p_3 - p_t) + c_p T_t\ [(p_3/p_t)^{(\gamma-1)/\gamma} - 1]}\ , \tag{32}$$

and

$$m_{34} = C_D{}'\ A_4\ \rho_t\ v_t\ . \tag{33}$$

The discharge coefficient $C_D{}'$ is as before an empirical correction for loss terms. Due to lack of better information, this is usually set to one. If the injection velocity approaches the speed of sound, choking may occur. Since all the cases considered so far involve injection velocities well below the speed of sound, a test for choking has not been implemented. It is not really known how good an approximation eqs. (32) and (33) are to the actual flow rate in a gun.

V. VENT OPTIONS

For a lumped parameter model, the details of the shape of the gun system are unimportant. For an in-line gun system all that is needed is the volume of the liquid reservoir and combustion chamber, the liquid and chamber side piston areas, and the vent area between the regions. For each option described below, there is a separate subroutine. Each subroutine reads the input data and, at each time step, calculates the time derivatives of the volumes, the piston acceleration, and the vent area. Because of this modular construction, additional options can be easily added. A number of options have in fact been added and discarded since the first report on this code.

A. VENT1

This option assumes the gun fixture of Fig. 1. The equations have been given in the previous section. The vent area is allowed to vary over time. While there is no physical mechanism that will change the vent area arbitrarily, this capacity in the code makes it easy to study the effects of making any desired changes in vent area. The physically reasonable case of constant vent area is a special case of this option.

A table of vent areas is read in as a function of relative piston travel. The maximum piston travel is calculated to match the initial liquid reservoir volume, and the input table is scaled so the last input piston travel matches the maximum piston travel. The advantage is that in doing parametric studies, the vent area table can be read in using either absolute or relative distances. Linear interpolation is used to determine the vent area for any given piston travel.

The vents may also be considered as valves that require a certain pressure to open. If the liquid pressure is below this input opening pressure, the vent area is zero. It would be more reasonable to open the vents when the pressure difference between the liquid reservoir and

the chamber reached a specified level, but the above has been implemented to allow comparisons with a German code with this vent opening algorithm.[12]

C. VENT2

Recent regenerative guns have been designed with an annular piston (see fig. 2). The piston has a circular hole in the center which surrounds a central rod or bolt. The propellant is stored between the bolt and the piston. The bolt remains fixed as the piston moves. The motion of the piston increases the size of the annular vent, and propellant is forced between the piston and the bolt. The back taper in the bolt decelerates the piston at the end of the stroke.

As before, a table is read in of vent area versus piston travel. The radius of the central bolt is assumed to vary linearly between table entries. The piston is assumed to be infinitely thin (the shape is unimportant for a lumped parameter model). The area A_h of the hole in the center of the piston is read in. These guns often have a grease dyke between the piston and the wall. The piston only touches the chamber walls at the very front. The pressure in the grease dyke is very similar to the chamber pressure. The area A_g of this grease dyke is also read in (if there is no grease dyke, A_g=0).

From this data, the radii of the central bolt and the volume of the reservoir can be computed. As before, the table is scaled to match the initial reservoir volume. Parametric studies varying the bolt shape but keeping the charge weight constant can then be easily performed.

At any given time step, the piston travel is between two input distances x_{i-1} and x_i. The radius of the central bolt is found by linear interpolation

$$r = r_{i-1} + \frac{(s_{ps} - x_{i-1})}{(x_i - x_{i-1})} (r_i - r_{i-1}) \ . \tag{34}$$

The vent area is then given by

$$A_v = A_h - \pi r^2 \ . \tag{35}$$

The rate of change of the volumes must include the central bolt. The derivative of the radius of the bolt under the vent is required

$$\frac{dr}{dt} = v_{ps} \frac{(r_i - r_{i-1})}{(x_i - x_{i-1})} \ . \tag{36}$$

After some algebra

[1]
$$\frac{dV_1}{dt} = -v_{ps} A_1 + \frac{\pi}{3} [v_{ps} (r^2 + r\, r_{i-1} + r_{i-1}^2) + (s_{ps} - x_{i-1}) (2r + r_{i-1}) \frac{dr}{dt}] \ . \tag{37}$$

Similarly,

[6]
$$\frac{dV_3}{dt} = v_{ps} A_3 - \frac{\pi}{3} [v_{ps} (r^2 + r\, r_{i-1} + r_{i-1}^2) + (s_{ps} - x_{i-1}) (2r + r_{i-1}) \frac{dr}{dt}] \ . \tag{38}$$

The piston acceleration is given by

[2]
$$\frac{dv_{ps}}{dt} = \frac{g_o}{M_{ps}} [p_3 (A_3 - A_h - A_g) - (p_1 + p_{ps}) (A_1 - A_h)] \ . \tag{39}$$

The acceleration on the piston no longer depends on the vent area. The

other governing equations are unchanged.

VENT3.

The above option is useful for parametric studies involving a concept VI gun. If an actual gun fixture is to be modeled, a slightly different interpretation is more useful.

The same data as for the VENT2 option are read in. The piston travels are now interpreted as absolute numbers. The piston is assumed to take up a definite volume, although the exact shape is still unimportant. The initial liquid volume has previously been read in. (The liquid volume can be measured, or computed using the specifications for the piston and bolt). The code then computes how far the piston must move to inject the appropriate volume of propellant. This is taken as the maximum piston travel. The piston is assumed to hit the back wall at this point, and injection ceases. This is not absolutely correct, since the piston will normally hit the back wall while there is still a small amount of liquid between the piston and the bolt, but the errors will be small, and the behavior at the end of the injection stroke has very little effect on performance. The governing equations are now exactly the same as in the VENT2 option.

An additional option has been added. Early models of the concept VI gun, such at the one at BRL, have a movable block at the end of the liquid reservoir mounted on Belleville springs. The injection area between the piston and the bolt is originally sealed by an O-ring. As the combustion chamber pressurizes, the liquid pressure rises. But since the liquid is almost incompressible, it is difficult to move the piston enough to open the vent. So the block moves backward and allows the piston to clear the O-ring and begin the injection process. Later gun fixtures use a metal-to-metal seal instead of the O-ring and do not require a movable block. But in order to model the BRL gun fixture, a Belleville spring option is included.

A table is read in of the distance the block moves versus the force exerted by the Belleville springs. For the BRL system, this has been measured. The last entry in the table is the maximum distance the block can move before the springs bottom out. The area and mass of the block are also read in. Two additional ordinary differential equations to describe the block motion are required

$$[B1] \qquad \frac{dv_{bk}}{dt} = \frac{g_o}{M_{bk}} (p_1 A_{bk} - f_{bk}) , \qquad (40)$$

and

$$[B2] \qquad \frac{ds_{bk}}{dt} = v_{bk} , \qquad (41)$$

where s_{bk} is the block travel, v_{bk} is the block velocity, A_{bk} is the block area, M_{bk} is the block mass, and f_{bk} is the force exerted on the block by the Belleville springs. When the springs bottom out, the block velocity is set equal to zero. The only other equation that needs to be changed is for the liquid reservoir volume

$$[1] \qquad \frac{dV_1}{dt} = \ldots + v_{bk} A_{bk} . \qquad (42)$$

VI. PISTON RESISTANCE OPTIONS

As the piston moves, there is frictional resistance between the piston and the chamber walls. There is no good estimate for the size of this frictional resistance. Because of the large pressures involved and the relatively slow speed of the piston, this effect is not expected to be important. Nevertheless, piston resistance options are included so the effects of friction can be studied. Only one option is presently in the code.

A. PIS1

The resistance is considered to be solely a function of piston travel. A table of piston travel versus resistive pressures is read in. The table will be normalized to the maximum piston travel. The piston resistive pressure p_{ps} at any given piston travel s_{ps} is found by interpolation. The actual resistive force is $p_{ps} A_1$. An equivalent pressure is read in rather than the actual force to make it easier to compare the braking force exerted by friction with the braking force exerted by the liquid pressure.

VII. PROJECTILE RESISTANCE OPTIONS

Similarly, as the projectile moves, there is friction between the projectile and the gun tube. More important is the shot start pressure. The projectile is restrained from moving until the pressure at its base reaches an appropriate value. The choice of shot start pressure can have a large effect on performance and on the maximum pressures in the gun. At present there is only one option.

A. PROJ1

As with the piston, a table of projectile travel versus resistive pressure is read in. The table is not normalized, since the maximum projectile travel is always known (input parameter). The resistive pressure p_{pj} for any given projectile travel s_{pj} is found by interpolation. If s_{pj} is larger than the last table entry for travel, the last table entry for pressure is chosen. The actual resistive force is $p_{pj} A_4$. The first entry in the table is the shot start pressure. The projectile will not move until the chamber pressure reaches the shot start pressure.

VIII. DISCHARGE COEFFICIENT - INTO CHAMBER

The discharge coefficients needed in equation (9) are input parameters.

A. DIS1

A table of piston travel versus discharge coefficient is read in. The table is normalized to the maximum piston travel. The discharge coefficient C_D for any given piston travel s_{ps} is found by interpolation.

IX. DISCHARGE COEFFICIENT - INTO GUN TUBE

The discharge coefficients needed in equation (33) are input parameters.

A. DIS1

A table of projectile travel versus discharge coefficient is read in. The discharge coefficient C_D' for any given piston travel s_{pj} is found by interpolation.

X. MASS FLUX OPTIONS - INTO CHAMBER

A. FLUX1

Steady state Bernoulli flow is assumed. The mass flux m_{13} is computed using equations (9). This routine also reads in the number of vent holes (there is more than one hole only for the first gun design). The routine computes the Weber number, the Reynold's number, and the third Lagrange number. These quantities are expected to effect the behaviour of the injection. While this code does not use these numbers, they are printed out as additional information about the injection

process.

B. FLUX2

Since the gun environment is highly transient, steady state flow may not be a good approximation. A transient model for injection has been developed (gun design 2).[4,13] The basic assumption is that the space derivative of the mass flux ρvA of the fluid in the reservoir is zero. Then the one-dimensional momentum equations can be integrated from the back wall to the vent with the result

$$\text{[F1]} \qquad \frac{d(\rho vA)}{dt} = [0.5\ \rho_1\ (v_{ps}^2 - v_3^2) + g_o C_D^2 (p_1 - p_3) / \int dx/A \qquad (43)$$

The integral of the inverse of the cross sectional area is approximated assuming a simplified piston shape. This additional ordinary differential equation is integrated to obtain the mass flux rate into the chamber. This equation shows a very rapid rise to steady state.

C. FLUX3

Heiser[12] has used a transient injection model more appropriate for the first gun design. Only the flow in the holes in the piston is considered; the liquid in the actual reservoir is considered a stagnant source. The result is an ordinary differential equation

$$\text{[F1]} \qquad \rho_1\ L \frac{dv_3}{dt} = g_o\ (p_1 - p_3) - 0.5\ \rho_1 \frac{v_3^2}{C_D^2}\ . \qquad (44)$$

The piston thickness L must be read in. This option was implemented to allow comparisons with the code developed by Heiser.

XI. MASS FLUX OPTIONS - INTO GUN TUBE

A. FLUX1.

Steady state isentropic flow is assumed. The mass flux into the gun tube is computed using eq. (32) and (33).

B. FLUX2

Steady state isentropic flow is still assumed. However, the entrance velocity v_t is considered known. This is calculated based on the assumed pressure distribution in the gun tube (see gun tube options TUBE3 and TUBE4). The governing equation (32) is solved for p_L using Newton-Raphson iteration.

XII. GUN TUBE PRESSURE DISTRIBUTION OPTIONS

Recently a number of different assumptions for the gun tube pressure distribution were implemented and tested against a one-dimensional code. The results will be published in an upcoming BRL report,[6] so the details are not included here. A brief description of the options presently in the code is included.

A. TUBE1

The standard Lagrange pressure distribution is assumed, that is, the density is constant in the tube, which implies that the velocity is linear. For the purpose of computing the pressure distribution, the entrance velocity v_t is set equal to zero. The momentum equation is integrated to obtain a formula for the pressure p(x) in the tube. The pressure p_R at the base of the projectile and the pressure p_L at the gun tube throat are computed using eq. (22) and (23). Since v_t will become large, this is not a very good approximation. However, for low performance guns with a relatively short gun barrel it is still

accurate.

B. TUBE2

The velocity v_t is allowed to be non-zero, but the time derivative of v_t is set to zero. The two equations for pressure are somewhat more complicated, and must be solved simultaneously with the equation for isentropic flow (32). The three equations are solved iteratively to obtain values for v_t, p_L, and p_R.

Since v_t does vary rapidly during the injection cycle, this approximation is still not very accurate. However, it is much more reasonable than simply ignoring the entrance velocity, and will predict performance much more accurately for high performance cases.

C. TUBE3

The term for the time derivative of v_t is left in the pressure equations. An additional ordinary differential equation for v_t is derived from the two pressure equations. The equation for steady state isentropic flow is solved for p_L (see FLUX2, gun tube injection options). Then p_R and the time derivative of v_t can be found from the pressure equations.

This is quite accurate until the point when the liquid propellant burns out (end of stroke). At this point the one-dimensional model shows a rarefaction wave moving toward the projectile. Both velocity and pressure profiles show a sharp slope break at the wave front.

There is an option to model this wave. At the end of piston stroke the code assumes that a rarefaction wave begins to move down the gun tube. The velocity of the wave is the speed of sound relative to the fluid. The fluid velocity is assumed to be bi-linear, with a knot point at the wave front. The fluid in front of the wave does not know

that burnout has occured. So the fluid velocity at the wave front is found by linearly interpolating between the throat velocity at burnout and the present projectile velocity. After much more algebra, the desired quantities can still be computed. The approximation is still fairly crude. But just assuming the velocity profile is bi-linear with a knot point at about the right location gives very good agreement after burnout with the one-dimensional model.

D. TUBE4

The primary error in the above approximation is due to the assumption that the density is constant in the gun tube. The one-dimensional model shows rather large changes in density, especially as the projectile moves further down the gun tube. So the assumption is made that the density profile is linear (after burnout, bi-linear). The velocity profile can still consistently be taken to be linear. The resulting model has very complicated algebra. However, the agreement with the one-dimensional model is extremely good.

XIII. PRIMER OPTIONS

In present liquid propellant guns, a solid primer is used. The primer injects hot gas into the combustion chamber to begin the firing cycle. The exact details of the primer model have only a small effect on pressure, so simplifications have been made. First, the primer is assumed to be the same material as the liquid propellant, to save having to read in a new set of properties for the actual solid primer. The three primer options then offer varying levels of simplification.

A. PRIM1

It is assumed that the primer completely combusts before the start of the calculation, pressurizing the chamber. The piston movement is ignored. The code computes how much propellant would be necessary to

create the input chamber pressure, and records this as the primer weight.

B. PRIM2

The initial mass of the primer is read in. Then the primer is distributed in the chamber as liquid droplets. A droplet burning option must be chosen (see below). The size of the droplets is determined from the drop diameter in the droplet burning option. This option can be used to mimic the delay in time to reach the primer pressure.

C. PRIM3

The primer is now considered to be out of the chamber. The mass of the primer and the injection time are read in. The primer is then injected at a steady rate over the desired injection time. The primer is assumed to combust instantaneously as it enters the chamber. During the injection process, the chamber density and pressure equations are modified

[7] $$\frac{d\rho_3}{dt} = \ldots + \frac{m_{p3}}{V_3} \tag{45}$$

[8] $$\frac{dp_3}{dt} = \ldots + \frac{m_{p3}\ (e_1 - h_{G3})\ (\gamma - 1)}{V_3 - b\ M_3} \tag{46}$$

where m_{p3} is the mass flux of primer into the chamber. This option was added to facilitate comparisons with the code developed by Heiser.[12]

XIV. GUN TUBE HEAT LOSS OPTIONS

In gun systems there is a large energy flux from the hot gas to the gun tube. This is important for actual systems primarily because it

causes erosion of the gun tube. The effect on muzzle velocity and pressure is on the order of a few percent. Heat loss is often treated as an adjustable parameter for fine tuning a model to agree with experiment.

A. HEAT1

The heat loss to the gun tube walls is ignored. This causes a slight increase in muzzle velocity and maximum pressures.

B. HEAT2

The gun tube temperature T_w and a heat loss factor are read in. The gun tube temperature is assumed to remain constant (infinite sink). On the short time scale of the ballistic event, the tube wall will heat up, but treating the heat flux into the solid makes the problem much more complicated. Then the heat loss can be represented as

$$Q_w = 4\ h_w\ (T_4 - T_w)\ /\ d_4\ , \qquad (47)$$

where T_4 is the space mean temperature in the tube, d_4 is the diameter of the tube, h_w is the heat transfer coefficient, and Q_w is the heat loss.[14] The variation of temperature in the gun tube is ignored. The difficulty is in computing the heat loss coefficient. In the code the correlation of Sieder and Tate for pipe flow is used. This assumes fully developed flow in a smooth pipe with a nearly constant wall temperature. For highly turbulent flow,

$$h_w = (k/d_4)\ 0.026\ Re^{0.8}\ Pr^{1/3}\ (\mu/\mu_w)^{0.14} \qquad (48)$$

where k is the thermal conductivity of the gas, Re is the Reynold's number, Pr is the Prandtl number, and μ is the viscosity. The correlation is for steady state flow, while the gun conditions are

highly transient. More important, the correlation has been found accurate for Reynold's numbers up to about 10^5. Reynold's numbers in the gun tube can be two orders of magniture higher.

If a HAN based propellant is completely burned, it will form a mixture of CO_2, H_2O, and N_2. Procedures have been developed to find the viscosity and thermal conductivity of a mixture of gases.[15] The procedures were developed for the low density limit. Fortunately, for high temperatures, the low density limit is very accurate even for very high pressures.[14] Fits were made for the viscosity and thermal conductivity of the gases resulting from HAN1845 between 1500K and 3500K. Values for other HAN based propellants are almost the same. A separate low temperature fit was made to determine the viscosity at the gun tube wall μ_w. The Reynold's number is given by

$$Re = \frac{\rho \ v \ d_4}{\mu} , \tag{49}$$

where ρv is the space mean average over the gun tube. The Prandtl number is given by

$$Pr = \frac{c_p \ \mu}{k} . \tag{50}$$

The equation for the space mean pressure is modified by

$$[13] \qquad \frac{dp_4}{dt} = \ldots - \frac{Q_w \ (\gamma - 1)}{(1 - b \ \rho_4)} \tag{51}$$

Simulations run so far indicate a heat loss of 3% to 5% for 120mm guns, and 10% to 12% for 30mm guns. These numbers are in the range reported by Nordheim, Soodak, and Nordheim[16] for their analysis of experimental data, and comparable with the heat loss normally used in solid

propellant gun modeling. In solid propellant gun modeling, the heat loss is often modified to improve agreement between model and experiment. The heat loss factor read in above multiplies eq. (51), and can be used to adjust the heat loss up or down.

XV. CHAMBER HEAT LOSS OPTIONS

It is not known whether heat loss in the combustion chamber is important. The surface area of the chamber and central bolt are relatively large, and the gas velocity past the chamber walls is unknown. To model the possible effects of heat loss in the chamber, a totally empirical formula is implemented.

A. HEAT1

There is no heat loss to the combustion chamber walls.

B. HEAT2

The combustion chamber wall temperature T_c is read in. The heat loss is assume to be determined by

$$Q_c = h_c (T_3 - T_c) / V_3 . \qquad (52)$$

Note that the heat transfer coefficient h_c has different units than h_w. Since the flow in the chamber is recirculation flow rather than pipe flow, a correlation based on the diameter of the chamber is inappropriate. Since there is no way to estimate h_c without knowing the flow pattern in the chamber, a table of heat transfer coefficient versus piston travel is read in. The heat transfer coefficient for any given piston travel is found by interpolation. The equations for chamber pressure is modified by

$$[8] \qquad \frac{dp_3}{dt} = \ldots - \frac{Q_c\ (\gamma - 1)}{(1 - b\ \rho_3)} . \tag{53}$$

The effect of heat loss can now be studied, but the size of the heat loss is totally arbitrary.

XVI. AIR SHOCK

The projectile will compress the air in the tube as it accelerates. This will have a minor effect on the velocity of the projectile.

A. SHOCK1

The resistance due to the air shock in front of the projectile is ignored.

B. SHOCK2

Corner[5] developed a formula for the air shock based on the Rankine-Hugoniot relations. The initial pressure p_a and temperature T_a of the air are read in. The molecular weight of the air and the ratio of specific heats are read in. The specific gas constant R_a is calculated (universal gas constant divided by molecular weight). Then the resistance pressure p_s is given by

$$\frac{p_s}{p_a} = 1 + \frac{(\gamma+1)\ {v_{pj}}^2}{4\ g_o\ R_a\ T_a} + \frac{v_{pj}}{(g_o\ R_a\ T_a)^{0.5}} \left[\gamma + \frac{(\gamma+1)^2\ {v_{pj}}^2}{16\ g_o\ R_a\ T_a}\right]^{0.5} . \tag{54}$$

This new resistance pressure p_s is just added on to the frictional resistance pressure p_{pj}.

XVII. BUFFER OPTIONS

More recent gun fixtures use a water buffer to slow up the piston at the end of stroke rather than a taper on the central bolt. This option was implemented, but has not been checked carefully against an actual fixture. Some changes may need to be made to the idealization.

A. BUFF1

There is no buffer.

B. BUFF2

When the piston moves back, it enters a chamber filled with liquid. The piston pressurizes the chamber, which then slows down the piston. The buffer fluid eventually is forced from the chamber to ambient conditions.

The area of the piston that enters the buffer is read in, as well as the area of the exit holes and the discharge coefficient. The initial volume and pressure of the buffer must be entered, as well as the bulk modulus coefficients and the density at atmosphric pressure. Three additional ordinary differential equations are required for the buffer volume, density, and pressure.

The buffer fluid is treated as an adiabatic isothermal fluid like the propellant in the reservoir. The speed of sound is determined analagously to eq. (6) and the mass flow out of the buffer by steady state Bernoulli flow (eq. (9)). The new differential equations are

[B1] $$\frac{dV_{bf}}{dt} = - v_{ps} A_{bf} , \qquad (55)$$

where V_{bf} is the volume of the buffer and A_{bf} is the area of the piston that enters the buffer volume. The density equation is

$$[B2] \qquad \frac{d\rho_{bf}}{dt} = - \frac{\rho_{bf}}{V_{bf}} \frac{dV_{bf}}{dt} - \frac{m_{bf}}{V_{bf}} , \qquad (56)$$

where ρ_{bf} is the density, and m_{bf} is the mass flux out of the buffer. The pressure equation is

$$[B3] \qquad \frac{dp_{bf}}{dt} = \frac{c_{bf}^2}{g_o} \frac{d\rho_{bf}}{dt} , \qquad (57)$$

where p_{bf} is the pressure in the buffer and c_{bf} is the speed of sound. The piston velocity equation is modified by

$$[2] \qquad \frac{dv_{ps}}{dt} = \ldots - \frac{g_o}{M_{ps}} p_{bf} A_{bf} . \qquad (58)$$

XVIII. REPEAT OPTIONS

In systems studies, there is often a physical constraint on the class of acceptable solutions. Two common constraints are implemented in the code. The code will integrate repeatedly until the constraints are satisfied.

A. REP1

The code integrates once. This is the standard option.

B. REP2

A solution is sought with a given maximum liquid pressure. The liquid pressure is adjusted by changing the vent area (or areas). The

desired liquid pressure and a first guess for the vent increment is read in.

The problem is first integrated with the input conditions. If the maximum liquid pressure is too low, the first vent area is incremented by the input value. The other vent areas in the table are changed proportionally. If the liquid pressure is too low, the vent areas are decremented. Once values are obtained both above and below the desired maximum liquid pressure, interpolation is used to obtain the new set of vent areas. Convergence normally occurs after a small number of integrations.

C. REP3

A solution is sought with a given muzzle velocity. The muzzle velocity is adjusted by changing the charge weight (initial reservoir volume). The desired muzzle velocity and a first guess for the reservoir volume increment is read in. The same iteration procedure is used to find the initial reservoir volume that gives the requested muzzle velocity.

XIX. CHAMBER PRESSURE OPTIONS

It is convenient to isolate part of the model for study. When comparing the model against experimental data, small differences will become large quickly. For instance, suppose that the chamber pressure is slightly high. This will accelerate the piston more and increase the rate of injection of the propellant. The propellant burns, and increases the pressure rise in the chamber. So to study the liquid injection process, it is better to disconnect the chamber pressure from the injection.

A. CHAM1

The chamber pressure is computed using the usual equations.

B. CHAM2

The experimental chamber pressure versus time is read in. At each time step, an interpolated experimental chamber pressure overwrites the pressure computed using the ordinary differential equations. This allows a study of the injection process using the experimental data as a boundary condition.

XX. DROPLET BURNING OPTIONS

So far the liquid has been assumed to combust instantaneously upon entering the combustion chamber. There is evidence, however, that liquid accumulates in the combustion chamber. So simple rules for the formation and combustion of droplets in the combustion chamber are derived.

The behavior of the liquid as it enters the combustion chamber is very complicated. A liquid jet is formed in the chamber. After some time, the jet will break up into droplets, ligaments, or slugs. The jet may impinge upon the walls of the chamber. At present, there is no way of predicting the behaviour of the jet. In the model, the liquid is assumed to instantaneously form droplets of fixed size as the liquid enters the combustion chamber. The droplets will then combust at some given rate. The initial size of the droplets is an input parameter. This simplified model has no basis in reality, except to allow the code to determine the effects of liquid accumulation.

In the earlier version of the code, there was an option to allow the droplets to decrease in size as combustion proceeded. But since the initial droplet size is arbitrary, this did not really improve the model. To simplify the code, this option was removed. The droplet size is assumed to be uniform with respect to space. However, the droplet

size may vary over time.

The derivation of the relevant equations is very similar to the previous report. Let M_{L3} be the liquid mass in region 3, V_{L3} be the liquid volume, M_{G3} be the gas mass, and V_{G3} be the gas volume. Then

$$\rho_{L3} = \frac{M_{L3}}{V_{L3}} , \tag{59}$$

and

$$\rho_{G3} = \frac{M_{G3}}{M_{L3}} , \tag{60}$$

where ρ_{L3} is the density of the liquid and ρ_{G3} is the density of the gas. Define the porosity

$$\epsilon_3 = \frac{V_{G3}}{V_3} . \tag{61}$$

Then

$$\rho_3 = \frac{M_3}{V_3} = (1 - \epsilon_3)\ \rho_{L3} + \epsilon_3\ \rho_{G3} \tag{62}$$

Following eq. (6), the speed of sound in the liquid is

$$c_{L3} = \sqrt{g_o\ K\ /\ \rho_{L3}} , \tag{63}$$

and following eq. (15) the speed of sound in the gas is

$$c_{G3} = \sqrt{\frac{g_o\ \gamma\ p_3}{\rho_{G3}\ (1 - b\ \rho_{G3})}} \tag{64}$$

After some manipulation, the speed of sound c_3 in the mixture is given

by

$$c_3 = \sqrt{\frac{1}{\rho_3} \left[\frac{1}{\epsilon_3/(\rho_{G3}\, c_{G3}{}^2) + (1 - \epsilon_3)/(\rho_{L3}\, c_{L3}{}^2)} \right.} \quad . \tag{65}$$

The enthalpy of the liquid is

$$h_{L3} = e_1 + p_3 \;/\; \rho_{L3} \;, \tag{66}$$

where e_1 is the chemical energy of the liquid, and the enthalpy of the gas is

$$h_{G3} = c_p\; T_3 + b\; p_3 \;. \tag{67}$$

Let m_3 be the rate at which the liquid in region 3 is combusting and forming the final gas products.

The thirteen equations derived in Section III are the same except for the energy equations [8] and [13]. The equation from the previous report is written in a more general fashion to make it easier to apply to different gun systems.

[8]

$$\frac{dp_3}{dt} = \frac{\rho_3\; c_3{}^2}{g_o\; V_3} \left(- \frac{dV_3}{dt} + \frac{m_{L3}}{\rho_{L3}} + \frac{m_{G3}}{\rho_{G3}} + \frac{S_3\; g_o\; (\gamma - 1)}{q_{G3}\; c_{G3}{}^2\; (1 - b\; \rho_{G3})} \right) , \tag{68}$$

where m_{L3} is the rate of production of liquid: in this case,

$$m_{L3} = m_{13} - m_3 - m_{34} \frac{M_{L3}}{M_3} \;, \tag{69}$$

and m_{G3} is the rate of production of gas,

$$m_{G3} = m_3 - m_{34} \frac{M_{G3}}{M_3} + m_{p3} , \tag{70}$$

and S_3 is the rate of production of mass times the change in enthalpy

$$S_3 = m_3 (h_{L3} - h_{G3}) + m_{13} (h_{L1} - h_{L3}) + \tag{71}$$

$$m_{p3} (e_1 - h_{G3}) .$$

If there is heat loss in the chamber, the modification term from eq. (53) is added on.

In the gun tube, the equations are exactly analogous. The only difference is in the coefficients for the pressure equation

[13]
$$\frac{dp_4}{dt} = \frac{\rho_4 c_4^2}{g_o V_4} \left(- \frac{dV_4}{dt} + \frac{m_{L4}}{\rho_{L4}} + \frac{m_{G4}}{\rho_{G4}} + \frac{S_4 g_o (\gamma - 1)}{q_{G4} c_{G4}^2 (1 - b \rho_{G4})} \right) . \tag{72}$$

In the gun tube

$$m_{L4} = - m_4 + m_{34} \frac{M_{L3}}{M_3} , \tag{73}$$

$$m_{G4} = m_4 + m_{34} \frac{M_{G3}}{M_3} , \tag{74}$$

$$S_4 = m_4\ (h_{L4} - h_{G4}) + m_{34}\ (h_{L3} - h_{L4})\ \frac{M_{L3}}{M_3} + \qquad (75)$$

$$m_{34}\ (h_{G3} - h_{G4})\ \frac{M_{G3}}{M_3}\ .$$

If there is heat loss in the gun tube, the modification term from eq. (51) is added on.

To complete the system, ordinary differential equations are required to determine the liquid density and mass in the regions. The corresponding gas quantities can be easily derived. The basic assumption is that the pressure in the liquid and the gas in a given region is the same. Since the gas pressure is known, the liquid equation of state can be written in differential form as

[14] $$\frac{d\rho_{L3}}{dt} = \frac{g_o}{{c_{L3}}^2}\ \frac{dp_3}{dt}\ , \qquad (76)$$

and

[16] $$\frac{d\rho_{L4}}{dt} = \frac{g_o}{{c_{L4}}^2}\ \frac{dp_4}{dt}\ . \qquad (77)$$

The mass conservation equations for the liquid have already been derived

[15] $$\frac{dM_{L3}}{dt} = m_{L3}\ , \qquad (78)$$

and

[17] $$\frac{dM_{L4}}{dt} = m_{L4}\ . \qquad (79)$$

To close the system, the rate at which the liquid droplets are combusting must be known. The rate of surface regression is assumed to be of the form

$$\text{rate of surface regression} = Ap^B \ . \tag{80}$$

Liquid propellant burning rates have been measured by McBratney[16,17]. The rate of combustion

$$m_3 = \rho_{L3} \ S \ Ap^B \ . \tag{81}$$

where S is the total surface area of the droplets in a region. All the droplets are assumed to have a constant diameter d. So the total surface area in the region

$$S = 6 \ V_{L3} \ /d \ . \tag{82}$$

and eq. (81) can be written as

$$m_3 = M_{L3} \ (6/d) \ Ap_3{}^B. \tag{83}$$

For region 4, the pressure is no longer constant over the region, but follows the Lagrange pressure distribution. But this would be quite complicated to keep track of, and very little liquid goes into region 4 for most problems. So the combustion rate is assumed to depend on the average pressure p4, and

$$m_4 = M_{L4} \ (6/d) \ Ap_4{}^B. \tag{84}$$

The droplet options can now be described.

A. DROP1

The liquid is assumed to combust instantaneously as soon as it

enters the combustion chamber. This is the model described in section III.

B. DROP2

The liquid enters the combustion chamber and instantaneously froms droplets of diameter d. The size of the droplets is fixed in time and space. As the droplets burn, the number of droplets may decrease, but the size of the droplets remains unchanged.

The droplet diameter and the burning rate coefficients are read in. There is some evidence that the burning rate for liquid monopropellants has a sharp slope break around 100 MPa. So the burning rate is read in as two fits, and the pressure is read in at which the change is made from the low pressure rate to the high pressure rate.

C. DROP3

The droplet size is fixed in space, but not in time. A table of droplet diameters versus piston travel is read in. As usual, the table is scaled to the maximum piston travel.

While this model is unrealistic, it allows the modeling of various accumulation rates at different times in the firing cycle.

XXI. MASS AND ENERGY BALANCE

As a check on the equations derived, both mass and energy should be conserved. The mass balance is straightforward.

$$M_T = M_1 + M_{L3} + M_{G3} + M_{L4} + M_{G4} + M_p \tag{85}$$

where M_p is the mass of the primer and M_T is the total mass of the propellant and primer. M_T should be constant throughout the

integration.

The energy balance is more complicated. The liquid is considered to be an isothermal fluid, and its internal energy e_1 is just the chemical energy of the propellant. The total energy in region 1 is

$$E_1 = e_1 M_1 \ . \tag{86}$$

If the outside primer option is chosen (PRIM3) then

$$E_p = e_1 M_p \ . \tag{87}$$

The internal energy of the liquid in region 3 is given by

$$E_{L3} = e_1 M_{L3} \ , \tag{88}$$

and the internal gas energy is

$$E_{G3} = c_v T_3 M_{G3} \ . \tag{89}$$

Similarly for region 4

$$E_{L4} = e_1 M_{L4} \ , \tag{90}$$

and

$$E_{G4} = c_v T_4 M_{G4} \ . \tag{91}$$

The kinetic energy of the piston is given by

$$EK_{ps} = 0.5 M_{ps} v_{ps}^2 / g_o \ , \tag{92}$$

and the kinetic energy of the projectile by

$$EK_{pj} = 0.5\ M_{pj}\ v_{pj}^2\ /\ g_o\ . \tag{93}$$

The liquid and gas in region 4 are moving, and are assumed to have the same velocity. The kinetic energy of the liquid is

$$EK_{L4} = 0.5\ M_{L4}\ v_{pj}^2\ x_R\ /(3g_o)\ , \tag{94}$$

where x_R is the distance from the entrance to the gun tube to the base of the projectile. The kinetic energy of the gas is

$$EK_{G4} = 0.5\ M_{G4}\ v_{pj}^2\ x_R\ /(3g_o)\ . \tag{95}$$

The fluid in the combustion chamber is considered stagnant. When the fluid enters the gun tube, it instantaneously acquires kinetic energy. To keep the energy balanced, the enthalpy of the liquid in the gun tube is redefined as

$$h_{L4} = e_1 + p_4\ /\ \rho_{L4} + EK_{L4}\ /\ M_4\ , \tag{96}$$

and the enthalpy of the gas in the gun tube is

$$h_{G4} = c_p\ T_4 + b\ p_4 + EK_{G4}\ /\ M_4\ . \tag{97}$$

The heat loss to the chamber and gun tube is energy that leaves the system. The total energy loss is approximated by finite differences. The code is set up to print out information at designated time intervals. After each time interval, the heat loss from the chamber is approximated by

$$EH_3(t) = EH_3(t_o) + Q_c\ V_3\ (t - t_o)\ , \tag{98}$$

where Q_c and V_3 are averages of the values at the present time t and the old time t_o. Similarly

$$EH_4(t) = EH_4(t_o) + Q_w V_4 (t - t_o) . \tag{99}$$

The energy lost through friction is approximated in a similar fashion. The energy lost is equal to force times distance, or

$$EF_{ps}(t) = EF_{ps}(t_o) + p_{ps} A_3 (s_{ps}(t) - s_{ps}(t_o)) , \tag{100}$$

for the piston and

$$EF_{pj}(t) = EF_{pj}(t_o) + p_{pj} A_4 (s_{pj}(t) - s_{pj}(t_o)) , \tag{101}$$

for the projectile.

Then the total energy of the system is

$$E_T = E_{L1} + E_p + E_{L3} + E_{G3} + E_{L4} + E_{G4} + EK_{ps} + \tag{102}$$

$$EK_{pj} + EK_{L4} + EK_{G4} + EH_3 + EH_4 + EF_{ps} + EF_{pj} .$$

This should be constant throughout the integration.

XXII. NUMERICAL METHOD

Because of the length (over 100 pages) the code listing is not given. Appendix A gives comments from the beginning of the code. This is a complete description of the input options and the notation actually used in the code for the input variables. A copy of the code is available from the author on request.

The ordinary differential equations derived above are solved using EPISODE.[19] This is a robust and efficient code for the solution of ordinary differential equations. EPISODE proper consists of the subroutines DRIVE to SING. A few minor changes have been made in in the subroutines DRIVE and TSTEP.

The subroutine DRIVE controls the integrator. The error control is defined in DRIVE, based on the input error bound EPS. Originally the error control could be either relative or absolute. A relative error control can be wasteful if some of the quantities being integrated become negligably small. However, an absolute error control is inaccurate if the quantities integrated vary widely in magnitude. A solution to this problem was developed during work on integrating chemical kinetics networks, where the concentrations of species differ by many orders of magnitude.[20] This is a semi-relative error control. If the quantities are above some cutoff value (SREC) a relative error control is used. If they are below SREC, an absolute error control is used. While an absolute error control would be adequate for the simpler equations now being considered, the semi-relative error control has been left in the code. SREC has normally been chosen three orders of magnitude smaller than EPS.

Also in DRIVE are various error messages. Among other things, the code prints out a warning if the time step size must be decreased dramatically to meet the error criterion. But in the gun code there are several discontinuities. For example, when the chamber pressure first exceeds the shot start pressure, the ordinary differential equations for the projectile motion are suddenly changed. The code normally has to cut back on the time step to integrate through this and similar changes. The normal warning messages are suppressed unless the write option is turned on (KWRITE=1).

The routine TSTEP actually takes the integration steps. A number of tests have been implemented here. For example, Eq. [4] for the volume of the liquid reservoir becomes singular as V_1 approaches zero. So when V_1 becomes less then the initial volume divided by a thousand, the region is closed. That is, region 1 is ignored in the integration from then on. The error resulting from ignoring the small amount of remaining propellant is negligable. If V_1 becomes negative, the time

step was too large, and it must be reduced and the time step taken over. There is a similar problem with region 4, since the projectile may start at the throat, and V4 will be zero. In this case region 4 starts out as closed. When the projectile is at least .1 cm. down the gun tube, the region is opened. Before this, region 4 is considered as an extension of region 3. Also, diagnostic printouts of the quantities of interest may be made after each time step (KWRITE=1).

There are two main integration routines included in EPISODE. The first is the Adams method, suitable for non-stiff problems (METH=1). The second is the backward differentiation method, suitable for stiff problems (METH=2). We have normally used METH=2. However, the governing equations are not very stiff, and METH=1 can also be used. The run times are about equivalent for the two methods.

There are also several methods for the nonlinear system solution required at each step of the integration. We have used the Newton method with an internally computed finite difference approximation to the Jacobian. So the only subroutine that needs to be supplied by the user is DIFFUN. Given a set of values for the unknowns, DIFFUN computes the time derivatives of the unknowns.

Subroutine DIFFUN in this case only calls one of two possible subroutines (FDROP1 or FDROP2). These routines correspond to the instantaneous burning option and the droplet burning option. Since the governing equations are different, it is easier to set these up as separate subroutines.

The main routine RLGD reads in the input data. Initial values are assigned in INITAL. The subroutine INTEG actually calls the integrator DRIVE. If a repeat option has been specified, INTEG will reset the initial conditions and repeat until convergence has occured.

Most of the subroutines are for the different options. To make it

easier to add or change options, some of the input is in separate subroutines. For instance, subroutines VENT1, VENT2, and VENT3 read in the required data for the three vent options. These routines also compute the vent area for a given piston travel. So if a new vent option is desired, it is only necessary to add a new subroutine and change the few lines that call the VENT subroutines. The subroutines for the other options are set up similarly.

Subroutines CAPTION and OUT control the output files. Subroutine OUTGRA creates a graphics file, so that any of the quantities computed may later be graphed.

XXIII. BRL 3ՐMM GUN FIXTURE

A set of experimental measurements have been made on a 30mm regenerative liquid propellant gun at the BRL.[21,22] The liquid reservoir pressure, combustion chamber pressure, piston travel, and projectile velocity have been measured. The data has been filtered to remove the acoustic oscillations. A number of cases have been measured for a 2/3 charge and a 1/3 charge. The gun has not been fired with a full charge. The injection thickness of the annular jet has not been optimized, and the performance of the gun is low. In this paper only one experiment will be considered (Round 8, 2/3 charge).

Figure 3 shows a scale model drawing of the liquid reservoir before firing. The piston is flush against a crash ring in the combustion chamber (not shown). The crash ring is for protection in case of a piston reversal. An O-ring initially seals the liquid reservoir. The block should be exactly at the end of the back taper of the central bolt. However, when the fixture is assembled, the block actually protudes about an eighth of the inch forward.[23] When the liquid propellant is loaded, the reservoir is presurized to 7 MPa. This is enough to push the block back, so the block will be only slightly forward of the back taper.

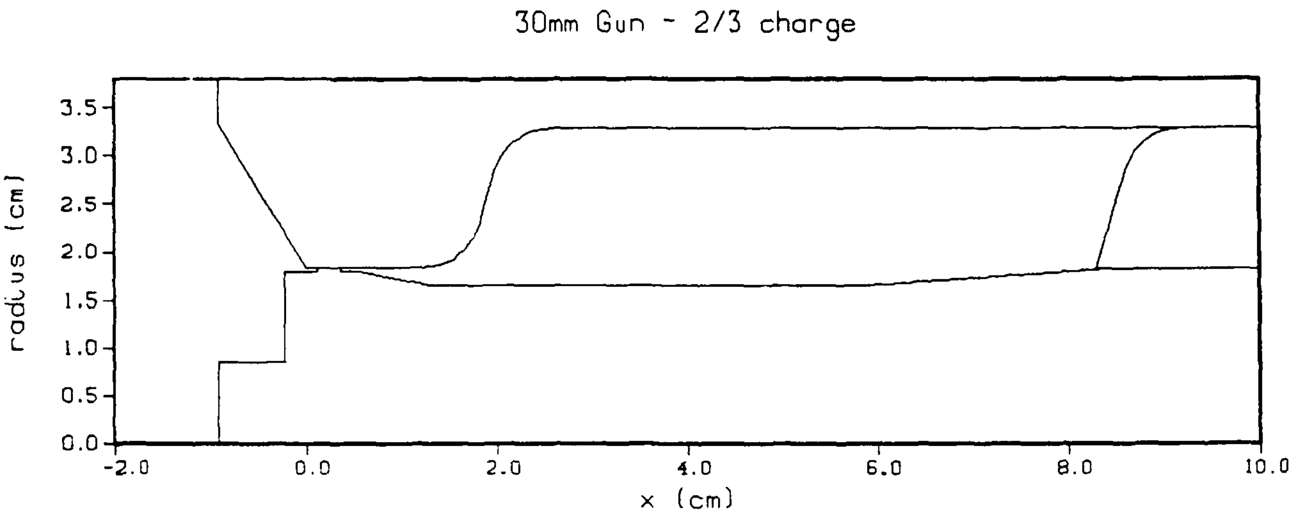

Figure 3. Scale Model Drawing of the Liquid Reservoir, Initial Position (after Pre-pressurization).

Figure 4 shows the experimental pressure profiles. The primer causes the initial pressure rise in the chamber. The chamber pressure then remains constant while the liquid pressure slowly rises. Both the piston and the block are in motion. When the Belleville springs bottom out, the momentum of the piston causes a pressure rise in the reservoir. This sets up oscillations in the liquid pressure. The injected liquid begins to combust and the chamber and liquid pressures increase rapidly.

Figure 5 shows the experimental piston travel. The piston moves relatively slowly at first. When the Belleville springs bottom out, the pressure rise in the liquid causes the piston to stop. After this the main injection stroke takes place. Figure 6 gives the experimental projectile velocity. This is only accurate over a period of time near the initial projectile motion. The muzzle velocity (measured separately) is around 1020 m/s.

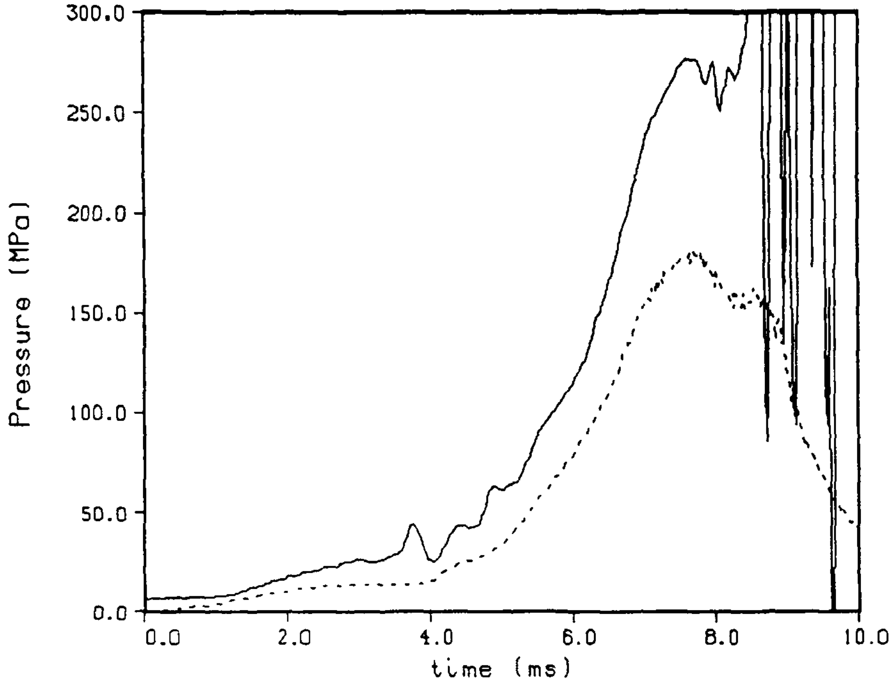

Figure 4. Experimental Liquid Pressure (line) and Chamber Pressure (dot).

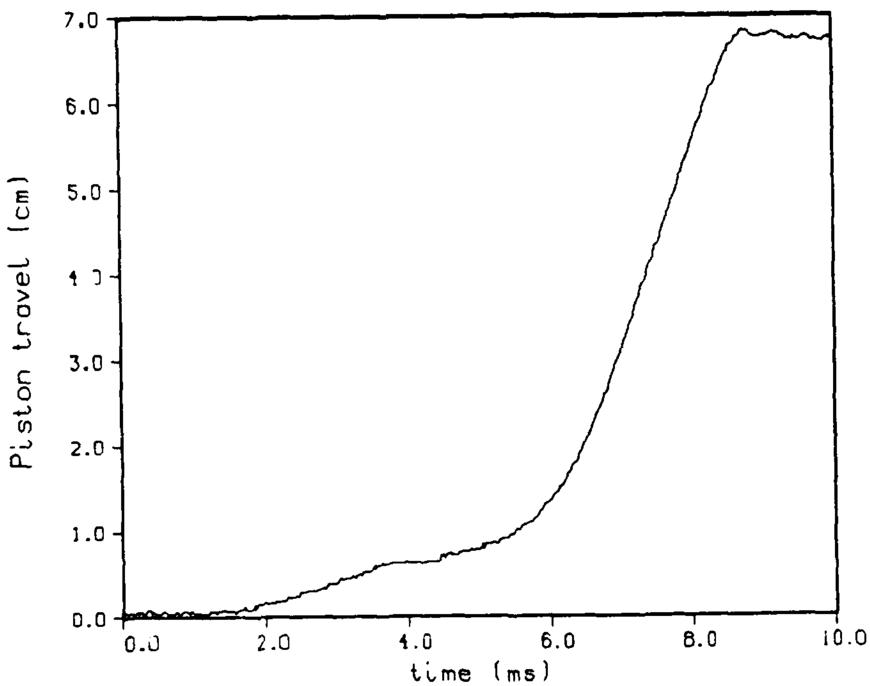

Figure 5. Experimental Piston Travel.

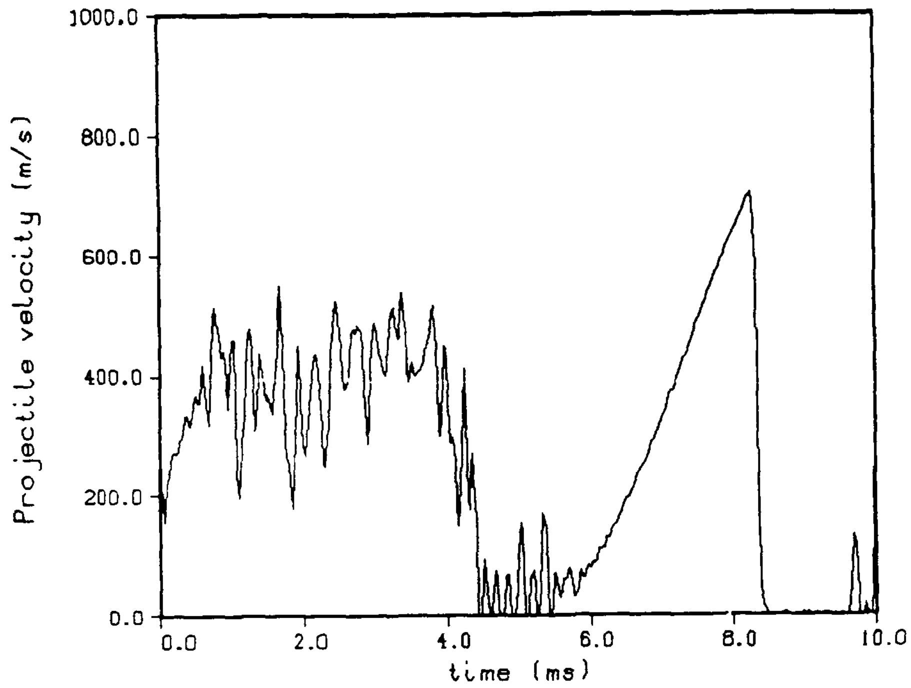

Figure 6. Experimental Projectile Velocity.

In a previous report[13] the data was analyzed using an inverse code. Values of the discharge coefficient and the liquid accumulation were derived. The discharge coefficient started small and took several milliseconds to rise to a value near one (see Figure 7). It is sometimes more convenient to consider the discharge coefficient versus the piston travel (Figure 8). At early times the derived discharge coefficient is not expected to be accurate. A small error in the piston position can lead to a relatively large change in the vent area. It is interesting that even after the piston is past the front taper (piston travel = 1.32 cm.) the discharge coefficient is still small.

More recently[4] an attempt was made to duplicate this behavior using transient models of the liquid injection (lumped parameter, one-dimensional, and two-dimensional). The two-dimensional model has only been applied to simplified cases where the central bolt does not have a

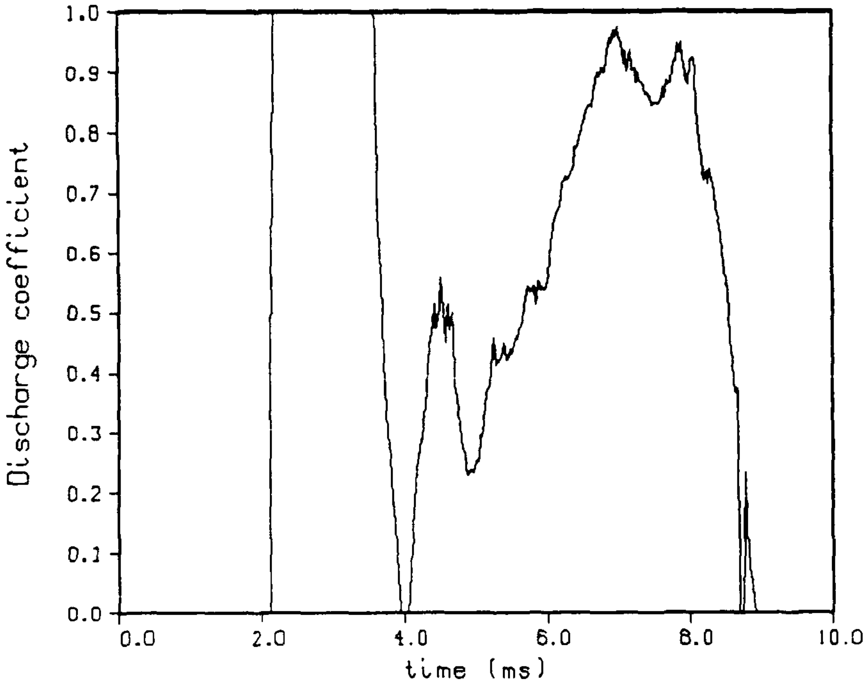

Figure 7. Derived Discharge Coefficient versus Time.

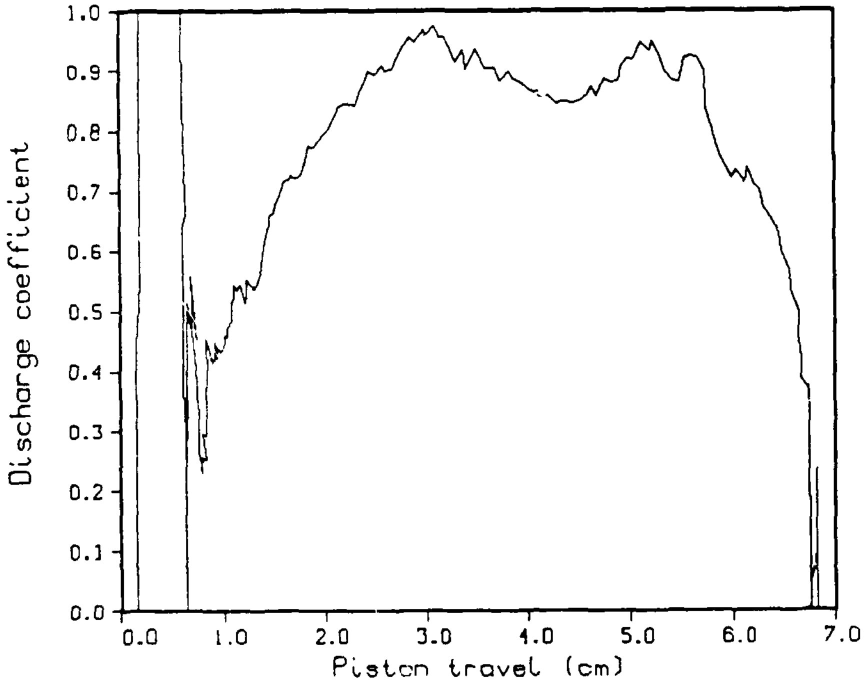

Figure 8. Derived Discharge Coefficient versus Piston Travel.

taper. All the models indicated a rapid rise to a discharge coefficient near one. This led to a more careful look at the inverse procedure. The derivation of the discharge coefficients depends on very accurate measurements of the piston travel. In fact, the discharge coefficients depend on the piston velocity, so the data must be numerically differentiated. However, the block motion has not been measured, so this must be estimated. And the recoil of the gun has not been measured. Since only the relative piston motion is measured, and this must be scaled against the expected maximum piston travel, an error anywhere during the gun firing will effect the entire profile. Also, it is known that the mini-transducer used in the liquid reservoir is less accurate than the transducers in the combustion chamber. If the flow was actually steady state, the liquid pressure would just be the chamber pressure times the hydraulic difference. However, the oscillations in the liquid pressure lead to substantial differences in the ratio of the liquid to the chamber pressure, and the accuracy of the liquid pressure measurement is unknown. Therefore the derivation of the discharge coefficient is here given less weight, and an attempt is made to model the experiment assuming a constant large discharge coefficient.

Appendix B shows the input for the code for this problem. The numbers and labels at the left are read in by the code. The comments at the right are for identification by the user and do not effect the actual code. The corresponding output follows.

The first line is merely a label for the problem. It lists the filename of the input job stream and a brief description of the problem.

The initial offset of the projectile and the total distance traveled by the projectile before muzzle exit are given. The diameter of the gun tube is given. The projectile and piston weights are entered (measured).

The initial volumes of the reservoir and chamber are given. The

reservoir volume is computed from the drawings. The crash ring in the chamber makes computing the volume difficult, so the initial volume is measured.[23] The initial gun tube volume will be computed from the offset and the gun tube diameter.

The initial areas of the reservoir and chamber are given (from the engineering drawings). The gun tube area is computed from the gun tube diameter.

The vent option is chosen. In this case the actual piston option is picked (VENT3). This requires a table of the bolt radii versus distance (from drawings). The zero distance is the initial position of the front of the piston. The vent area is the area between the front of the piston and the bolt. The area of this central hole in the piston is given, as well as the area of the grease dyke. The O-ring originally is between 0.127 and 0.363 cm. measured from the initial piston position. As the O-ring is uncovered, the high liquid pressure will push out the O-ring before the piston has moved out to 0.363 cm. The exact behavior of the vent is not known here. As an approximation, the bolt radius is assumed to vary linearly from the beginning to the end of the initial location of the O-ring.

The Belleville spring option is chosen. The force exerted by the Belleville springs has been measured as a function of distance.[23] The springs bottom out at 0.422 cm. The pre-presurization is sufficient to compress the springs 0.184 cm., so the block only moves 0.238 cm. during the gun firing. The surface area of the block (from the drawings) and the weight of the block (measured) must also be known.

For lack of better information, the piston resistance is set equal to zero. The discharge coefficient into the chamber is set at a constant 0.95. This agrees well with higher dimensional transient models.[4] The discharge coefficient into the gun tube is chosen as one (no losses).

The flow into the chamber is modeled as steady state Bernoulli flow (FLUX1). There is only one vent hole. The piston thickness is irrelevant for this option. The flow into the gun tube is steady state isentropic flow (FLUX1).

The shot start pressure is taken as 50 MPa. Previously a value of 68 MPa has been used. An analysis of the radar traces of the projectile indicate the projectile moves somewhat sooner.[23] The initial projectile motion may not be reproducible, and there is some evidence that the projectile sometimes moves a few centimeters, stops, and then later moves again.[24] After shot start the resistance pressure is taken as 5 MPa. This is a typical value from solid propellant gun modeling.

Next the physical properties of the propellant HAN1846 are given. The density at atmospheric pressure has been measured[8] and the bulk modulus has been fitted.[7] The chemical energy, the ratios of specific heats, the molecular weight of the propellant final produces gas, and the covolume have been computed using BLAKE.[9] The surface tension and the kinematic viscosity of the liquid[8] are not actually required, but are used to compute the Weber number, the Reynold's number, and the third Lagrange number.

The liquid is pre-presurized to 7.0 MPa. The initial chamber pressure is one atmosphere.

As a first approximation, the liquid is assumed to combust instantaneously as it enters the combustion chamber (DROP1). Later the effects of accumulation will be studied.

The primer is assumed to be injected in the form of hot gas (PRIM3). From the experimental chamber pressure, once the pressure starts to rise, it takes about 2.5 ms. to reach a pressure of 13 MPa. The chamber pressure then stays almost constant for another 1.5 ms. The

initial pressure rise is assumed to be due solely to the primer. So the injection time is taken to be 2.5 ms. The primer mass is chosen as 1.5 grams in order to obtain the proper pressure. The actual primer is 3.0 grams. But since the primer is injected through a relatively long narrow tube, there should be large energy losses.[24] The code does not model these losses directly, so a smaller amount of primer must be chosen.

The heat loss to the combustion chamber is ignored. Heat loss to the gun tube walls is calculated. The gun tube wall temperature is taken to be 300K. The heat loss algorithm in the code is not adjusted.

The air shock in front of the projectile is calculated. The air in the tube is initially assumed to be at 1 atm. and 300K. The values of the molecular weight and ratio of specific heats are taken at these conditions.

Since this is a low performance gun, the choice of the pressure distribution in the gun tube is not critical. The modified Lagrange distribution is chosen (TUBE2). This does take into account the velocity at the entrance to the tube, but is still easy to calculate. There is no water buffer in this fixture (BUFF1).

The code will print out results every 0.1 ms. (TINC). Because the code must often change the time step, it is more efficient to restrict the maximum time step (HTOP). The error controls EPS and SREC are given typical values.

The integration method flag MF is set to 22 (backwards differentiation formulas with an internally computed Jacobian). KWRITE is set to zero to eliminate diagnostic messages. A time limit TMAX is set. If the code takes longer than TMAX seconds to execute, the code will stop and write the usual summary pages so all the information will not be lost.

The code is only to be integrated once (REP1) and the chamber pressure will be computed normally (CHAM1).

Appendix B also gives the output for this problem. The code was run on the BRL Cray-2. The input is echoed back, along with other calculated initial values. Once the integration begins, output is given every 0.1 ms. The pressures, piston travel and velocity, and projectile travel and velocity are given. At the end of the integration, a summary page is given. A second page shows when various maximum values are achieved. There are many other variables of interest in the simulation. As the integration proceeds, these are written onto other files, and can be appended to the output. In Appendix B, only the minimal output is given.

Figure 9 shows the resulting chamber pressure profile. Because of the instantaneous burning option, the pressure starts to rise as soon as the vent opens. The only way to delay the pressure rise would be to delay the opening of the vent.

To make comparisons more easily, the model results are shifted (Figures 10-13). The curves are moved over so that the model chamber pressure reaches the shot start pressure (50 MPa) at the same time as the experimental chamber pressure. All the model curves are moved the same amount. After the initial disturbances caused by the Belleville springs, the agreement in the pressure curves is reasonable. The agreement in piston travel is poor. The model projectile velocities are consistently high, due to the higher chamber pressure, and the predicted muzzle velocity is about 6% high.

A droplet option was also calculated to see if improved agreement could be obtained. The inverse code was not used to obtain liquid accumulation because of doubts concerning the accuracy of the piston travel. Instead, the drop size versus piston travel table was adjusted

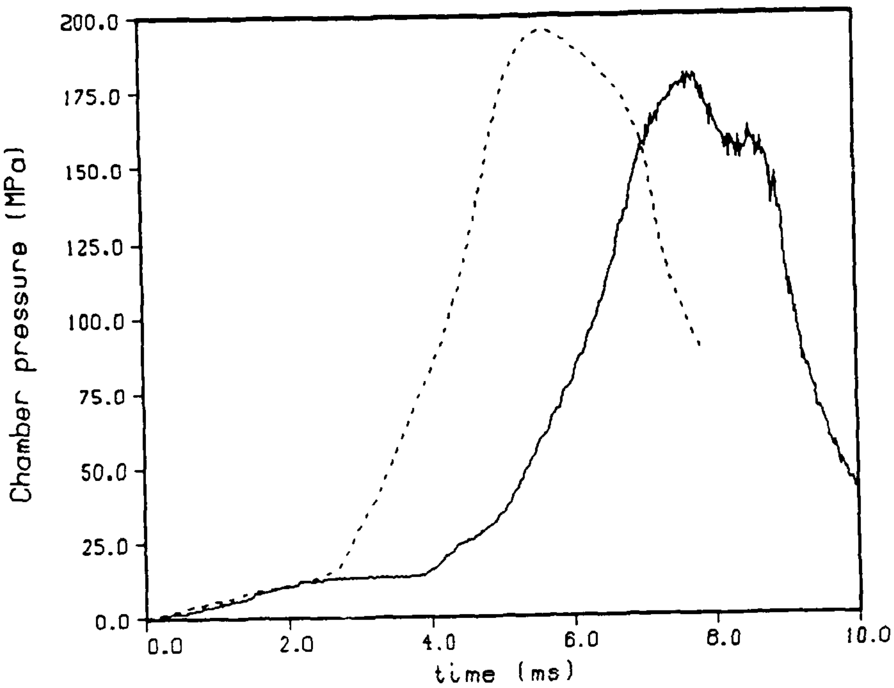

Figure 9. Chamber Pressure. Experiment (line).
Model - Instantaneous Burning - C_D = 0.95 (dot).

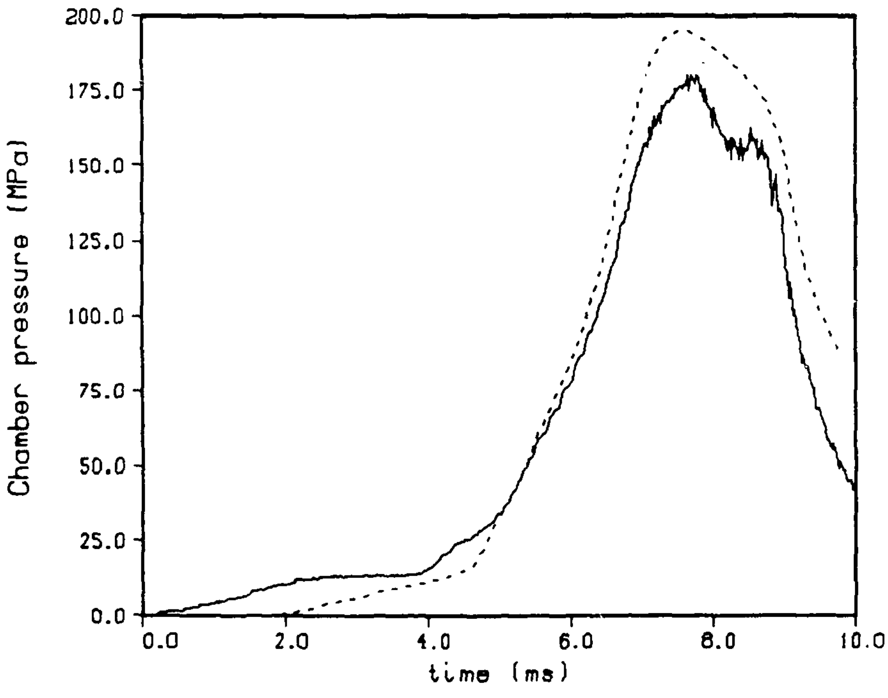

Figure 10. Chamber Pressure - Centered. Experiment (line).
Model - Instantaneous Burning - C_D = 0.95 (dot).

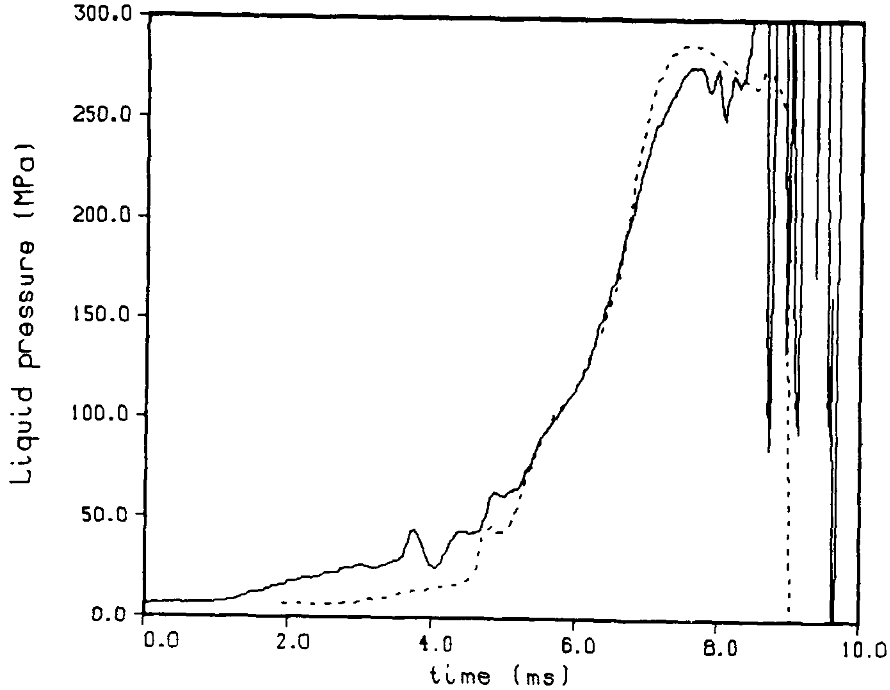

Figure 11. Liquid Pressure - Centered. Experiment (line). Model - Instantaneous Burning - C_D = 0.95 (dot).

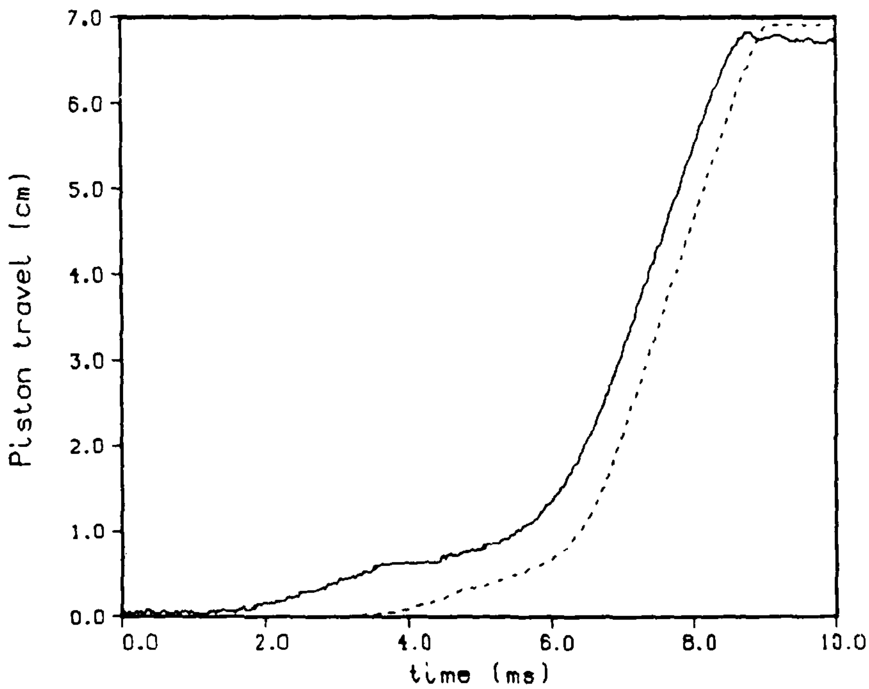

Figure 12. Piston Travel - Centered. Experiment (line). Model - Instantaneous Burning - C_D = 0.95 (dot).

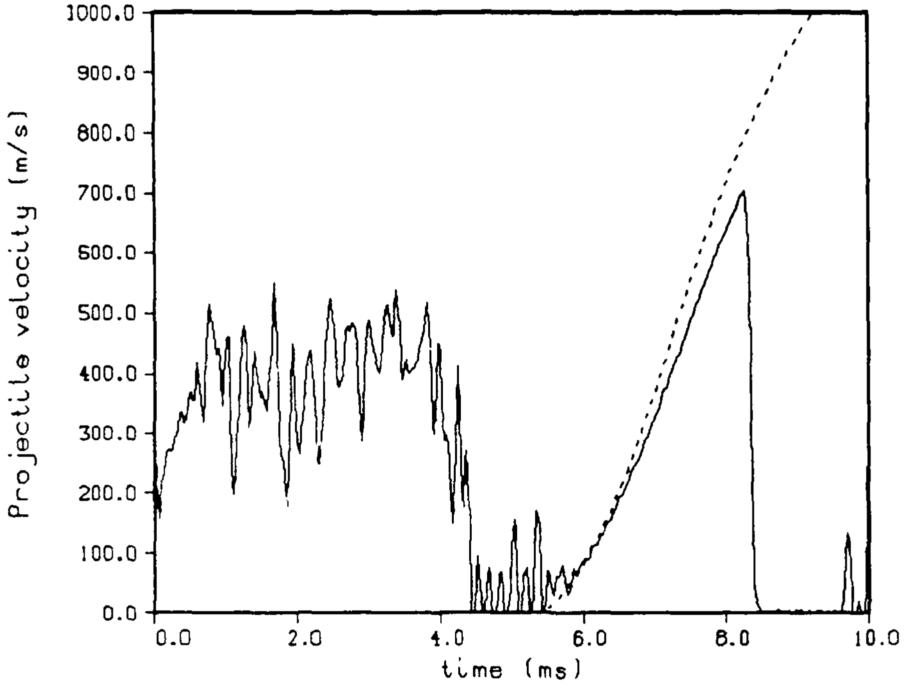

Figure 13. Projectile Velocity - Centered. Experiment (line). Model - Instantaneous Burning - C_D = 0.95 (dot).

by trial and error until reasonable agreement in the chamber pressures was obtained. The DROP1 option then is replaced by the DROP3 option. This is the only change made in the code. The input and the summary page of the output are given in Appendix C. The results (Figures 14-17) no longer require centering, since the delay in the experimental pressure rise is now being modeled.

The agreement in the combustion chamber pressures is much better. The oscillations in the liquid pressure are now reproduced. However, in the model the Belleville springs bottom out too early. This can be seen in the liquid pressure profile, where the pressure bump comes too early, and in the piston travel profile, where the piston stops sooner. The later agreement in the piston travel may or may not be coincidental. The muzzle velocity is still 3% high.

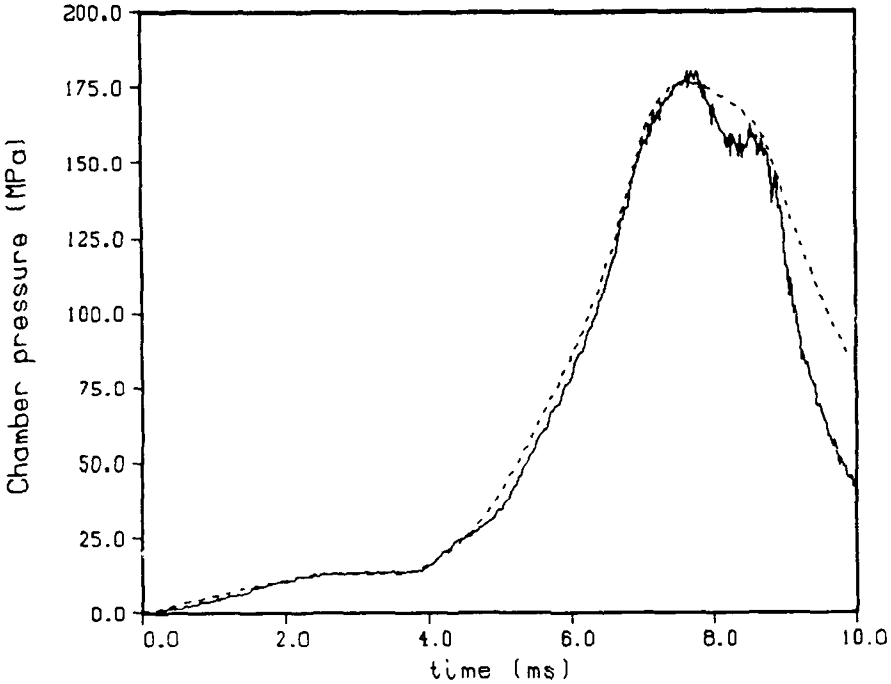

Figure 14. Chamber Pressure. Experiment (line).
Model - Droplet Formation - C_D = 0.95 (dot).

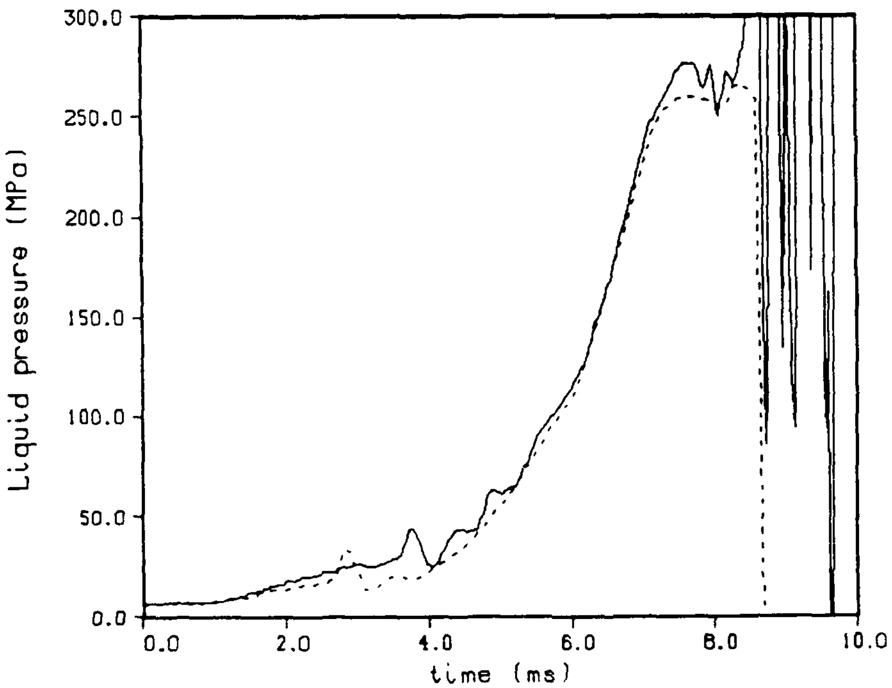

Figure 15. Liquid Pressure. Experiment (line).
Model - Droplet Formation - C_D = 0.95 (dot).

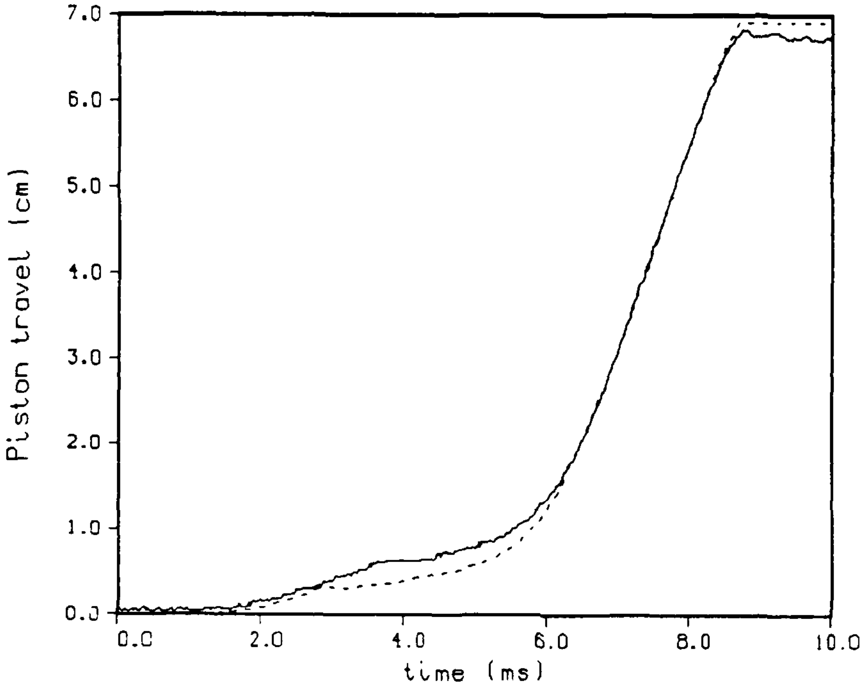

Figure 16. Piston Travel. Experiment (line).
Model - Droplet Formation - C_D = 0.95 (dot).

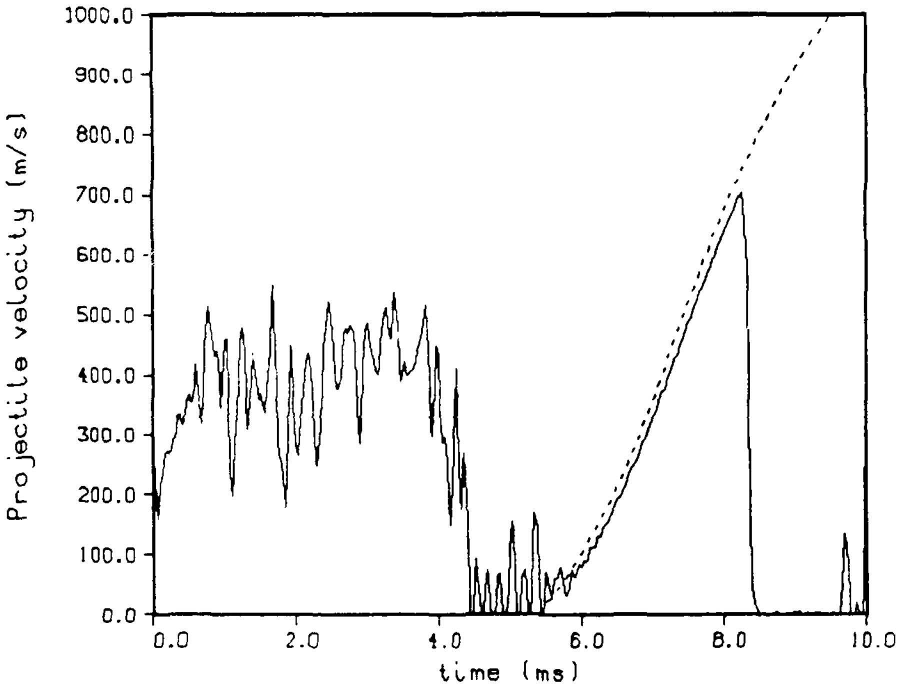

Figure 17. Projectile Velocity. Experiment (line).
Model - Droplet Formation - C_D = 0.95 (dot).

The experiment indicates that the block should move further before the Belleville springs bottom out. So calculations were made where the block is assumed to move 2 mm. further. This would indicate a small error in the measurement of the spring behavior. Note that the experimental piston travel must now be scaled to a slightly longer total piston travel.

The model with instantaneous burning is calculated first. The input is in Appendix D, and Figures 18-21 show the results. The agreement is now very poor. The piston moves another 2 mm. before the block stops moving. Therefore the vent area is larger, and the injection starts more rapidly. Because of the assumption of instantaneous burning, the initial small difference in the injection rate grows as time goes on. The unfortunate fact here is that the initial piston position must be known very accurately to model this gun fixture properly. Fortunately later gun fixtures do not use Belleville springs or an O-ring, but a metal-to-metal seal, and the vent area versus piston travel is much better known.

Next droplet burning was assumed, and again the droplet size table was chosen so that the chamber pressure profile was reasonably accurate (Appendix E, Figures 22-25). The agreement in the piston travel is still rather poor. Despite experimentation with the code, it proved impossible to get reasonable agreement with the piston travel under the assumption that the discharge coefficient was uniformly equal to 0.95.

So an attempt was made to get agreement in the piston travel making minimal changes in the discharge coefficient. This proved to be possible by decreasing the discharge coefficient when the piston was over the front taper of the bolt and increasing it back to 0.95 when the piston moved to the flat part of the bolt (Appendix F, Figures 26-29). The agreement with the chamber pressure and the piston travel is now very good.

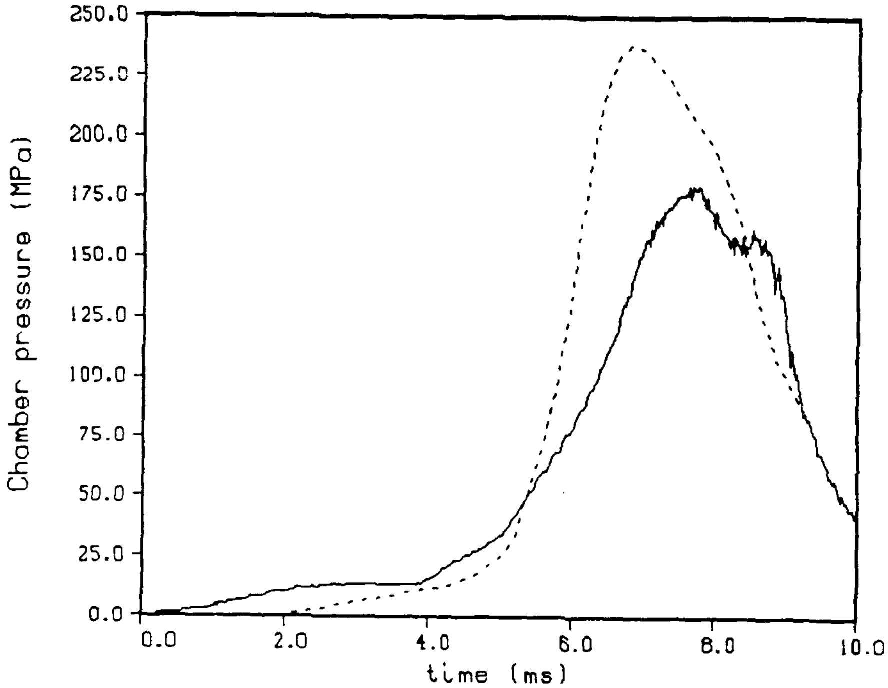

Figure 18. Chamber Pressure - Centered. Experiment (line). Model - Instantaneous Burning - C_D = 0.95 - Long Belleville (dot).

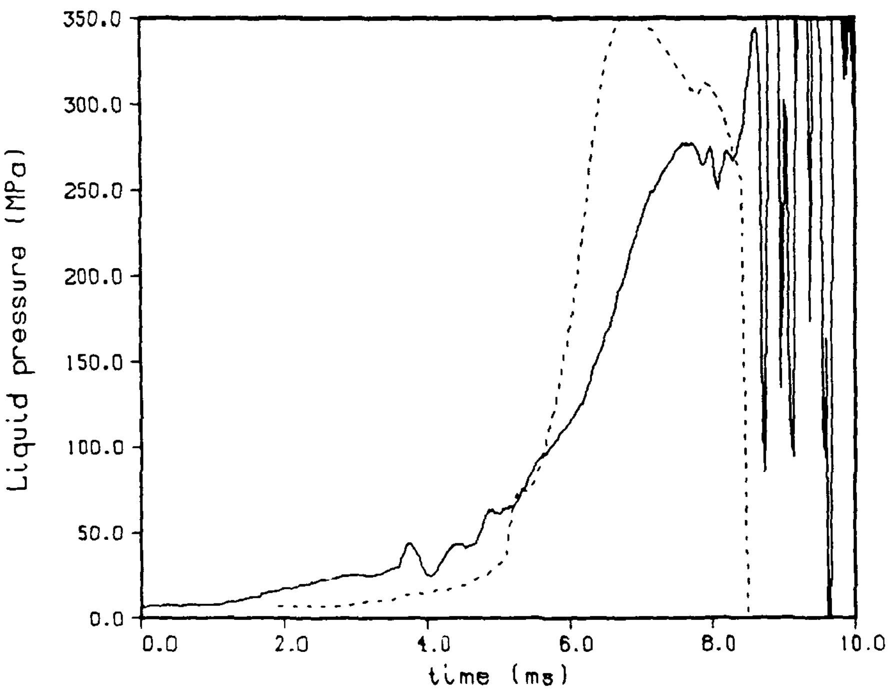

Figure 19. Liquid Pressure - Centered. Experiment (line). Model - Instantaneous Burning - C_D = 0.95 - Long Belleville (dot).

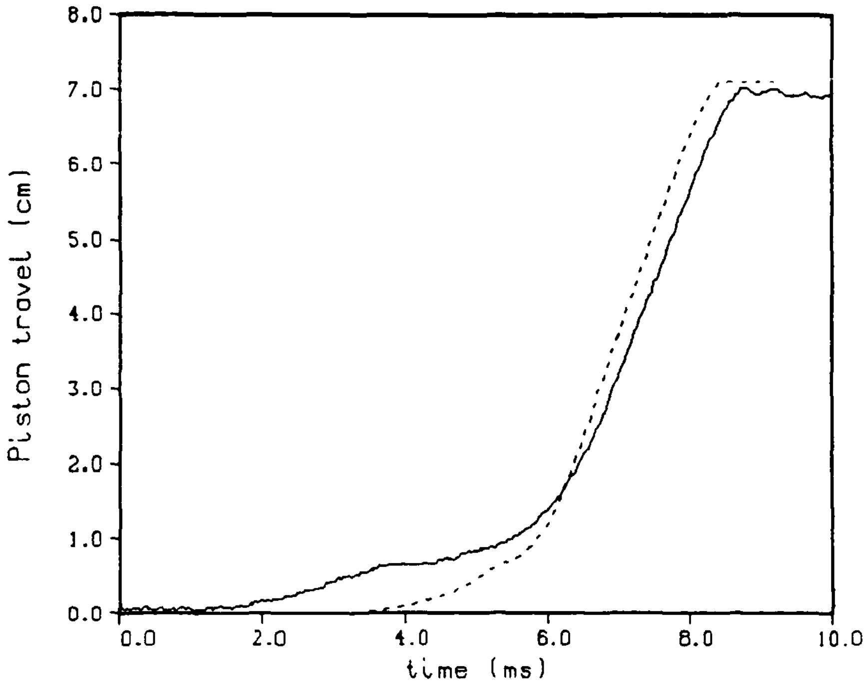

Figure 20. Piston Travel - Centered. Experiment (line).
Model - Instantaneous Burning - C_D = 0.95 - Long Belleville (dot).

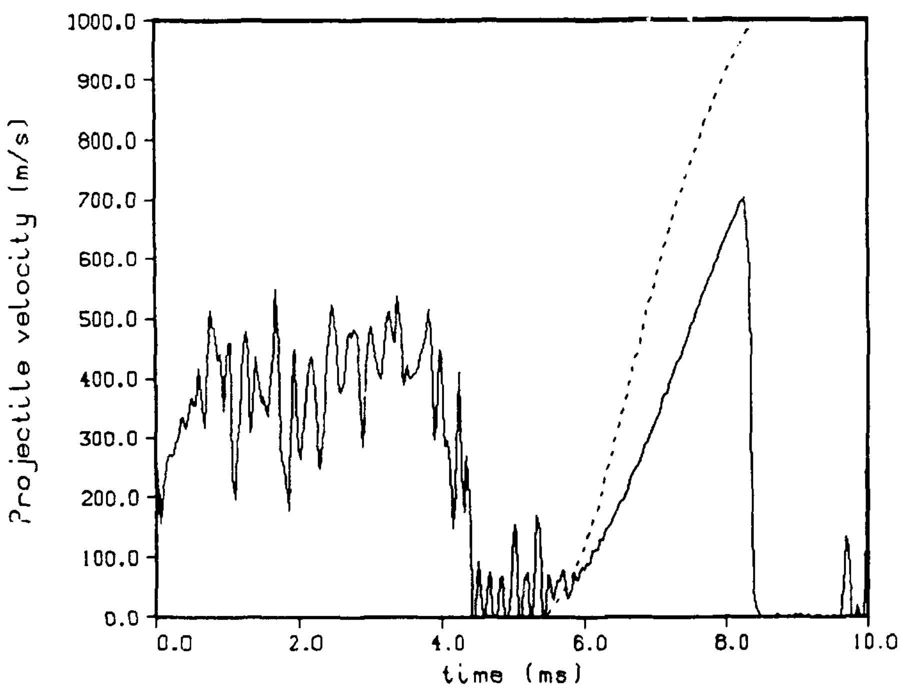

Figure 21. Projectile Velocity - Centered. Experiment (line).
Model - Instantaneous Burning - C_D = 0.95 - Long Belleville (dot).

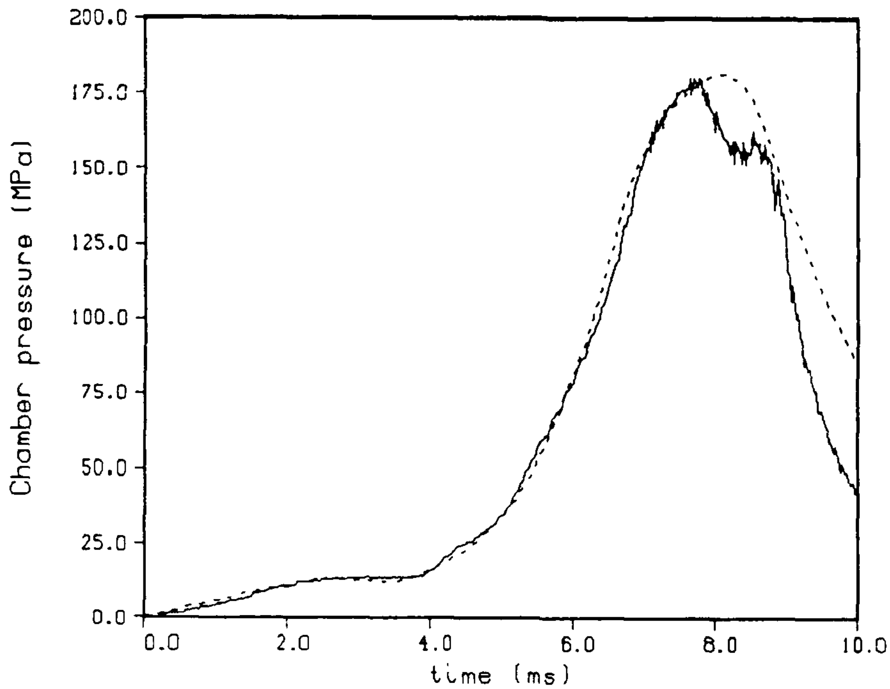

Figure 22. Chamber Pressure. Experiment (line).
Model - Droplet Formation - C_D = 0.95 - Long Belleville (dot).

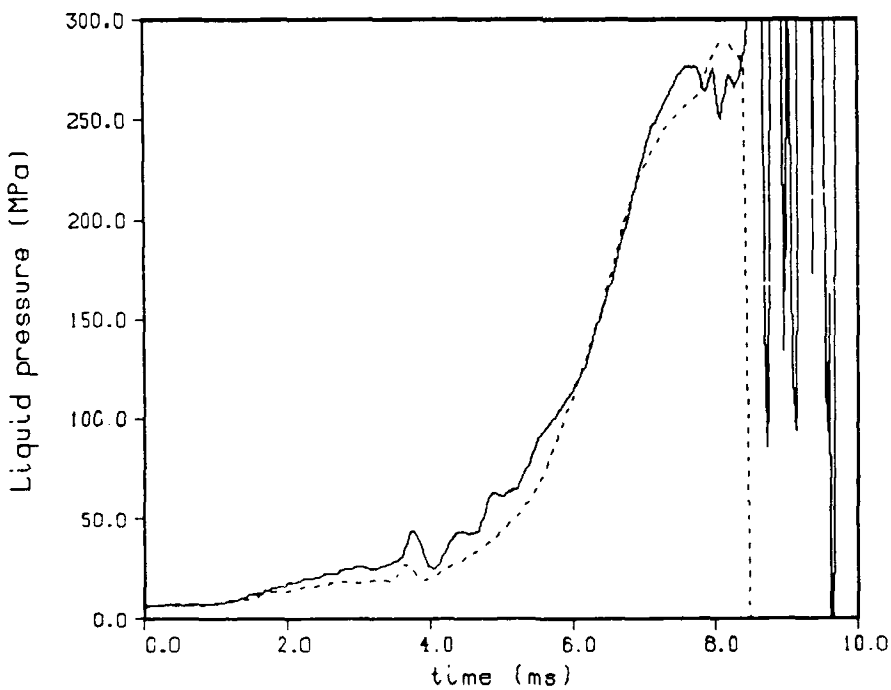

Figure 23. Liquid Pressure. Experiment (line).
Model - Droplet Formation - C_D = 0.95 - Long Belleville (dot).

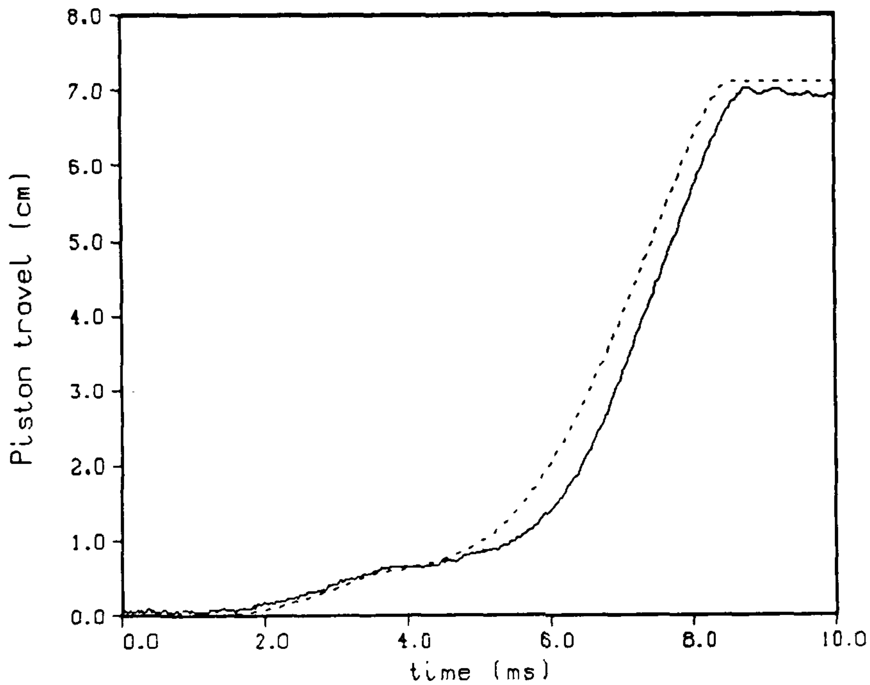

Figure 24. Piston Travel. Experiment (line).
Model - Droplet Formation - $C_D = 0.95$ - Long Belleville (dot).

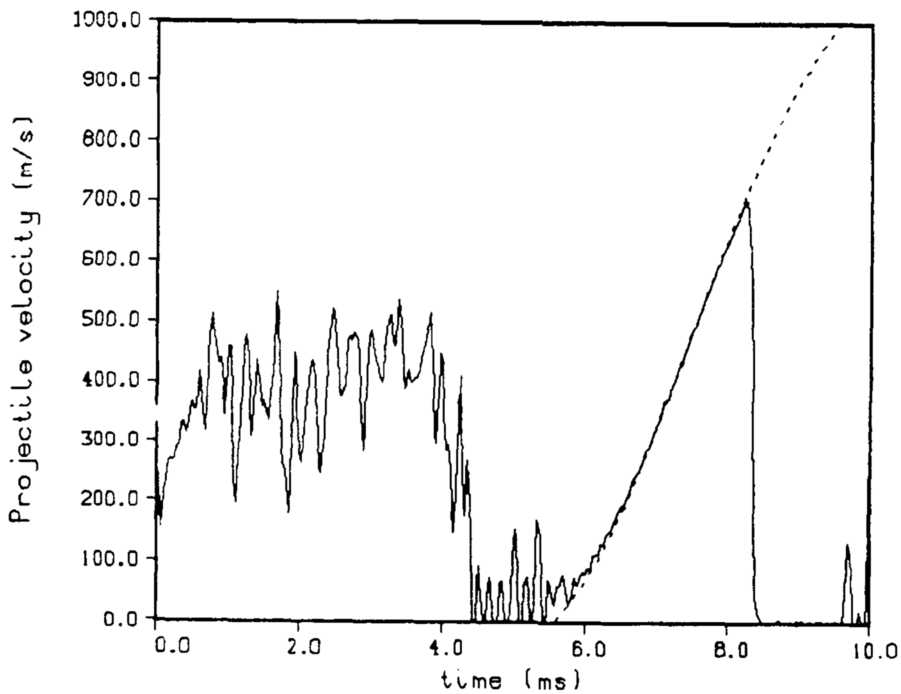

Figure 25. Projectile Velocity. Experiment (line).
Model - Droplet Formation - $C_D = 0.95$ - Long Belleville (dot).

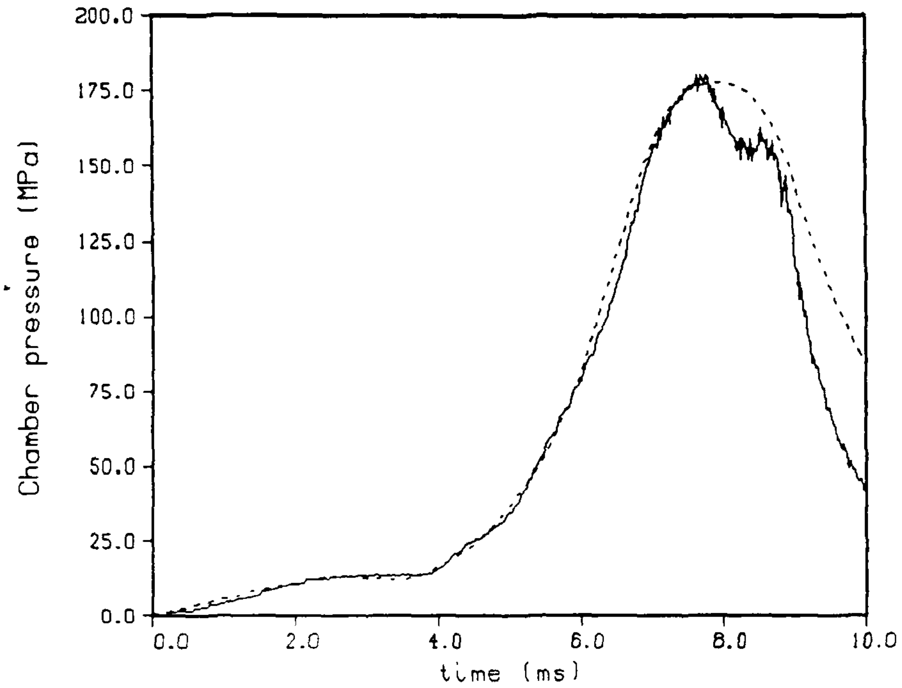

Figure 26. Chamber Pressure. Experiment (line).
Model Droplet Formation - C_D Adjusted - Long Belleville (dot).

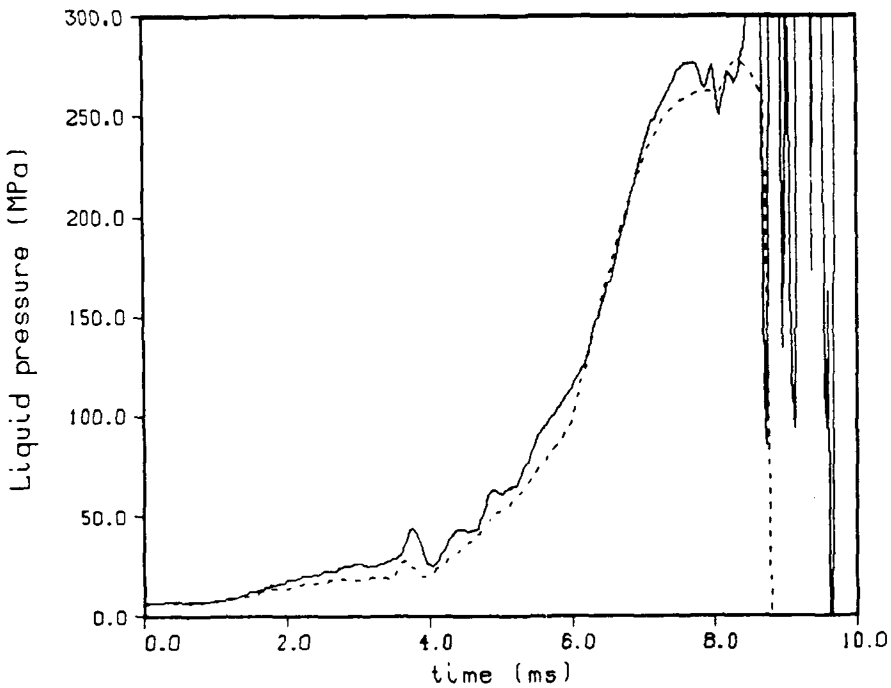

Figure 27. Liquid Pressure. Experiment (line).
Model - Droplet Formation - C_D Adjusted - Long Belleville (dot).

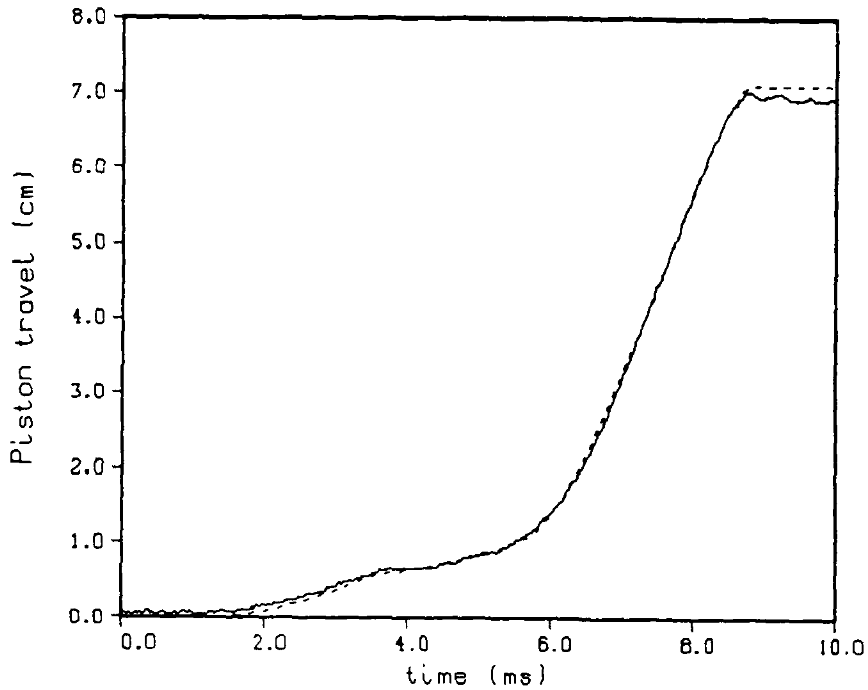

Figure 28. Piston Travel. Experiment (line).
Model - Droplet Formation - C_D Adjusted - Long Belleville (dot).

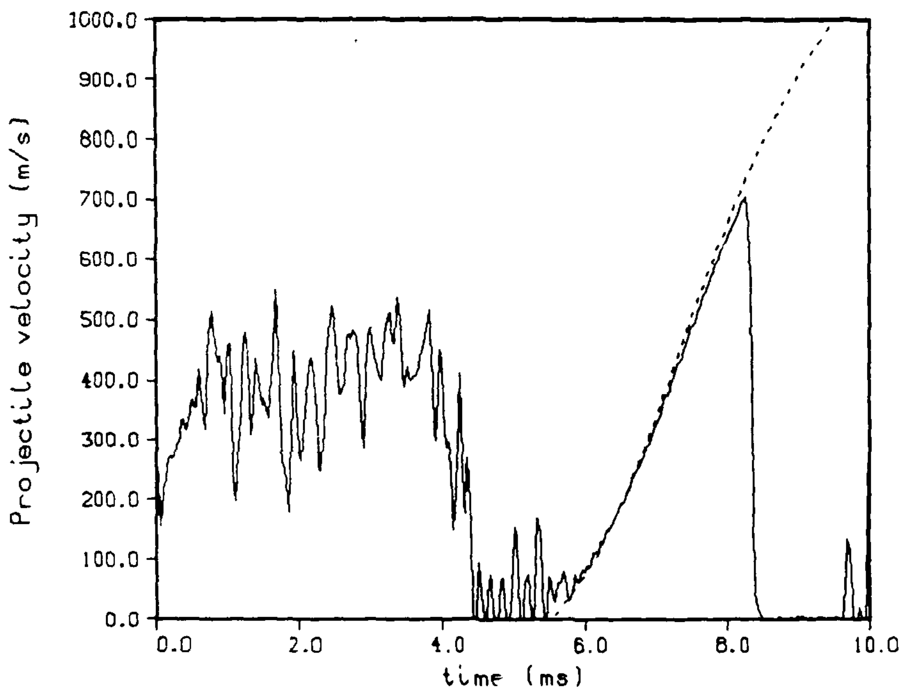

Figure 29. Projectile Velocity. Experiment (line).
Model - Droplet Formation - C_D Adjusted - Long Belleville (dot).

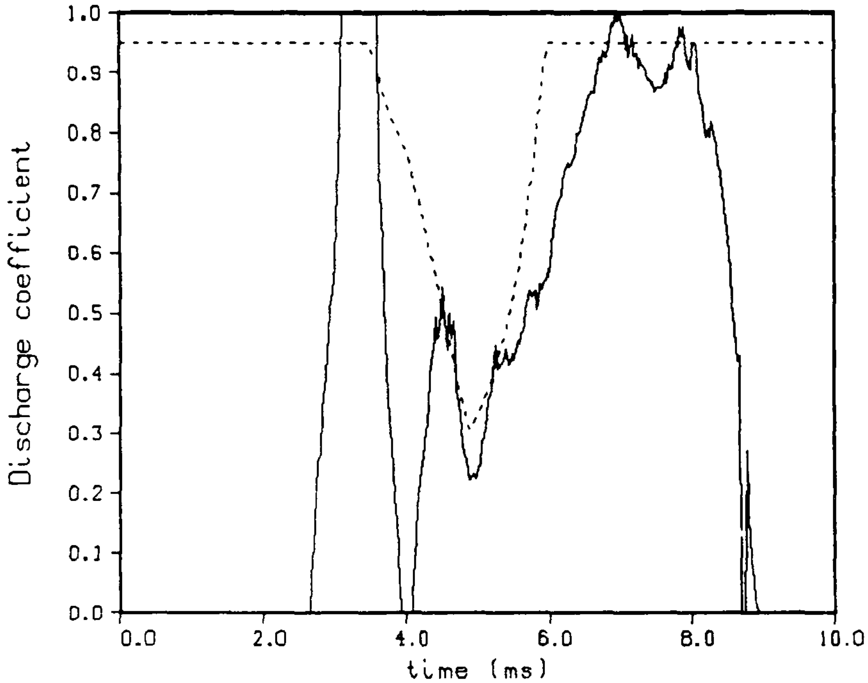

Figure 30. Discharge Coefficient. Derived from Experiment (line). Model - Droplet Formation - C_D Adjusted - Long Belleville (dot).

Figure 30 shows a comparison of the present profile for the discharge coefficient with the experimentally derived values. The differences are due partly to the small differences in the piston travel, since the discharge coefficient depends on the slope of the piston travel. The early differences are due to the differences in the liquid pressure. Since the liquid pressure transducer is known to be less accurate, and since the ratio of the liquid to chamber pressure is equal to the hydraulic difference only at steady state, the model liquid pressures are still plausible.

To summarize, the last model shows very good agreement with experiment. The assumption must be made that the discharge coefficient is small when the piston is over the front taper of the bolt. This occurs right after the Belleville springs bottom out. The liquid pressure oscillations could lead to turbulence and/or flow separation at the exit. At this point, the opening is essentially a

converging/diverging nozzle. The earlier lumped parameter and one-dimensional transient models would not be able to predict this type of behavior, and the two-dimensional model has not been applied to a problem with a tapered bolt.

The model does not reproduce the pressure behavior after the maximum pressure. At this stage the piston is near the end of its stroke. Hydrodynamic effects may be important. Since the model pressure is uniformly higher than the experimental pressure after the maximum, there are probably loss terms not implemented in the model. The muzzle velocity is also slightly too large.

XXIV. CONCLUSIONS

An update is given to a lumped parameter model for regenerative liquid propellant guns. While the basic structure is the same, many more options have been added. A complete discussion of the governing equations and the different options is given. The code has been used to test the effect of various assumptions, so additional options will be added as needed.

The model results are compared with experimental data from a 30mm gun fixture. A discussion is given of the procedure for choosing a set of input parameters. The code predicts the overall behavior of the gun fixture extremely well. Some of the details are not reproduced, and the probable shortcomings in the code are discussed.

ACKNOWLEDGEMENT

I would like to thank Cris Watson, BRL, for his help in understanding the gun fixture and the experimental data.

GLOSSARY

A_1	Area of the liquid reservoir, cm^2.
A_3	Area of the chamber, cm^2.
A_4	Area of the gun tube, cm^2.
A_{bf}	Area of the piston in the buffer, cm^2.
A_{bk}	Area of the block in the reservoir, cm^2.
A_g	Area of the grease dyke around an annular piston, cm^2.
A_h	Area of the central hole in the annular piston, cm^2.
A_v	Area of the piston vents, cm^2.
b	Covolume, cm^3/g.
c_1	Speed of sound in the liquid in the reservoir, cm/s.
c_3	Speed of sound in the mixture in the chamber, cm/s.
c_4	Speed of sound in the mixture in the gun tube, cm/s.
c_{L3}	Speed of sound in the liquid in the chamber, cm/s.
c_{L4}	Speed of sound in the liquid in the gun tube, cm/s.
c_{G3}	Speed of sound in the gas in the chamber, cm/s.
c_{G4}	Average speed of sound in the gas in the gun tube, cm/s.

c_{bf} Speed of sound in the buffer liquid, cm/s.

c_p Specific heat at constant pressure, j/g-K.

c_v Specific heat at constant volume, j/g-K.

C_D Discharge coefficient for the mass flux through the piston.

C_D' Discharge coefficient for the mass flux into the gun tube.

d_4 Diameter of the gun tube, cm.

e_1 Chemical energy of the liquid, j/g.

e_3 Internal energy of the gas in the chamber, j/g.

e_4 Internal energy of the gas in the gun tube, j/g.

E_{L1} Total internal energy in the liquid reservoir, j.

E_{L3} Total internal energy in the liquid in the chamber, j.

E_{L4} Total internal energy in the liquid in the gun tube, j.

E_{G3} Total internal energy in the gas in the chamber, j.

E_{G4} Total internal energy in the gas in the gun tube, j.

E_p Total internal energy in the unburned primer, j.

EK_{L4} Kinetic energy of the liquid in the gun tube, j.

EK_{G4} Kinetic energy of the gas in the gun tube, j.

EK_{pj} Kinetic energy of the projectile, j.

EK_{ps} Kinetic energy of the piston, j.

EH_3 Total heat loss to the chamber walls, j.

EH_4 Total heat loss to the gun tube walls, j.

EF_{pj} Total energy loss due to projectile friction, j.

EF_{ps} Total energy loss due to piston friction, j.

E_T Total energy of the system, j.

f_{bk} Force exerted by the Belleville springs, MPa-cm^2.

g_o Conversion constant = 10^7 g/MPa-cm-s^2.

h_{L1} Liquid enthalpy in the reservoir, j/g.

h_{L3} Liquid enthalpy in the combustion chamber, j/g.

h_{L4} Liquid enthalpy in the gun tube, j/g.

h_{G3} Gas enthalpy in the chamber, j/g.

h_{G4} Gas enthalpy in the gun tube, j/g.

h_c Heat transfer coefficient to the chamber walls, j/cm^2-K-s.

h_w Heat transfer coefficient to the gun tube walls, j/cm^2-K-s.

K Bulk modulus, MPa.

K_1	Bulk modulus at zero pressure, MPa.
K_2	Derivative of the bulk modulus.
L	Piston thickness, cm.
m_{13}	Mass flux from the reservoir into the chamber, g/s.
m_{34}	Mass flux from the chamber into the gun tube, g/s.
m_{p3}	Mass flux of the primer into the chamber, g/s.
m_{bf}	Mass flux out of the buffer, g/s.
m_3	Chamber rate of production of gas by combustion, g/s.
m_4	Gun tube rate of production of gas by combustion, g/s.
m_{L3}	Total rate of production of liquid in the chamber, g/s.
m_{L4}	Total rate of production of liquid in the gun tube, g/s.
m_{G3}	Total rate of production of gas in the chamber, g/s.
m_{G4}	Total rate of production of gas in the gun tube, g/s.
M_1	Total mass in the reservoir, g.
M_3	Total mass in the chamber, g.
M_4	Total mass in the gun tube, g.
M_{L3}	Liquid mass in the chamber, g.

M_{L4} Liquid mass in the gun tube, g.

M_{G3} Gas mass in the chamber, g.

M_{G4} Gas mass in the gun tube, g.

M_p Unburned primer mass, g.

M_T Total propellant mass in the system, g.

M_{bk} Mass of the block, g.

M_{pj} Mass of the projectile, g.

M_{ps} Mass of the piston, g.

M_g Molecular weight of the gas, g/mole.

p_1 Pressure in the liquid reservoir, MPa.

p_3 Pressure in the chamber, MPa.

p_4 Space mean pressure in the gun tube, MPa.

p_L Pressure at the gun throat, MPa.

p_R Pressure at the base of the projectile, MPa.

p_t Pressure at the gun tube entrance = p_L, MPa.

p_{pj} Projectile resistance pressure, MPa.

p_{ps} Piston resistance pressure, MPa.

P_s Air shock pressure ahead of the projectile, MPa.

P_{bf} Pressure in the buffer, MPa.

Pr Prandtl number.

Q_c Heat loss to the chamber walls, j/cm^3-s.

Q_w Heat loss to the gun tube walls, j/cm^3-s.

Re Reynold's number.

R_s Specific gas constant, j/g-K.

R_u Universal gas constant = 8.318 j/mole-K.

s_{bk} Block travel, cm.

s_{pj} Projectile travel, cm.

s_{ps} Piston travel, cm.

S_3 Chamber mass production rate times enthalpy change , j/s.

S_4 Gun tube mass production rate times enthalpy change , j/s.

t Time, s.

T_3 Temperature in the combustion chamber, K.

T_4 Average temperature in the gun tube, K.

T_o Isoc' ɔric temperature of the propellant, K.

T_t Temperature at the gun tube entrance, K.

T_c Temperature of the chamber walls, K.

T_w Temperature of the gun tube walls, K.

v_3 Injection velocity of the liquid into the chamber, cm/s.

v_{bk} Velocity of the block, cm/s.

v_{pj} Velocity of the projectile, cm/s.

v_{ps} Velocity of the piston, cm/s.

V_1 Volume of the liquid reservoir, cm^3.

V_3 Volume of the chamber, cm^3.

V_4 Volume of the gun tube behind the projectile, cm^3.

V_{L3} Volume of the liquid in the chamber, cm^3.

V_{L4} Volume of the liquid in the gun tube, cm^3.

V_{G3} Volume of the gas in the chamber, cm^3.

V_{G4} Volume of the gas in the gun tube, cm^3.

V_{bf} Volume of the buffer, cm^3.

v_t Fluid velocity at the gun tube entrance, cm/s.

x_R Distance from the tube entrance to the projectile base, cm.

γ	Ratio of specific heats.
ϵ_3	Porosity of the mixture in the combustion chamber.
ϵ_4	Porosity of the mixture in the gun tube.
λ	Impetus of the propellant, j/g.
μ	Viscosity of the gas, poise = g/cm-s.
μ_w	Viscosity of the gas at the wall temperature, poise.
ρ_o	Liquid density at zero pressure, g/cm^3.
ρ_1	Liquid density in the reservoir, g/cm^3.
ρ_3	Mixture density in the chamber, g/cm^3.
ρ_4	Mixture density in the gun tube, g/cm^3.
ρ_{L3}	Liquid density in the chamber, g/cm^3.
ρ_{L4}	Liquid density in the gun tube, g/cm^3.
ρ_{G3}	Gas density in the chamber, g/cm^3.
ρ_{G4}	Gas density in the gun tube, g/cm^3.
ρ_{bf}	Liquid density in the buffer, g/cm^3.

REFERENCES

1. Coffee, T.P., "A Lumped Parameter Code for Regenerative Liquid Propellant Guns," BRL-TR-2703, December 1985.

2. Morrison, W.F., Bulman, M.J., Baer, P.G., and Banz, C.F., "The Interior Ballistics of Regenerative Liquid Propellant Guns," 1984 JANNAF Propulsion Meeting, New Orleans, LA, CPIA Publication 390, February 1984.

3. Morrison, W.F., Banz, C.F., May, I.W., and Morrison, W.F., "A Propulsion System Comparison Study for the 120-MM Anti-Armor Cannon," 1984 JANNAF Propulsion Meeting, New Orleans, LA, CPIA Publication 390, February 1984.

4. Coffee, T.P., "One-Dimensional Modeling of Liquid Injection in a Regenerative Propellant Gun," BRL-TR-2897, March 1988.

5. Corner, J., Theory of the Interior Ballistics of Guns, Wiley, New York, 1950.

6. Morrison, W.F., and Coffee, T.P., "A Modified Lagrange Pressure Gradient for the Regenerative Liquid Propellant Gun," BRL report, to be written.

7. Constantino, M., "The High Pressure Equations of State of LGP 1845 and LGP 1846," UCRL-93985, Preprint.

8. Decker, M.M., Klein, N., Freedman, E., Leveritt, C.S., and Wojciechowski, J.Q., "HAN-Based Liquid Gun Propellants: Physical Properties," BRL-TR-2864, November 1987.

9. Freedman, E., "BLAKE - A Thermodynamics Code Based on TIGER: Users' Guide and Manual," ARBRL-TR-02411, July 1982.

10. Sears, F.W., An Introduction to Thermodynamics, the Kinetic Theory of Gases, and Statistical Mechanics, 2nd ed., Addison-Wesley Publishing

Company, Inc., London, England, 1959.

11. Fox, R.W., and McDonald, A.T., Introduction to Fluid Mechanics, 2nd ed., John Wiley and Sons, NY, 1978.

12. Heiser, R.W., "A Gasdynamic Model for Regenerative Liquid Propellant Guns," Journal of Ballistics, Vol. 9, No. 4, pp. 2403-2441, 1988.

13. Coffee, T.P., "Injection Processes in Liquid Regenerative Propellant Guns," BRL-TR-2846, August 1987.

14. Bird, R.B., Stewart, W.E., and Lightfoot, E.N., Transport Phenomena, John Wiley & Sons, Inc., New York, 1960.

15. Coffee, T.P., and Heimerl, J.M., "Transport Algorithms for Premixed, Laminar Steady State Flames," ARBRL-TR-02302, March 1981.

16. Nordheim, L.W., Soodak, H., and Nordheim, G., "Thermal Effects of Propellant Gases in Erosion Vents and in Guns," National Defense Research Committee, Armor and Ordnance Report No. A-262 (OSRD No. 3447), May 1944.

17. McBratney, W.F., "Windowed Chamber Investigation of the Burning Rate of Liquid Monopropellants for Guns," ARBRL-MR-03018, April 1980.

18. McBratney, W.F., "Burning Rate Data, LPG 1845," ARBRL-MR- 03128, August, 1981.

19. Hindmarsh, A.C., and Byrne, G.D., "EPISODE: An Effective Package for the Integration of Systems of Ordinary Differential Equations," UCID-30112-Rev.1, Lawrence Livermore Laboratory, 1977.

20. Coffee, T.P., "A Computer Code for the Solution of the Equations Governing a Laminar, Premixed, One-Dimensional Flame," ARBRL-MR-03165, April 1982.

21. Knapton, J.D., Watson, C., and DeSpirito, J., "Test Data from a Regenerative Sheet Injector Type of Liquid Propellant Gun," 22nd JANNAF Combustion Meeting, October 1985.

22. Watson, C., DeSpirito, J., Knapton, J.D., and Boyer, N., "A Study on High Frequency Pressure Ocsillations Observed in a 20-mm Regenerative RLG," 22nd JANNAF Combustion Meeting, October 1985.

23. Watson, C., Private Communication, 1987.

24. Watson, C., Knapton, J.D., Boyer, N., and Stobie, I.C., "Sensitivity of Muzzle Velocity Repeatability to Variations in Initial Conditions," BRL report, to be published.

APPENDIX A

The computer code is long (around 100 pages), so a complete listing is not given. Instead, only the description of the input options from the beginning of the code is given. A complete listing of the code (tape, disk, or hardcopy) may be obtained from the author.

```
C   **********************************************
C    FEBRUARY 23, 1988.
C    DESCRIPTION OF INPUT
C
C     FILE 1: PROBLEM TITLE
C     80 ALPHANUMERIC CHARACTERS.
C     WILL BE TITLE ON GRAPHICS FILES.
C
C     FILE 2: OFFSET, TRAVEL
C     OFFSET=DISTANCE FROM END OF TUBE TO PROJECTILE (CM).
C     TRAVEL=TOTAL PROJECTILE TRAVEL (CM).
C
C     FILE 3:D4
C     D4 = GUN TUBE DIAMETER (CM).
C
C     FILE 4: PJWT
C     PJWT = PROJECTILE WEIGHT (GM).
C
C     FILE 5: PSWT
C     PSWT = PISTON WEIGHT (GM).
C
C     FILE 6: V1I,V3I
C     V1I = INITIAL LIQUID RESERVOIR VOLUME (CM**3).
C     V3I = INITIAL COMBUSTION CHAMBER VOLUME (CM**3).
C
C     FILE 7: A1,A3
C     A1 = AREA OF LIQUID SIDE PISTON FACE (INCLUDING VENTS) (CM**2).
C     A3 = AREA OF CHAMBER SIDE PISTON FACE (INCLUDING VENTS) (CM**2).
C
C     FILE 8: TVENT - VENT OPTION SWITCH
C
C       IF VENT1 THEN PISTON WITH HOLES.
C       AREA OF HOLES MAY VARY WITH PISTON TRAVEL.
C       ENTER VENT AREA TABLE.
C       FILE 8.1: NVENT
C       NVENT = NO. OF TABLE ENTRIES.
C       FILE 8.2...:SVT(I),AVT(I)
C       SVT(I) = FRACTION OF PISTON TRAVEL (CM).
C       WILL BE NORMALIZED TO MAX PISTON TRAVEL.
C       MAX PISTON TRAVEL CHOSEN TO AGREE WITH INITIAL LIQUID VOLUME.
C       AVT(I) = CORRESPONDING VENT AREA (CM**2).
C       FIND VENT AREA BY INTERPOLATING TABLE.
```

```
C        FILE 8.NVENT+2:POPEN
C        POPEN = LIQUID PRESSURE AT WHICH VENT WILL OPEN.
C
C        IF VENT2 THEN CENTRAL ROD OR BOLT
C        WITH INFINITELY THIN PISTON.
C        FILE 8.1: NVENT
C        NVENT = NO. OF TABLE ENTRIES.
C        FILE 8.2...:SVT(I),AVT(I)
C        SVT(I) = FRACTION OF PISTON TRAVEL (CM).
C        WILL BE NORMALIZED TO MAX PISTON TRAVEL.
C        MAX PISTON TRAVEL CHOSEN TO AGREE WITH INITIAL LIQUID VOLUME.
C        AVT(I) = CORRESPONDING VENT AREA (CM**2).
C        FILE 8.NVENT+2: AHOLE,AGRES
C        AHOLE = AREA OF CENTRAL HOLE IN ANNULAR PISTON (CM**2).
C        AGRES = AREA OF GREASE DYKE.
C        INTERPOLATE CENTRAL ROD RADII TO FIND VENT AREA.
C
C        IF VENT3 THEN CENTRAL ROD OR BOLT
C        WITH ACTUAL PISTON.
C        FILE 8.1: NVENT
C        NVENT = NO. OF TABLE ENTRIES.
C        FILE 8.2...:SVT(I),RROD(I)
C        SVT(I) = DISTANCE FROM FRONT OF ROD.
C        RROD(I) = CORRESPONDING ROD RADIUS.
C        FILE 8.NVENT+2: AHOLE,AGRES
C        AHOLE = AREA OF CENTRAL HOLE IN ANNULAP PISTON (CM**2).
C        AGRES = AREA OF GREASE DYKE.
C        INITIAL LIQUID VOLUME V1 IS CONSIDERED ACCURATE.
C        WHEN THIS MUCH LIQUID HAS BEEN INJECTED,
C        THE PISTON STOPS.
C        SOME PART OF THE PISTON IS ASSUMED TO HAVE HIT
C        THE BACK WALL.
C        ACTUAL SHAPE OF PISTON IS IRRELEVANT.C
C        FILE 8.NVENT+3: NBLOC
C        IF NBLOC > 0, THEN BLOCK IS MOUNTED ON BELLEVILLE SPRINGS.
C        BLOCK WILL MOVE BACK UNTIL SPRINGS BOTTOM OUT.
C        FILE 8.NVENT+4...:SBLOC(I),FBLOC(I)
C        SBLOC(I) = DISTANCE SPRINGS ARE COMPRESSED (CM).
C        FBLOC(I) = FORCE EXERTED BY SPRINGS (MPA-CM**3).
C        FILE 8.NVENT+4+NBLOC: ABLOC,BLWT
C        ABLOC = AREA OF BLOCK (CM**2).
C        BLWT = MASS OF BLOCK (G).
C
C      FILE 9: TPIS - PISTON FRICTION RESISTANCE OPTION
C
C        IF PIS1 THEN RESISTANCE IS A FUNCTION OF PISTON TRAVEL.
C        FILE 9.1: NPIS
C        NPIS = NO. OF ENTRIES IN PISTON RESISTANCE TABLE.
C        FILE 9.1...: SFRAC(I),PRS(I)
C        SFRAC(I) = FRACTION OF PISTON TRAVEL.
C        WILL BE NORMALIZED TO MAX PISTON TRAVEL.
C        PRS(I) = PISTON RESISTANCE (MPA).
```

```
C        PISTON RESISTANCE IS FOUND BY INTERPOLATING TABLE.
C
C      FILE 10: TDIS - DISCHARGE COEFFICIENT OPTION SWITCH
C
C        IF DIS1 THEN DC FUNCTION OF PISTON TRAVEL.
C        FILE 10.1: NDC
C        NDC = NO. OF TABLE ENTRIES.
C        FILE 10.2...: SFRAC(I),DCF(I)
C        SFRAC(I) = FRACTION OF PISTON TRAVEL.
C        WILL BE NORMALIZED TO MAX PISTON TRAVEL.
C        DCF(I) = DISCHARGE COEFFICIENT.
C        DC IS FOUND BY INTERPOLATING TABLE.
C
C      FILE 11: TDIS34 - DISCHARGE COEFFICIENT OPTION SWITCH-TUBE
C
C        IF DIS1 THEN DC34 FUNCTION OF PROJ TRAVEL.
C        FILE 11.1: NDC
C        NDC = NO. OF TABLE ENTRIES.
C        FILE 11.2...: SFRAC(I),DCF(I)
C        SPROJ(I) = PROJECTILE TRAVEL.
C        DCF(I) = DISCHARGE COEFFICIENT.
C        DC34 IS FOUND BY INTERPOLATING TABLE.
C
C      FILE 12: TFLUX - MASS FLUX OPTION SWITCH FOR ORIFICE
C
C        IF FLUX1 THEN STEADY STATE FORMULATION.
C        FLUID ENTRANCE VELOCITY = 0.
C        FILE 12.1: NVO
C        NVO = NO. OF OPENINGS IN PISTON.
C        USED TO FIND REYNOLDS NO.
C
C        IF FLUX2 THEN UNSTEADY MASS FLUX FORMULATION.
C        TAKE TIME DERIVATIVE OF MASS FLUX.
C        ASSUME MASS FLUX CONSTANT WRT X.
C        FILE 12.1: NVO
C        NVO = NO. OF OPENINGS IN PISTON.
C        USED TO FIND REYNOLDS NO.
C
C        IF FLUX3 THEN UNSTEADY MASS FLUX FORMULATION.
C        TAKE TIME DERIVATIVE OF INFLUX VELOCITY.
C        HEISER FORMULATION.
C        ASSUME MASS FLUX CONSTANT WRT X.
C        FILE 12.1: NVO,PISTH
C        NVO = NO. OF OPENINGS IN PISTON.
C        USED TO FIND REYNOLDS NO.
C        PISTH = THICKNESS OF PISTON (CM).
C
C      FILE 13: TFLUXP - MASS FLUX OPTION SWITCH FOR TUBE
C
C        IF FLUX1 THEN STEADY STATE FORMULATION.
C        GENERALIZED BERNOULLI WITH ENERGY DIFFERENCE.
C        ISENTROPIC FLOW.
```

```
C        FLUID ENTRANCE VELOCITY = 0.
C
C        IF FLUX2 THEN STEADY STATE FORMULATION.
C        ISENTROPIC FLOW.
C        BUT SOLVE FOR PL INSTEAD OF U34.
C        USE WITH TUBE3 OR TUBE4 OPTION.
C
C      FILE 14: TPROJ - PROJECTILE RESISTANCE OPTION SWITCH
C
C        IF PROJ1 THEN PROJECTILE RESISTANCE FUNCTION OF PROJ TRAVEL.
C        FILE 14.1: NPROJ
C        NPROJ = NO. OF TABLE ENTRIES.
C        FILE 14.2...:STR(I),PTR(I)
C        STR(I) = PROJECTILE TRAVEL (CM).
C        PTR(I) = RESISTIVE PRESSURE (MPA).
C        INTERPOLATE TABLE TO FIND PROJECTILE RESISTANCE PRESSURE.
C
C      FILE 15: RH1I,RK1,RK2
C      RH1I = LIQUID DENSITY AT ZERO PRESSURE (GM/CM**3).
C      RK1 = BULK MODULUS AT ZERO PRESSURE (MPA).
C      RK2 = DERIVATIVE OF BULK MODULUS.
C
C      FILE 16: ENER,GAM
C      ENER = CHEMICAL ENERGY OF PROPELLANT (JOULES/GM).
C      GAM = RATIO OF SPECIFIC HEATS.
C
C      FILE 17: SIGMA,VISK
C      SIGMA = SURFACE TENSION OF PROPELLANT (DYNES/CM).
C      VISK = KINEMATIC VISCOSITY (CM**2/SEC).
C
C      FILE 18: WG,COV
C      WG = MOLECULAR WEIGHT OF THE GASES (GM/MOLE).
C      COV = COVOLUME OF THE GAS (CM**3/GM).
C
C      FILE 19: PLI,PGI
C      PLI = INITIAL LIQUID PRESSURE (MPA).
C      PGI = INITIAL GAS PRESSURE (MPA).
C
C      FILE 20: TDROP - DROPLET OPTION SWITCH
C
C        IF DROP1 THEN INSTANTANEOUS BURNING.
C
C        IF DROP2 THEN FIXED SIZE DROPLETS.
C        FILE 20.1:DDR,PBR
C        DDR = DIAMETER OF DROPLETS (CM).
C        PBR = BREAK PRESSURE FOR CHANGE IN BURNING RATE (MPA).
C        FILE 20.2:ADR1,BDR1
C        BURNING RATE = ADR1 * (P**DBR1)
C        IF P<PBR.
C        FILE 20.3:ADR2,BDR2
C        BURNING RATE = ADR2 * (P**DBR2)
C        IF P>PBR.
```

```
C
C         IF DROP3 THEN FIXED SIZE DROPLETS WRT SPACE.
C         DROPLET SIZE CHANGES WITH SIZE.
C         FILE 20.1:DDR,PBR
C         DDR IS IGNORED.
C         PBR = BREAK PRESSURE FOR CHANGE IN BURNING RATE (MPA).
C         FILE 20.2:ADR1,BDR1
C         BURNING RATE = ADR1 * (P**DBR1)
C         IF P<PBR.
C         FILE 20.3:ADR2,BDR2
C         BURNING RATE = ADR2 * (P**DBR2)
C         IF P>PBR.
C         FILE 20.4:NDIAM
C         NDIAM = NO. OF TABLE ENTRIES.
C         FILE 20.5...:SFRAC(I),DIAM(I)
C         SFRAC(I) = FRACTION OF PISTON TRAVEL.
C         WILL BE NORMALIZED TO MAX PISTON TRAVEL.
C         DIAM(I) = DROPLET DIAMETER
C         THE DROPLET DIAMETER AT ANY TIME WILL BE FOUND BY
C         INTERPOLATING THE ABOVE TABLE.
C
C       FILE 21: TPRIM - PRIMER OPTION SWITCH
C
C         IF PRIM1 THEN PRIMER INSTANTANEOUSLY GOES TO GAS.
C         THE PRIMER MASS IS THE MASS OF GAS IN THE CHAMBER.
C
C         IF PRIM2 SET PRIMER AS LIQUID DROPLETS.
C         ASSUME PRIMER HAS SAME PROPERTIES AS LIQUID PROPELLANT.
C         FILE 21.1: RMPRIM
C         RMPRIM = MASS OF PRIMER (G).
C         SET PRIMER AS LIQUID DROPLETS IN COMBUSTION CHAMBER.
C         THE INITIAL GAS PRESSURE IS ASSUMED TO HAVE BEEN
C         GENERATED BY PRIMER THAT HAS ALREADY BURNED.
C
C         IF PRIM3 THEN INJECT PRIMER AT A CONSTANT RATE.
C         ASSUME PRIMER HAS SAME PROPERTIES AS LIQUID PROPELLANT.
C         FILE 21.1: RMPRIM, TINJEC
C         RMPRIM = MASS OF PRIMER (G).
C         TINJEC = TIME FOR COMPLETE INJECTION (S).
C
C       FILE 22: THEATC - HEAT LOSS OPTION (CHAMBER)
C
C         IF HEAT1 THEN NO HEAT LOSS TO THE CHAMBER WALLS.
C
C         IF HEAT2 THEN CONVECTIVE HEAT LOSS TO THE CHAMBER.
C         Q = H * A * DELTA T.
C         FILE 22.1:TEMPC
C         TEMPC = CHAMBER WALL TEMPERATURE (K).
C         FILE 22.2:NCHAM
C         NCHAM = NUMBER OF HEAT LOSS TERMS.
C         FILE 22.3...25.NCHAM+2:SPS,HTRAN
C         SPS = PISTON TRAVEL (CM).
```

```
C        HTRAN = HEAT TRANSFER COEFF. TIMES AREA (JOULES/S-K).
C
C      FILE 23:THEAT - HEAT LOSS OPTION (GUN TUBE)
C
C        IF HEAT1 THEN NO HEAT LOSS TO THE TUBE WALLS.
C
C        IF HEAT2 THEN CONVECTIVE HEAT LOSS TO THE GUN TUBE.
C        USE FITS FOR VISCOSITY AND THERMAL CONDUCTIVITY.
C        FITS WERE MADE FOR HAN1845 BETWEEN 1500K AND 3500K.
C        FILE 23.1:TEMPW,HLFAC
C        TEMPW = TUBE WALL TEMPERATURE (K).
C        HLFAC = FUDGE FACTOR.
C
C      FILE 24: TSHOCK
C
C        IF SHOCK1 NO AIR SHOCK TERM.
C
C        IF SHOCK2 INCLUDE AIR SHOCK EFFECT.
C        FILE 24.1:AIRP,AIRT
C        AIRP = INITIAL PRESSURE IN GUN TUBE (MPA).
C        AIRT = INITIAL TEMPERATURE IN GUN TUBE (K).
C        FILE 24.2:AIRGAM,AIRMW
C        AIRGAM = RATIO OF SPECIFIC HEATS OF GAS IN BARREL.
C        AIRMW = MOLECULAR WEIGHT OF GAS IN BARREL (GM/MOLE).
C
C      FILE 25: TTUBE
C
C        IF TUBE1 THEN STANDARD LAGRANGE DISTRIBUTION.
C
C        IF TUBE2 THEN LAGRANGE WITH NON-ZERO ENTRANCE VELOCITY.
C        ASSUME DENSITY IS CONSTANT WRT X.
C
C        IF TUBE3 THEN UNSTEADY LAGRANGE WITH NON-ZERO ENTRANCE VELOCIT
C        ASSUME DENSITY IS CONSTANT WRT X.
C        SET UP ODE FOR U34.
C        USE WITH FLUX2 OPTION.
C        FILE 25.1: TTUBE
C        IF BURN1 THEN TRACK RAREFACTION WAVE AFTER BURNOUT.
C        OTHERWISE DO NOT.
C
C        IF TUBE4 THEN UNSTEADY LAGRANGE WITH NON-ZERO ENTRANCE VELOCIT
C        ASSUME DENSITY IS LINEAR WRT X.
C        SET UP ODE FOR U34.
C        USE WITH FLUX2 OPTION.
C        FILE 25.1: TTUBE
C        IF BURN1 THEN TRACK RAREFACTION WAVE AFTER BURNOUT.
C        OTHERWISE DO NOT.
C
C      FILE 26: TBUFF
C
C        IF BUFF1 THEN NO WATER BUFFER.
C
```

```
C         IF BUFF2 THEN WATER BUFFER.
C         FILE 26.1: APIS5, AOUT5
C         APIS5 = AREA OF BACK OF PISTON IN BUFFER.
C         AOUT5 = AREA OF EXIT FROM BUFFER TO OUTSIDE.
C         FILE 26.2: CD5
C         CD5 = DISCHARGE COEFFICIENT INTO OUTSIDE.
C         FILE 26.3: V5
C         V5 = INITIAL VOLUME OF THE BUFFER.
C         FILE 26.4: P5
C         P5 = INITIAL PRESSURE OF THE BUFFER.
C         FILE 26.5: RH50, RK51, RK52
C         RH50 = DENSITY AT ZERO PRESSURE.
C         RK51 = BULK MODULUS AT ZERO PRESSURE.
C         RK52 = DERIVATIVE OF BULK MODULUS.
C
C       FILE 27: TINC,HTOP
C       TINC = TIME INCREMENT BETWEEN OUTPUT LINES (SEC).
C       HTOP = MAX TIME STEP ALLOWED IN THE INTEGRATION (SEC).
C
C       FILE 28: EPS,SREC
C       EPS = ERROR CONTROL FOR TIME INTEGRATION.
C       SREC = CUTOFF BETWEEN RELATIVE AND ABSOLUTE ERROR CONTROL.
C
C       FILE 29:MF,KWRITE
C       MF = METHOD OF INTEGRATION.
C       USUALLY MF=22 (STIFF INTEGRATION SCHEME WITH INTERNALLY
C       GENERATED JACOBIAN).
C       KWRITE = DIAGNOSTIC
C       IF KWRITE=1, THEN PRINT OUT AFTER EACH TIME STEP.
C       ALSO TURN ON EPISODE ERROR MESSAGES.
C
C       FILE 30:TMAX
C       TMAX = MAX RUN TIME ALLOWED.
C
C       FILE 31:TREP
C
C         IF REP1 THEN INTEGRATE ONCE.
C
C         IF REP2 ITERATE: CHANGE VENT AREA TO ADJUST LIQUID PRESSURE.
C         FILE 31.1: PTAR, VINC
C         PTAR = DESIRED LIQUID PRESSURE (MPA).
C         VINC = INITIAL INCREMENT FOR CHANGING VENT AREA (CM**2).
C
C         IF REP3 ITERATE: CHANGE RESERVOIR VOLUME TO ADJUST MUZZLE V.
C         FILE 31.1: VMTAR, VINC
C         VMTAR = DESIRED MUZZLE VELOCITY (M/S).
C         VINC  = INITIAL INCREMENT FOR CHANGING RESERVOIR VOLUME (CM**3
C
C       FILE 32:TCHAM
C
C         IF CHAM1 THEN COMPUTE CHAMBER PRESSURE.
C
```

```
C       IF CHAM2 THEN USE EXPERIMENTAL CHAMBER PRESSURE.
C       READ IN FROM STANDARD GRAPHICS FILE (TAPE1).
C       FIRST COLUMN  = TIME (MS).
C       THIRD COLUMN  = CHAMBER PRESSURE (MPA).
C   ***********************************************
```

APPENDIX B

Below is a listing of the job stream for the first test problem (instantaneous burning with constant discharge coefficient). Following is a listing of the output. Since there are many variables to keep track of, the output is on multiple files. Only the ones of interest for a particular problem need to be printed out. Here only the minimal output is given.

```
30LC21 - 2/3 Charge - Instan - CD=0.95
   0.0        243.84            OFFSET   PROJ TRAVEL
   3.0                          GUN TUBE DIAMETER
   287.1                        PROJ WEIGHT
  2109.1                        PISTON WEIGHT
   166.98     95.0              V1   V3
   33.778      45.508           A1   A3
VENT3                           CENTRAL BOLT WITH ACTUAL PISTON
   7                              BOLT RADIUS VERSUS PISTON TRAVEL
  0.0       1.826
  0.127     1.826
  0.363     1.800
  0.558     1.800
  1.320     1.651
  5.889     1.651
  8.103     1.822
10.475       .666                 AHOLE    AGRES
  11                              NBLOC
  .000    163.443                 SBLOC    FBLOC
  .007    171.470
  .034    202.162
  .058    229.517
  .085    265.323
  .110    288.898
  .135    316.253
  .160    344.275
  .185    370.963
  .210    398.318
  .238    427.675
23.349  3921.0                    ABLOC    BLOCK WEIGHT
PIS1                            PISTON RESISTANCE
   2
    0.0       0.0
    1.0       0.0
DIS1                            DIS. COEFF. VERSUS PISTON TRAVEL
   2
    0.0      .95
    1.0      .95
DIS1                            DIS. COEFF. VS. PROJ TRAVEL - TUBE
   2
    0.0     1.0
```

```
  243.84   1.0
FLUX1                            STEADY STATE MASS FLUX FORMULATION
   1          1.0                  NVO   PTH
FLUX1                            ISENTROPIC FLOW INTO TUBE
PROJ1                            PROJ RESISTANCE
   3
     0.0           50.0
     0.01           5.0
   243.84           5.0
  1.43   5350.0   9.11         RHO   K1   K2
  4035.5      1.2226           ENERGY   GAMMA
    66.9     .04988            SURFACE TENSION   KINEMATIC VISCOSITY
  22.848      .677             MOL WT GAS      COVOLUME
    7.0        0.1             P1   P3
DROP1                          INSTANTANEOUS BURNING
PRIM3                          INJECT HOT GAS
  1.5    0.0025                  PRIMER MASS   INJECTION TIME
HEAT1                          NO HEAT LOSS TO CHAMBER WALLS
HEAT2                          HEAT LOSS TO GUN TUBE WALLS
   300.0    1.0                  TUBE TEMP   FUDGE FACTOR
SHOCK2                         AIR SHOCK
    0.1    300.                  AIRP   AIRT
    1.4    28.84                 AIRGAM AIRMW
TUBE2                          MODIFIED LAGRANGE DISTRIBUTION
BUFF1                          NO WATER BUFFER
  1.00E-04    1.00E-05         TINC   HTOP
  1.00E-06    1.00E-09         EPS    SREC
  22   0                       MF      KWRITE
    40.0                       TMAX
REP1                           INTEGRATE ONCE
CHAM1                          COMPUTE P3
```

```
DATE:   3-08-88     TIME:  14:59:56

30LC21 - 2/3 Charge - Instan - CD=0.95

OFFSET = 0.00000          TRAVEL =  243.84

TUBE DIAM =  3.0000          TUBE AREA =  7.0686

PJWT =   287.10          PSWT =  2109.1

V1 IN =  166.98          V3 IN =  95.000

A1 =  33.778          A3 =  45.508

VENT3                         CENTRAL BOLT WITH ACTUAL PISTON

NVENT =   7

PISTON TRAV = 0.00000          ROD RADIUS =  1.8260
PISTON TRAV = 0.12700          ROD RADIUS =  1.8260
PISTON TRAV = 0.36300          ROD RADIUS =  1.8000
PISTON TRAV = 0.55800          ROD RADIUS =  1.8000
PISTON TRAV =  1.3200          ROD RADIUS =  1.6510
PISTON TRAV =  5.8890          ROD RADIUS =  1.6510
PISTON TRAV =  8.1030          ROD RADIUS =  1.8220

AREA OF CENTER HOLE =  10.475          AREA OF GREASE DYKE = 0.66600

HYDRAULIC DIFF =  1.4748

PIS TRAV = 0.00000     AVT = 6.30120E-05     AROD =  10.475     RROD =  1.8260     GAP = 5.49214E-06
PIS TRAV = 0.12700     AVT = 6.30120E-05     AROD =  10.475     RROD =  1.8260     GAP = 5.49214E-06
PIS TRAV = 0.36300     AVT = 0.29624         AROD =  10.179     RROD =  1.8000     GAP = 2.60055E-02
PIS TRAV = 0.55800     AVT = 0.29624         AROD =  10.179     RROD =  1.8000     GAP = 2.60055E-02
PIS TRAV =  1.3200     AVT =  1.9116         AROD =  8.5634     RROD =  1.6510     GAP = 0.17500
PIS TRAV =  5.8890     AVT =  1.9116         AROD =  8.5634     RROD =  1.6510     GAP = 0.17500
PIS TRAV =  8.1030     AVT = 4.59051E-02     AROD =  10.429     RROD =  1.8220     GAP = 4.00549E-03

MAX PISTON TRAVEL =  6.9227

NBLOC =  11  BLOCK MOUNTED ON BELLEVILLE SPRINGS

BLOCK TRAVEL = 0.00000          SPRING FORCE =  163.44
BLOCK TRAVEL = 7.00000E-03      SPRING FORCE =  171.47
BLOCK TRAVEL = 3.40000E-02      SPRING FORCE =  202.16
BLOCK TRAVEL = 5.80000E-02      SPRING FORCE =  229.52
BLOCK TRAVEL = 8.50000E-02      SPRING FORCE =  265.32
```

```
BLOCK TRAVEL = 0.11000        SPRING FORCE =  288.90
BLOCK TRAVEL = 0.13500        SPRING FORCE =  316.25
BLOCK TRAVEL = 0.16000        SPRING FORCE =  344.27
BLOCK TRAVEL = 0.18500        SPRING FORCE =  370.96
BLOCK TRAVEL = 0.21000        SPRING FORCE =  398.32
BLOCK TRAVEL = 0.23800        SPRING FORCE =  427.67

BLOCK AREA =  23.349        BLOCK WEIGHT =  3921.0

BORE =  7.6120        BORE/STROKE =  1.0996

PIS1                        PISTON RESISTANCE

NPIS =   2

FRAC PIS TRAV = 0.00000       PIS TRAV = 0.00000       PIS RESISTANCE = 0.00000
FRAC PIS TRAV =  1.0000       PIS TRAV =  6.9227       PIS RESISTANCE = 0.00000

DIS1                        DIS. COEFF. VERSUS PISTON TRAVEL

NDC =   2

FRAC PIS TRAV = 0.00000       PIS TRAV = 0.00000       DIS COEFF = 0.95000
FRAC PIS TRAV =  1.0000       PIS TRAV =  6.9227       DIS COEFF = 0.95000

DIS1                        DIS. COEFF. VS. PROJ TRAVEL - TUBE

NDC =   2

PROJ TRAV = 0.00000        DIS COEFF =  1.0000
PROJ TRAV =  243.84        DIS COEFF =  1.0000

FLUX1                       STEADY STATE MASS FLUX FORMULATION

NO. OF VENT OPENINGS =   1

FLUX1                       ISENTROPIC FLOW INTO TUBE

PROJ1                       PROJ RESISTANCE

NPROJ =   3

TRAVEL = 0.00000        RESISTIVE PRESS =  50.000
TRAVEL = 1.00000E-02    RESISTIVE PRESS =  5.0000
```

```
TRAVEL =  243.84          RESISTIVE PRESS =  5.0000
DENS LIQUID =  1.4300          K1 =  5350.0          K2 =  9.1100
CHEM ENERGY =  4035.5          GAM =  1.2226
SURFACE TENSION =  66.900          KINEMATIC VISCOSITY = 4.98800E-02
MOL WT GAS =  22.848          COVOLUME = 0.67700
PRES LIQUID =  7.0000          PRES GAS = 0.10000
SPECIFIC GAS CONSTANT = 0.36390
CV =  1.6348          CP =  1.9987

DROP1                    INSTANTANEOUS BURNING

PRIM3                    INJECT HOT GAS
MASS PRIMER =  1.5000
TIME FOR INJECTION = 2.50000E-03
RATE OF INJECTION =  600.00

HEAT1                    NO HEAT LOSS TO CHAMBER WALLS

HEAT2                    HEAT LOSS TO GUN TUBE WALLS
TUBE TEMPERATURE =  300.00
HEAT LOSS FUDGE FACTOR =  1.0000

SHOCK2                   AIR SHOCK
AIRP = 0.10000          AIRT =  300.00
AIRGAM =  1.4000          AIRMW =  28.840

TUBE2                    MODIFIED LAGRANGE DISTRIBUTION

BUFF1                    NO WATER BUFFER
```

```
TINC = 1.00000E-04     HTOP = 1.00000E-05

MF =  22     EPS = 1.00000E-06     SREC = 1.00000E-09

TMAX =  40.000

REP1                          INTEGRATE ONCE

CHAM1                         COMPUTE P3


CHARGE =  239.09          PRIMER =  1.5106          C/M = 0.83278

INITIAL GAS VOLUME =   95.000

INITIAL TOTAL VOLUME =  261.98

LOADING DENSITY = 0.91263

COMBUSTOR LENGTH =  33.264

TOTAL MASS =  240.60

TOTAL ENERGY = 9.70952E+05
```

T (MS)	P1	P3	PL	P4	PR	S PS	V PS.	S PJ	V PJ
0.000	7.000	0.100	0.100	0.100	0.100	0.000	0.000	0.000	0.000
0.100	6.998	0.668	0.668	0.668	0.668	0.000	0.000	0.000	0.000
0.200	6.997	1.237	1.237	1.237	1.237	0.000	0.000	0.000	0.000
0.300	6.998	1.807	1.807	1.807	1.807	0.000	0.000	0.000	0.000
0.400	6.999	2.377	2.377	2.377	2.377	0.000	0.000	0.000	0.000
0.500	7.001	2.947	2.947	2.947	2.947	0.000	0.000	0.000	0.000
0.600	7.003	3.518	3.518	3.518	3.518	0.000	0.000	0.000	0.000
0.700	7.003	4.089	4.089	4.089	4.089	0.000	0.000	0.000	0.000
0.800	7.002	4.660	4.660	4.660	4.660	0.000	0.000	0.000	0.000
0.900	7.069	5.232	5.232	5.232	5.232	0.000	3.184	0.000	0.000
1.000	7.593	5.803	5.803	5.803	5.803	0.001	12.645	0.000	0.000
1.100	8.603	6.370	6.370	6.370	6.370	0.003	22.613	0.000	0.000
1.200	9.570	6.935	6.935	6.935	6.935	0.005	30.298	0.000	0.000
1.300	10.028	7.496	7.496	7.496	7.496	0.009	39.091	0.000	0.000
1.400	10.125	8.052	8.052	8.052	8.052	0.013	54.360	0.000	0.000
1.500	10.454	8.599	8.599	8.599	8.599	0.020	76.824	0.000	0.000
1.600	11.361	9.134	9.134	9.134	9.134	0.029	101.303	0.000	0.000
1.700	12.543	9.655	9.655	9.655	9.655	0.040	122.309	0.000	0.000
1.800	13.398	10.164	10.164	10.164	10.164	0.053	139.984	0.000	0.000
1.900	13.735	10.659	10.659	10.659	10.659	0.068	159.406	0.000	0.000
2.000	14.012	11.138	11.138	11.138	11.138	0.085	183.999	0.000	0.000
2.100	14.820	11.597	11.597	11.597	11.597	0.105	210.595	0.000	0.000
2.200	16.100	12.037	12.037	12.037	12.037	0.127	232.538	0.000	0.000
2.300	16.903	12.607	12.607	12.607	12.607	0.151	249.689	0.000	0.000
2.400	17.075	13.439	13.439	13.439	13.439	0.177	273.807	0.000	0.000
2.500	17.865	14.500	14.500	14.500	14.500	0.206	309.152	0.000	0.000
2.600	19.664	15.369	15.369	15.369	15.369	0.239	345.112	0.000	0.000
2.700	25.451	16.781	16.781	16.781	16.781	0.275	373.943	0.000	0.000
2.800	42.494	20.359	20.359	20.359	20.359	0.309	285.906	0.000	0.000
2.900	46.113	25.359	25.359	25.359	25.359	0.331	157.408	0.000	0.000
3.000	43.178	30.106	30.106	30.106	30.106	0.344	116.192	0.000	0.000
3.100	43.185	34.030	34.030	34.030	34.030	0.358	167.738	0.000	0.000
3.200	49.036	37.877	37.877	37.877	37.877	0.378	248.700	0.000	0.000
3.300	58.901	42.362	42.362	42.362	42.362	0.407	307.223	0.000	0.000
3.400	69.725	47.660	47.660	47.660	47.660	0.439	328.757	0.000	0.000
3.500	79.496	53.560	53.560	53.560	53.560	0.471	327.071	0.001	32.877
3.600	87.924	59.652	59.652	59.652	59.652	0.504	323.840	0.032	842.551
3.700	95.729	65.284	65.265	65.262	65.256	0.536	327.742	0.185	2255.915
3.800	102.958	70.310	70.250	70.241	70.221	0.570	333.589	0.487	3798.525
3.900	106.778	75.609	75.464	75.450	75.411	0.604	361.029	0.949	5464.867

4.000	110.413	80.947	80.665	80.641	80.567	0.643	438.468	1.584	7259.000
4.100	116.453	86.435	85.929	85.896	85.771	0.693	550.609	2.405	9179.616
4.200	124.243	92.549	91.692	91.652	91.457	0.754	678.976	3.425	11233.267
4.300	132.643	99.545	98.151	98.113	97.819	0.829	823.994	4.657	13434.866
4.400	141.548	107.450	105.267	105.241	104.811	0.920	995.110	6.117	15800.678

T (MS)	P1	P3	PL	P4	PR	S PS	V PS	S PJ	V PJ
4.500	151.353	116.299	112.976	112.980	112.366	1.029	1199.606	7.823	18345.242
4.600	162.343	126.208	121.268	121.332	120.472	1.161	1442.035	9.793	21082.153
4.700	174.689	137.327	130.127	130.297	129.112	1.319	1726.825	12.046	24024.728
4.800	196.008	148.330	138.869	138.921	137.195	1.507	2016.398	14.605	27176.251
4.900	219.951	159.197	146.814	146.757	144.381	1.719	2222.638	17.488	30514.290
5.000	240.495	169.200	153.915	153.502	150.248	1.949	2352.295	20.713	34013.674
5.100	256.538	177.627	159.632	158.599	154.257	2.188	2430.479	24.294	37634.387
5.200	268.370	184.210	163.724	161.854	156.276	2.434	2477.642	28.242	41328.197
5.300	276.710	188.995	166.220	163.359	156.462	2.683	2506.479	32.561	45047.500
5.400	282.266	192.190	167.300	163.357	155.109	2.935	2523.822	37.251	48750.544
5.500	285.616	194.050	167.209	162.135	152.549	3.188	2533.264	42.309	52403.462
5.600	287.222	194.828	166.191	159.973	149.091	3.441	2536.880	47.729	55980.354
5.700	287.462	194.752	164.466	157.115	145.002	3.695	2536.054	53.502	59462.456
5.800	286.646	194.015	162.217	153.766	140.500	3.948	2531.800	59.618	62836.965
5.900	285.028	192.776	159.594	150.089	135.755	4.201	2524.902	66.066	66095.868
6.000	282.814	191.166	156.716	146.211	130.898	4.453	2515.975	72.833	69234.871
6.100	280.166	189.289	153.675	142.231	126.029	4.704	2505.506	79.909	72252.496
6.200	277.214	187.227	150.542	138.221	121.218	4.954	2493.886	87.280	75149.345
6.300	274.058	185.044	147.369	134.236	116.515	5.203	2481.425	94.935	77927.511
6.400	270.777	182.789	144.197	130.314	111.955	5.450	2468.375	102.861	80590.130
6.500	267.431	180.502	141.053	126.483	107.560	5.697	2454.936	111.049	83141.025
6.600	266.205	178.167	137.978	122.767	103.343	5.941	2439.234	119.486	85584.453
6.700	274.299	175.294	135.129	119.207	99.288	6.181	2326.045	128.162	87924.742
6.800	273.548	171.262	132.591	115.797	95.352	6.404	2117.543	137.068	90165.325
6.900	266.369	165.931	130.207	112.455	91.503	6.603	1879.138	146.192	92308.784
7.000	255.649	159.661	127.669	109.059	87.719	6.780	1646.808	155.526	94356.975
7.100	0.000	151.229	125.238	105.811	84.149	6.917	0.000	165.060	96311.659
7.200	0.000	134.419	122.156	102.929	81.451	6.917	0.000	174.786	98191.311
7.300	0.000	122.883	115.889	98.231	77.882	6.917	0.000	184.696	99992.621
7.400	0.000	114.123	109.230	92.939	73.775	6.917	0.000	194.781	101697.149
7.500	0.000	106.854	102.926	87.670	69.585	6.917	0.000	205.032	103297.668
7.600	0.000	100.486	97.091	82.662	65.554	6.917	0.000	215.438	104795.575
7.700	0.000	94.747	91.706	77.986	61.778	6.917	0.000	225.988	106196.242
7.800	0.000	89.502	86.730	73.649	58.278	6.917	0.000	236.674	107506.341
7.866	0.000	86.252	83.633	70.949	56.103	6.917	0.000	243.840	108329.606

MUZZLE VEL (M/SEC)	1083.3
MAX V PIS (M/SEC)	25.4
MAX P1 (MPA)	287.5
MAX P3 (MPA)	194.8
MAX PL (MPA)	167.3
MAX PR (MPA)	163.4
MAX ACC (K-G)	37.9
MAX MASS ERROR	0.00
MAX ENERGY ERROR	0.11
BALLISTIC EFFICIENCY =	17.46 %
EXPANSION RATIO =	7.91
LOSS TO CHAMBER WALLS =	11.64 %

RUN TIME = 4.1 NSTEP = 1225

MAX	TIME	S PS	V PS	S PJ	V PJ	ACC	P1	P3	PL	P4	PR	Z BUR
P1	5.70	0.037	25.36	0.535	594.6	34.95	287.5	194.8	164.5	157.1	145.0	0.50
P3	5.60	0.034	25.37	0.477	559.8	35.99	287.2	194.8	166.2	160.0	149.1	0.46
PL	5.40	0.029	25.24	0.373	487.5	37.53	282.3	192.2	167.3	163.4	155.1	0.38
P4	5.30	0.027	25.06	0.326	450.5	37.88	276.7	189.0	166.2	163.4	156.5	0.34
PR	5.30	0.027	25.06	0.326	450.5	37.88	276.7	189.0	166.2	163.4	156.5	0.34
V PS	5.60	0.034	25.37	0.477	559.8	35.99	287.2	194.8	166.2	160.0	149.1	0.46
BURN	7.09	0.069	14.59	1.639	960.9	19.55	244.9	153.7	125.1	106.0	84.4	1.00
MUZ	7.87	0.069	0.00	2.438	1083.3	12.36	0.0	86.3	83.6	70.9	56.1	1.00

APPENDIX C

Below is a listing of the job stream for the second test problem (droplet formation with constant discharge coefficient). Following is the summary page from the output.

```
30LC31 - 2/3 Charge - Drop - CD=0.95
   0.0         243.84          OFFSET   PROJ TRAVEL
   3.0                         GUN TUBE DIAMETER
   287.1                       PROJ WEIGHT
  2109.1                       PISTON WEIGHT
   166.98     95.0             V1   V3
   33.778      45.508          A1   A3
VENT3                          CENTRAL BOLT WITH ACTUAL PISTON
   7                             BOLT RADIUS VERSUS PISTON TRAVEL
  0.0      1.826
  0.127    1.826
  0.363    1.800
  0.558    1.800
  1.320    1.651
  5.889    1.651
  8.103    1.822
10.475      .666                 AHOLE    AGRES
  11                             NBLOC
  .000   163.443                 SBLOC    FBLOC
  .007   171.470
  .034   202.162
  .058   229.517
  .085   265.323
  .110   288.898
  .135   316.253
  .160   344.275
  .185   370.963
  .210   398.318
  .238   427.675
23.349  3921.0                   ABLOC    BLOCK WEIGHT
PIS1                           PISTON RESISTANCE
   2
    0.0      0.0
    1.0      0.0
DIS1                           DIS. COEFF. VERSUS PISTON TRAVEL
   2
    0.0     .95
    1.0     .95
DIS1                           DIS. COEFF. VS. PROJ TRAVEL - TUBE
   2
    0.0    1.0
  243.84   1.0
FLUX1                          STEADY STATE MASS FLUX FORMULATION
   1           1.0               NVO   PTH
```

```
FLUX1                                 ISENTROPIC FLOW INTO TUBE
PROJ1                                 PROJ RESISTANCE
   3
     0.0           50.0
      0.01          5.0
   243.84           5.0
  1.43   5350.0   9.11          RHO    K1    K2
  4035.5       1.2226           ENERGY   GAMMA
    66.9      .04988            SURFACE TENSION   KINEMATIC VISCOSITY
  22.848       .677             MOL WT GAS      COVOLUME
   7.0          0.1             P1    P3
DROP3                           MONOSIZE DROPS- FUNC OF PISTON TRAVEL
  0.01       95.2590            DDR       PBR
  1.64        .103              ADR1      BDR1
  1.64        .103              ADR1      BDR1
    7
  0.00       1.00
  0.363      1.00
  0.364      0.04
  0.558      0.02
  1.320      0.016
  3.000      0.008
  6.9227     0.008
PRIM3                           INJECT HOT GAS
  1.5    0.0025                   PRIMER MASS   INJECTION TIME
HEAT1                           NO HEAT LOSS TO CHAMBER WALLS
HEAT2                           HEAT LOSS TO GUN TUBE WALLS
   300.0     1.0                  TUBE TEMP   FUDGE FACTOR
SHOCK2                          AIR SHOCK
    0.1     300.                  AIRP    AIRT
    1.4     28.84                 AIRGAM AIRMW
TUBE2                           MODIFIED LAGRANGE DISTRIBUTION
BUFF1                           NO WATER BUFFER
  1.00E-04     1.00E-05         TINC   HTOP
  1.00E-06     1.00E-09         EPS    SREC
  22    0                       MF     KWRITE
    40.0                        TMAX
REP1                            INTEGRATE ONCE
CHAM1                           COMPUTE P3
```

MUZZLE VEL (M/SEC)	1050.4
MAX V PIS (M/SEC)	24.1
MAX P1 (MPA)	266.4
MAX P3 (MPA)	176.2
MAX PL (MPA)	159.1
MAX PR (MPA)	150.6
MAX ACC (K-G)	33.9
MAX MASS ERROR	0.00
MAX ENERGY ERROR	0.18

BALLISTIC EFFICIENCY = 16.42 %

EXPANSION RATIO = 7.91

LOSS TO CHAMBER WALLS = 11.49 %

RUN TIME = 5.6 NSTEP = 1496

APPENDIX D

Below is a listing of the job stream for the third test problem (instantaneous burning; constant discharge coefficient; longer Belleville). Following is the summary page from the output.

```
30LC22 - 2/3 Charge - Instan - CD=0.95 - Long Belleville
   0.0          243.84            OFFSET    PROJ TRAVEL
   3.0                            GUN TUBE DIAMETER
   287.1                          PROJ WEIGHT
  2109.1                          PISTON WEIGHT
   166.98       95.0              V1    V3
   33.778        45.508           A1    A3
VENT3                             CENTRAL BOLT WITH ACTUAL PISTON
   7                                BOLT RADIUS VERSUS PISTON TRAVEL
  0.0       1.826
  0.127     1.826
  0.363     1.800
  0.558     1.800
  1.320     1.651
  5.889     1.651
  8.103     1.822
10.475       .666                   AHOLE     AGRES
  12                                NBLOC
  .000    163.443                   SBLOC     FBLOC
  .007    171.470
  .034    202.162
  .058    229.517
  .085    265.323
  .110    288.898
  .135    316.253
  .160    344.275
  .185    370.963
  .210    398.318
  .238    427.675
  .438    500.000
23.349   3921.0                     ABLOC     BLOCK WEIGHT
PIS1                              PISTON RESISTANCE
   2
    0.0       0.0
    1.0       0.0
DIS1                              DIS. COEFF. VERSUS PISTON TRAVEL
   2
    0.0      .95
    1.0      .95
DIS1                              DIS. COEFF. VS. PROJ TRAVEL - TUBE
   2
    0.0    1.0
  243.84   1.0
FLUX1                             STEADY STATE MASS FLUX FORMULATION
```

```
  1          1.0              NVO   PTH
FLUX1                       ISENTROPIC FLOW INTO TUBE
PROJ1                       PROJ RESISTANCE
  3
    0.0         50.0
    0.01         5.0
  243.84         5.0
  1.43   5350.0   9.11      RHO   K1   K2
  4035.5      1.2226        ENERGY   GAMMA
   66.9      .04988         SURFACE TENSION   KINEMATIC VISCOSITY
  22.848      .677          MOL WT GAS     COVOLUME
   7.0        0.1           P1   P3
DROP1                       INSTANTANEOUS BURNING
PRIM3                       INJECT HOT GAS
  1.5    0.0025               PRIMER MASS   INJECTION TIME
HEAT1                       NO HEAT LOSS TO CHAMBER WALLS
HEAT2                       HEAT LOSS TO GUN TUBE WALLS
  300.0    1.0                TUBE TEMP   FUDGE FACTOR
SHOCK2                      AIR SHOCK
   0.1    300.                AIRP   AIRT
   1.4     28.84              AIRGAM AIRMW
TUBE2                       MODIFIED LAGRANGE DISTRIBUTION
BUFF1                       NO WATER BUFFER
  1.00E-04    1.00E-05      TINC   HTOP
  1.00E-06    1.00E-09      EPS    SREC
  22   0                    MF     KWRITE
   40.0                     TMAX
REP1                        INTEGRATE ONCE
CHAM1                       COMPUTE P3
```

MUZZLE VEL (M/SEC)	1140.9
MAX V PIS (M/SEC)	28.0
MAX P1 (MPA)	351.8
MAX P3 (MPA)	238.1
MAX PL (MPA)	214.5
MAX PR (MPA)	210.8
MAX ACC (K-G)	50.0
MAX MASS ERROR	0.00
MAX ENERGY ERROR	0.14

BALLISTIC EFFICIENCY = 19.37 %

EXPANSION RATIO = 7.94

LOSS TO CHAMBER WALLS = 11.08 %

RUN TIME = 3.8 NSTEP = 1169

APPENDIX E

Below is a listing of the job stream for the fourth test problem (droplet formation; constant discharge coefficient; longer Belleville). Following is the summary page from the output.

```
30LC32- 2/3 Charge - Drop - CD=0.95 - Longer Belleville
   0.0        243.84            OFFSET   PROJ TRAVEL
   3.0                          GUN TUBE DIAMETER
   287.1                        PROJ WEIGHT
  2109.1                        PISTON WEIGHT
   166.98      95.0             V1   V3
   33.778       45.508          A1   A3
VENT3                           CENTRAL BOLT WITH ACTUAL PISTON
   7                              BOLT RADIUS VERSUS PISTON TRAVEL
  0.0       1.826
  0.127     1.826
  0.363     1.800
  0.558     1.800
  1.320     1.651
  5.889     1.651
  8.103     1.822
10.475       .666                 AHOLE     AGRES
  12                              NBLOC
  .000   163.443                  SBLOC     FBLOC
  .007   171.470
  .034   202.162
  .058   229.517
  .085   265.323
  .110   288.898
  .135   316.253
  .160   344.275
  .185   370.963
  .210   398.318
  .238   427.675
  .438   500.
23.349  3921.0                    ABLOC     BLOCK WEIGHT
PIS1                            PISTON RESISTANCE
   2
    0.0       0.0
    1.0       0.0
DIS1                            DIS. COEFF. VERSUS PISTON TRAVEL
   2
    0.0     .95
    1.0     .95
DIS1                            DIS. COEFF. VS. PROJ TRAVEL - TUBE
   2
    0.0    1.0
  243.84   1.0
FLUX1                           STEADY STATE MASS FLUX FORMULATION
```

```
   1            1.0              NVO   PTH
FLUX1                          ISENTROPIC FLOW INTO TUBE
PROJ1                          PROJ RESISTANCE
   3
     0.0          50.0
     0.01          5.0
   243.84          5.0
  1.43   5350.0   9.11       RHO   K1   K2
  4035.5      1.2226         ENERGY   GAMMA
    66.9     .04988          SURFACE TENSION   KINEMATIC VISCOSITY
  22.848      .677           MOL WT GAS      COVOLUME
   7.0         0.1           P1   P3
DROP3                        MONOSIZE DROPS- FUNC OF PISTON TRAVEL
  0.01     95.2590           DDR      PBR
  1.64       .103            ADR1     BDR1
  1.64       .103            ADR1     BDR1
     7
  0.00      1.00
  0.558     1.00
  0.559     0.05
  1.320     0.05
  3.000     0.02
  5.889     0.012
  7.115     0.01
PRIM3                        INJECT HOT GAS
  1.5    0.0025                PRIMER MASS   INJECTION TIME
HEAT1                        NO HEAT LOSS TO CHAMBER WALLS
HEAT2                        HEAT LOSS TO GUN TUBE WALLS
   300.0    1.0                TUBE TEMP   FUDGE FACTOR
SHOCK2                       AIR SHOCK
    0.1    300.                AIRP   AIRT
    1.4     28.84              AIRGAM AIRMW
TUBE2                        MODIFIED LAGRANGE DISTRIBUTION
BUFF1                        NO WATER BUFFER
  1.00E-04    1.00E-05       TINC   HTOP
  1.00E-06    1.00E-09       EPS    SREC
  22   0                     MF     KWRITE
    40.0                     TMAX
REP1                         INTEGRATE ONCE
CHAM1                        COMPUTE P3
```

MUZZLE VEL (M/SEC)	1058.8
MAX V PIS (M/SEC)	24.2
MAX P1 (MPA)	288.1
MAX P3 (MPA)	181.6
MAX PL (MPA)	160.1
MAX PR (MPA)	147.6
MAX ACC (K-G)	32.9
MAX MASS ERROR	0.00
MAX ENERGY ERROR	0.22

BALLISTIC EFFICIENCY = 16.68 %

EXPANSION RATIO = 7.94

LOSS TO CHAMBER WALLS = 11.63 %

RUN TIME = 5.4 NSTEP = 1485

APPENDIX F

Below is a listing of the job stream for the fifth test problem (droplet formation; adjusted discharge coefficient; longer Belleville). Following is the summary page from the output.

```
30LC42- 2/3 Charge - Drop - Simple CD - Long Belle
   0.0         243.84          OFFSET   PROJ TRAVEL
   3.0                         GUN TUBE DIAMETER
   287.1                       PROJ WEIGHT
  2109.1                       PISTON WEIGHT
   166.98      95.0            V1   V3
   33.778       45.508         A1   A3
VENT3                          CENTRAL BOLT WITH ACTUAL PISTON
   7                             BOLT RADIUS VERSUS PISTON TRAVEL
  0.0      1.826
  0.127    1.826
  0.363    1.800
  0.558    1.800
  1.320    1.651
  5.889    1.651
  8.103    1.822
10.475      .666                 AHOLE    AGRES
  12                             NBLOC
  .000    163.443                SBLOC    FBLOC
  .007    171.470
  .034    202.162
  .058    229.517
  .085    265.323
  .110    288.898
  .135    316.253
  .160    344.275
  .185    370.963
  .210    398.318
  .238    427.675
  .438    500.
23.349  3921.0                   ABLOC    BLOCK WEIGHT
PIS1                           PISTON RESISTANCE
   2
    0.0       0.0
    1.0       0.0
DIS1                           DIS. COEFF. VERSUS PISTON TRAVEL
   5
    0.0      .95
    0.558    .95
    0.800    .30
    1.320    .95
    7.115    .95
DIS1                           DIS. COEFF. VS. PROJ TRAVEL - TUBE
   2
```

```
   0.0      1.0
  243.84    1.0
FLUX1                                    STEADY STATE MASS FLUX FORMULATION
  1              1.0                       NVO    PTH
FLUX1                                    ISENTROPIC FLOW INTO TUBE
PROJ1                                    PROJ RESISTANCE
  3
    0.0            50.0
    0.01            5.0
   243.84           5.0
  1.43    5350.0   9.11                RHO    K1    K2
  4035.5       1.2226                  ENERGY   GAMMA
   66.9       .04988                   SURFACE TENSION   KINEMATIC VISCOSITY
  22.848       .677                    MOL WT GAS       COVOLUME
   7.0          0.1                    P1    P3
DROP3                                  MONOSIZE DROPS- FUNC OF PISTON TRAVEL
  0.01      95.2590                    DDR       PBR
  1.64        .103                     ADR1      BDR1
  1.64        .103                     ADR1      BDR1
    8
  0.00       1.0000
  0.558      1.0000
  0.559      0.0500
  0.800      0.0300
  1.320      0.0150
  3.000      0.0100
  5.889      0.0075
  7.115      0.0075
PRIM3                                  INJECT HOT GAS
  1.5     0.0025                         PRIMER MASS   INJECTION TIME
HEAT1                                  NO HEAT LOSS TO CHAMBER WALLS
HEAT2                                  HEAT LOSS TO GUN TUBE WALLS
   300.0     1.0                         TUBE TEMP   FUDGE FACTOR
SHOCK2                                 AIR SHOCK
    0.1     300.                         AIRP   AIRT
    1.4      28.84                       AIRGAM AIRMW
TUBE2                                  MODIFIED LAGRANGE DISTRIBUTION
BUFF1                                  NO WATER BUFFER
  1.00E-04     1.00E-05                TINC   HTOP
  1.00E-06     1.00E-09                EPS    SREC
  22    0                              MF      KWRITE
    40.0                               TMAX
REP1                                   INTEGRATE ONCE
CHAM1                                  COMPUTE P3
```

MUZZLE VEL (M/SEC)	1059.5
MAX V PIS (M/SEC)	24.2
MAX P1 (MPA)	277.7
MAX P3 (MPA)	177.9
MAX PL (MPA)	158.5
MAX PR (MPA)	149.8
MAX ACC (K-G)	33.8
MAX MASS ERROR	0.00
MAX ENERGY ERROR	0.15

BALLISTIC EFFICIENCY = 16.70 %

EXPANSION RATIO = 7.94

LOSS TO CHAMBER WALLS = 11.47 %

RUN TIME = 5.4 NSTEP = 1471

THIS PAGE IS BLANK

DISTRIBUTION LIST

No. of Copies	Organization
12	Administrator Defense Technical Info Center ATTN: DTIC-DDA Cameron Station Alexandria, VA 22304-6145
2	Director Defense Advanced Research Projects Agency ATTN: J. Lupo J. Richardson 1400 Wilson Boulevard Arlington, VA 22209
2	HQDA (SARD-TR/B. Zimmerman, I. Szkrybalo) Washington, DC 20310-0001
1	Commander US Army Materiel Command ATTN: AMCDRA-ST 5001 Eisenhower Avenue Alexandria, VA 22333-0001
1	HQ, US Army Materiel Command ATTN: AMCICP-AD, B. Dunetz 5001 Eisenhower Avenue Alexandria, VA 22333-0001
14	Cmdr, US Army Armament, Rsch, Development & Engr Center ATTN: SMCAR-TSS SMCAR-TDC (2 COPIES) SMCAR-MSI (2 COPIES) SMCAR-AEE-BR, B. Brodman SMCAR-AEE-B, D. Downs SMCAR-AEE-BR, W. Seals A. Beardell SMCAR-AEE-W, N. Slagg SMCAR-AEE, A. Bracuti J. Lannon SMCAR-FSS-D, L. Frauen SMCAR-FSA-S, H. Liberman Picatinny Arsenal, NJ07806-5000
5	Commander US Army Armament, Rsch, Development & Engr Center ATTN: SMCAR-FSS-DA, Bldg 94 C. Daly R. Kopmann J. Irizarry M. Oetken N. Kendl Picatinny Arsenal, NJ 07806-5000
5	Director Benet Weapons Laboratory US Army Armament, Rsch, Development & Engr Center ATTN: SMCAR-CCB-DS, E. Conroy A. Graham SMCAR-CCB, L. Johnson SMCAR-CCB-S, F. Heiser SMCAR-LCB-TL Watervliet NY 12189-4050
1	Commander US Army Armament, Munitions and Chemical Command ATTN: SMCAR-ESP-L Rock Island, IL 61299-5000
1	Commander US Army Aviation Systems Cmd ATTN: AMSAV-DACL 4300 Goodfellow Blvd St. Louis, MO 63120-1798
1	Commander Materials Technology Lab US Army Laboratory Cmd ATTN: SLCMT-MCM-SB M. Levy Watertown, MA 02172-0001

DISTRIBUTION LIST

No. of Copies	Organization
1	Director US Army Aviation Rsch and Technology Activity Ames Research Center Moffett Field, CA 94035-1099
1	Commander US Army Communications Electronics Command ATTN: AMSEL-ED Fort Monmouth, NJ 07703-5022
1	Commander ERADCOM Technical Library ATTN: STEI-L Ft. Monmouth, NJ 07703-5301
2	Commander US Army Laboratory Cmd ATTN: SLCHD-TA-L AMSLC-DL 2800 Powder Mill Rd Adelphi, MD 20783-1145
1	Commander US Army Missile Command ATTN: AMSMI-RD Redstone Arsenal, AL 35898-5000
1	Commander US Army Missile Command ATTN: AMSMI-AS Redstone Arsenal, AL 35898-5000
1	Commander US Army Belvoir RD&E Ctr ATTN: STRBE-WC Tech Library (Vault) B-315 Fort Belvoir, VA 22060-5606

No. of Copies	Organization
1	Commander US Army Tank Automotive Cmd ATTN: AMSTA-TSL Warren, MI 48397-5000
1	Director US Army Laboratory Cmd Army Research Office ATTN: Tech Library PO Box 12211 Research Triangle Park, NC 27709-2211
1	Director TRADOC Analysis Command ATTN: ATAA-SL White Sands Missile Range NM 88002-5502
1	Commandant US Army Infantry School ATTN: ATSH-CD-CSO-OR Fort Benning, GA 31905-5660
1	Commander US Army Armament, Rsch, Development and Engr Center ATTN: SMCAR-CCS-C, T Hung Picatinny Arsenal, NJ 07806-5000
2	Commandant US Army Field Artillery School ATTN: ATSF-CMW ATSF-TSM-CN, J. Spicer Fort Sill, OK 73503
1	Commandant US Army Armor Center ATTN: ATSB-CD-MLD Fort Knox, KY 40121

DISTRIBUTION LIST

No. of Copies	Organization
1	Commander Naval Surface Weapons Center ATTN: D.A. Wilson, Code G31 Dahlgren, VA 22448-5000
1	Commander Naval Surface Weapons Center ATTN: J. East, Code G33 Dahlgren, VA 22448-5000
2	Commander US Naval Surface Weapons Ctr ATTN: O. Dengel K. Thorsted Silver Spring, MD 20902-5000
1	Commander Naval Weapons Center China Lake, CA 93555-6001
1	Commander Naval Ordnance Station ATTN: C. Dale Code 5251 Indian Head, MD 20640
1	Superintendent Naval Postgraduate School Dept of Mechanical Engr ATTN: Code 1424, Library Monterey, CA 93943
1	AFWL/SUL Kirtland AFB, NM 87117-5800
1	Air Force Armament Lab ATTN: AFATL/DLODL Eglin AFB, FL 32542-5000
1	AFOSR/NA (L. Caveny) Bldg 410 Bolling AFB, DC 20332

No. of Copies	Organization
1	Commandant USAFAS ATTN: ATSF-TSM-CN Fort Sill, OK 73503-5600
1	Director Jet Propulsion Lab ATTN: Tech Library 4800 Oak Grove Drive Pasadena, CA 91109
2	Director National Aeronautics and Space Administration ATTN: MS-603, Tech Lib MS-86, Dr. Povinelli 21000 Brookpark Road Lewis Research Center Cleveland, OH 44135
1	Director National Aeronautics and Space Administration Manned Spacecraft Center Houston, TX 77058
10	Central Intelligence Agency Office of Central Reference Dissemination Branch Room GE-47 HQS Washington, DC 20502
1	Central Intelligence Agency ATTN: Joseph E. Backofen HQ Room 5F22 Washington, DC 20505
3	Bell Aerospace Textron ATTN: F. Boorady F. Picirillo A.J. Friona PO Box One Buffalo, NY 14240

DISTRIBUTION LIST

No. of Copies	Organization
1	Calspan Corporation ATTN: Tech Library PO Box 400 Buffalo, NY 14225
8	General Electric Ord Sys Div ATTN: J. Mandzy, OP43-220 R.E. Mayer H. West W. Pasko R. Pate I. Magoon J. Scudiere Minh Luu 100 Plastics Avenue Pittsfield, MA 01201-3698
1	General Electric Company Armament Systems Department ATTN: D. Maher Burlington, VT 05401
1	IITRI ATTN: Library 10 W. 35th St Chicago, IL 60616
1	Olin Chemicals Research ATTN: David Gavin PO Box 586 Chesire, CT 06410-0586
2	Olin Corporation ATTN: Victor A. Corso Dr. Ronald L. Dotson PO Box 30-9644 New Haven, CT 06536
1	Paul Gough Associates ATTN: Paul Gough PO Box 1614 Portsmouth, NH 03801

No. of Copies	Organization
1	Safety Consulting Engr ATTN: Mr. C. James Dahn 5240 Pearl St Rosemont, IL 60018
1	Science Applications, Inc. ATTN: R. Edelman 23146 Cumorah Crest Woodland Hills, CA 91364
2	Science Applications Int'l Corporation ATTN: Dr. F. T. Phillips Dr. Fred Su 10210 Campus Point Drive San Diego, CA 92121
1	Science Applications Int'l Corporation ATTN: Norman Banks 4900 Waters Edge Drive Suite 255 Raleigh, NC 27606
1	Sundstrand Aviation Operations ATTN: Mr. Owen Briles PO Box 7202 Rockford, IL 61125
1	Veritay Technology, Inc. ATTN: E.B. Fisher 4845 Millersport Highway PO Box 305 East Amherst, NY 14051-0305
1	Director Applied Physics Laboratory The Johns Hopkins Univ. Johns Hopkins Road Laurel, MD 20707

DISTRIBUTION LIST

No. of Copies	Organization
2	Director CPIA The Johns Hopkins Univ. ATTN: T. Christian Tech Library Johns Hopkins Road Laurel, MD 20707
1	U. of Illinois at Chicago ATTN: Professor Sohail Murad Dept of Chemical Engr Box 4348 Chicago, IL 60680
1	U. of MD at College Park ATTN: Professor Franz Kasler Department of Chemistry College Park, MD 20742
1	U. of Missouri at Columbia ATTN: Professor R. Thompson Department of Chemistry Columbia, MO 65211
1	U. of Michigan ATTN: Prof. Gerard M. Faeth Dept of Aerospace Engr Ann Arbor, MI 48109-3796
1	U. of Missouri at Columbia ATTN: Professor F.K. Ross Research Reactor Columbia, MO 65211
1	U. of Missouri at Kansas City Department of Physics ATTN: Prof. R.D. Murphy 1110 East 48th Street Kansas City, MO 64110-2499
1	Pennsylvania State University Dept of Mechanical Engr ATTN: Prof. K. Kuo University Park, PA 16802

No. of Copies	Organization
2	Princeton Combustion Rsch Laboratories, Inc. ATTN: N.A. Messina M. Summerfield 4275 US Highway One North Monmouth Junction, NJ 08852
1	University of Arkansas Dept of Chemical Engr ATTN: J. Havens 227 Engineering Building Fayetteville, AR 72701
3	University of Delaware Department of Chemistry ATTN: Mr. James Cronin Professor Thomas Brill Mr. Peter Spohn Newark, DE 19711
1	U. of Texas at Austin Bureau of Engineering Rsch ATTN: BRC EME133, Room 1.100 H. Fair 10100 Burnet Road Austin, TX 78758

Aberdeen Proving Ground

Dir, USAMSAA
ATTN: AMXSY-D
AMXSY-MP, H. Cohen

Cdr, USATECOM
ATTN: AMSTE-TO-F

DISTRIBUTION LIST

No. of Copies	Organization	No. of Copies	Organization
	Cdr, CRDEC, AMCCOM ATTN: SMCCR-RSP-A SMCCR-MU SMCCR-SPS-IL		

DISTRIBUTION LIST

No. of Copies	Organization
1	Dr. Clive Woodley GS2 Division Building R31 RARDE Ft. Halstead Sevenoaks, Kent TN14 7BT England

USER EVALUATION SHEET/CHANGE OF ADDRESS

This laboratory undertakes a continuing effort to improve the quality of the reports it publishes. Your comments/answers below will aid us in our efforts.

1. Does this report satisfy a need? (Comment on purpose, related project, or other area of interest for which the report will be used.) ______

2. How, specifically, is the report being used? (Information source, design data, procedure, source of ideas, etc.) ______

3. Has the information in this report led to any quantitative savings as far as man-hours or dollars saved, operating costs avoided, or efficiencies achieved, etc? If so, please elaborate. ______

4. General Comments. What do you think should be changed to improve future reports? (Indicate changes to organization, technical content, format, etc.) ______

BRL Report Number ______ Division Symbol ______

Check here if desire to be removed from distribution list. ____

Check here for address change. ____

Current address: Organization ______
Address ______

------FOLD AND TAPE CLOSED------

Director
U.S. Army Ballistic Research Laboratory
ATTN: SLCBR-DD-T(NEI)
Aberdeen Proving Ground, MD 21005-5066

OFFICIAL BUSINESS
PENALTY FOR PRIVATE USE $300

NO POSTAGE NECESSARY IF MAILED IN THE UNITED STATES

BUSINESS REPLY LABEL
FIRST CLASS PERMIT NO 12062 WASHINGTON D C

POSTAGE WILL BE PAID BY DEPARTMENT OF THE ARMY

Director
U.S. Army Ballistic Research Laboratory
ATTN: SLCBR-DD-T(NEI)
Aberdeen Proving Ground, MD 21005-9989

DTIC

4-89

END

DATE

FILMED